A characterization of tardigrade energetics from oxygen microgradients in relation to temperature, salinity and the termination of cryptobiosis.

By Bjarke Haldrup.
A Master's Thesis in Molecular and Medical Biology, Roskilde University.
In collaboration with the Department of Bioscience, Aarhus University.

August 17, 2018

Internal supervisor: Hans Ramløv
External supervisor: Kai Finster

Abstract

The aim of this project was to determine the metabolic rate of tardigrades and how it depends on conditions such as temperature and salinity, as well as how it changes during termination of the putatively ametabolic state of cryptobiosis and from this to discover novel insights into how tardigrade metabolism and the extraordinary abilities it facilitates may function. To this end, tardigrades were collected in Öland and a method was developed for measuring their metabolic rate (nmol $O_2 \cdot mg^{-1} \cdot hour^{-1}$) using oxygen microsensors and microgradients. The metabolic rate of active Richtersius coronifers at 22 °C and a salinity of 0 ppt was 10.8 ± 1.84 (n = 28) and for dead specimens, it was 0.21 ± 0.03 (n = 4). For the Macrobiotus macrocalix species, it was 13.4 ± 2.19 (n = 17). The metabolic rate of both species was found to be unaffected by scaling within the inherent size variation of the populations. The following metabolic rates (nmol $O_2 \cdot mg^{-1} \cdot hour^{-1}$) were also determined for R. coronifer at different temperatures and a salinity of 0 ppt. 2 °C: 2.28 ± 0.48 (n = 8); 11 °C: 3.56 ± 0.59 (n = 6); 16 °C: 8.42 ± 0.82 (n = 6) and 33 °C: 19.5 ± 1.19 (n = 6). Q_{10}-values were calculated to be ~ 1.5 in all temperature ranges – except from 11 – 16 °C where it was ~ 5.5. This was concluded to be a range of relative temperature dependence (RRTD). The activation energy of the rate-limiting step in the metabolic pathway was calculated to be 50.8 kJ/mole O_2. At 22 °C, the metabolic rate increased with salinity from 0 – 4 ppt and decreased from 14 – 32 ppt. Survival rate was 100 % at 0 – 4 ppt, 50 % at 14.4 ppt perchlorates and 0 % at 16 – 32 ppt NaCl. Plotting the metabolic rate over time revealed a spike to 286 % of the previous metabolic rate over 18 minutes for one tardigrade and 180 % over 8 minutes for another during exposure to 14.4 ppt perchlorates. Both spikes occurred after 60 minutes of exposure, where metabolic rate had been declining exponentially. The metabolic rate during termination of anhydrobiosis was determined for two R. coronifer tuns that successfully regained activity and 8 tuns that did not survive the process. For all 10 tuns, the metabolic rate was found to go through three distinct zones: heightened metabolic rate (~ 20 – 25 for successful tuns) with one or more local peaks for less than one hour, followed by an exponential decrease as the tardigrades hydrated over the next several hours and finally a period of low metabolic rate (~ 5 for successful tuns) that continued for more than 24 hours after rehydration. The method allows precise determination of the oxygen consumption for individual tardigrades and can be repurposed for a wide range of experimental set-ups – opening up a rich field of inquiry into the metabolism and energetics of tardigrade biology.

Acknowledgements

This report was written as the conclusion of a Master's project in Molecular and Medical Biology at the Department of Science and Environment, Roskilde University and in collaboration with the Faculty of Science and Technology, Department of Bioscience: Microbiology Section at Aarhus University. I want to thank my supervisors Hans Ramløv and Kai Finster for their guidance both before and during the work of this project, as well as the opportunities they have presented me with to share the results and meet interesting people in the fields of astrobiology and tardigrade biology. I would also like to thank Niels Peter Revsbech and Lars Riis Damgaard for their advice on the theory behind the microsensors and Klaus Koren for his advice on the experimental design suggested in Perspectives. Thank you to Lars Borregaard Pedersen for invaluable help on the practical challenges faced in the laboratory – without which this thesis could not have been written. Also, thanks to the Mars-group including Ebbe Norskov Bak, Per Nørnberg, Svend Knak Jensen and Jan Thøgersen for interesting perspectives that kept the work engaging and exciting. To my office mates Ugo Marzocchi, Lara Jochum, Thomas Leonhardt Husted and Carina Cupit Bayley as well as Jesper Tataru Bjerg and Cedric Herring for helpful discussions and to everybody at the microbiology section for their good company. Finally, I want to thank Wibeke and Michael Haldrup for their feedback and support throughout the writing process.

Contents

Introduction

Conceptualization of the Thesis

This thesis is about tardigrades and the energetics behind the protective mechanisms that give the phylum its extraordinary tolerance toward stress-factors such as temperature, salinity and desiccation, as well as its ability to return to normal activity from the putatively ametabolic state of cryptobiosis. The extraordinary abilities of tardigrades have made them a topic of interest both with regards to the development of medical and industrial biotechnologies, ecological and astrobiological research and even our philosophical understanding of what life is. By contributing to a detailed understanding of tardigrade energetics under normal and stressful conditions, the hope is that energy-requirements for specific processes of interest and thus their underlying mechanisms may be identified through chemical and biochemical analysis. The energetics will be investigated by measuring the oxygen consumption of tardigrades using microsensors developed at Aarhus University. The method has been customized for this project to determine the metabolic rate of tardigrades. The research question of the thesis is as follows:

To determine the metabolic rate of tardigrades and how it depends on conditions such as temperature and salinity, as well as how it changes during termination of the putatively ametabolic state of cryptobiosis. From this to discover novel insights into how tardigrade metabolism and the extraordinary abilities it facilitates may function.

The next section in this introduction will be on the broader context of tardigrade research, followed by a section on general tardigrade biology and finally a section on the theory behind the microsensors. In Chapter 1, the metabolic rate of the two species *Richtersius coronifer* and *Macrobiotus macrocalix* will be determined in MiliQ water at 22 °C and the reliability of the method will be validated. Chapters 2 – 4 will deal only with the *R. coronifer* species. Chapter 2 will investigate the effects of temperature and Chapter 3 the effects of salinity on metabolic rate. In Chapter 4, the metabolic rate during termination of cryptobiosis will be described. Chapter 5 will describe issues with the experimental set-ups and how those issues were solved. Finally, the conclusion will provide an answer to the research question and suggestions for future studies will be made under perspectives.

1. Context

Tardigrades were first described in 1773 by the German pastor and zoologist Johann Goeze who referred to them as *Kleine Wasserbär* – or water bears. The Latin name 'Tardigrade' – meaning "that which wanders slowly" was suggested 3 years later by the Italian biologist and catholic priest Lazzaro Spallanzani (Westh, 1990; Wright, 2001). Since then, tardigrades have been a topic of much interest – primarily because of their ability to survive a wide range of stressful conditions by entering a state called cryptobiosis where they lose 97 % of their water content as well as all detectable metabolic activity. The tardigrades can remain in this state for decades (Jönsson and Bertolani, 2001) before returning to normal activity when conditions become favorable – e.g. from exposure to water after desiccation. The phenomena of cryptobiosis had already been described in 1702 by Antonie van Leuwenhoek after he invented the light microscope and observed that microscopic animals would emerge from seemingly lifeless soil samples when adding water to them. Leuwenhoek mistakenly concluded that the surface of these animals must be so compact that water could not evaporation through it, thus allowing the animals to remain hydrated in the dry soil when in actuality the animals turned out to be desiccated and cryptobiotic bdelloid rotifers (Westh, 1990; Wright, 2001). Today, the commonly accepted definition of cryptobiosis is the one coined by David Keilin in 1959:

> "*The state of an organism when it shows no visible signs of life and when its metabolic activity becomes hardly measurable or comes reversibly to a standstill*" (Keilin, 1959).

It has since been objected that for cryptobiosis to be a qualitatively different phenomenon from other examples of reduced metabolism, such as hibernation, it is of central importance that the metabolism is not merely reduced to a hardly measurable level, but indeed comes reversibly to a standstill (Hinton and Needham, 1968; Clegg, 2001). Crowe, (1975) instead defines it as a general term for any reversible *cessation* of metabolism and distinguishes between subtypes of cryptobiosis related both to different stimuli and different mechanisms. The notion of cryptobiosis as an ametabolic state between life and death has sparked several controversies. Considering the cryptobiotic organism dead would then give credence to ideas of resurrection and spontaneous generation, whereas considering it alive would imply that life is something divorceable from dynamic processes such as metabolism, growth or reproduction but rather exists in the physical structures as a potential for active life (Westh, 1990). Such philosophical implications are explored in detail in *The Oxford Handbook of Philosophy of Death* under the rubric of *the cryptobiosis argument* (Gilmore, 2012). Debates on this topic have included speculations on ideas such as life evolving

on land in isolated pools that underwent periodic drying (Hinton and Needham, 1968), as well as discredited ideas of panspermia (May, Maria and Guimard, 1964; Crowe, 1971) and spontaneous generation (Brack, 1998) and prompting accusations of blasphemy for reducing life to chemical and physical processes (Pouchet, 1869; Westh, 1990). Despite 300 years of research on cryptobiosis, the phenomena remains a mystery (Wright, 2001; Watanabe *et al.*, 2002; Guppy, 2004; Schill, Steinbrück and Köhler, 2004) – both with regards to the underlying biochemistry and the ecological and evolutionary implications (Jönsson and Bertolani, 2001). Cryptobiosis has been observed in many invertebrates, as well as in plants and bacteria. However, it is of special interest with regards to tardigrades where it must maintain relatively complex organ systems – anatomically closer to humans than those of other cryptobiotic organisms. In addition to cryptobiosis, research into tardigrades have revealed surprising extremophilic capacities – both in cryptobiosis and to a lesser extend when active. Table 1 shows some of those durability studies concerning temperature, radiation, pressure, salinity, harmful chemicals and space conditions – which included many stress factors such as radiation, freezing and vacuum.

Table 1: *Tolerance of different tardigrade species to temperature, radiation, pressure, salinity, harmful chemicals and space conditions – i.e. low earth orbit 258–304 km above sea level. The state of the tardigrades during exposure is specified as 'cryptobiosis', 'active' or 'both'. Sources: [1] (Rebecchi, Altiero and Guidetti, 2007); [2] (Hengherr* et al.*, 2009); [3] (Horikawa* et al.*, 2008); [4] (Ramløv and Westh, 2001); [5] (Ramløv and Westh, 1992); [6] (Altiero* et al.*, 2011); [7] (Horikawa* et al.*, 2006); [8] (Jönsson and Wojcik, 2017); [9] (Jönsson, Harms-Ringdahl and Torudd, 2005); [10] (Seki and Toyoshima, 1998); [11] (Ono* et al.*, 2016); [12] (Halberg* et al.*, 2009); [13] (Møbjerg* et al.*, 2011); [14]* (Dennis Persson *et al.*, 2011)*; [15] (Jönsson* et al.*, 2016); [16] (Rizzo* et al.*, 2015); [17] (Rebecchi* et al.*, 2011); [18] (Jönsson* et al.*, 2008).*

Species	Temperature	Radiation	Pressure	Salinity	Chemicals	Space
Richtersius coronifer	Cryptobiosis: 70 °C[4] Both: -196 °C[5]	Cryptobiosis: 2 kGy heavy ion- and 0.5 kGy X-ray radiation[8] Both: 3 kGy γ-radiation[9]		Active: 0 – 500 mOsm/kg[13]	Cryptobiosis: Ethanol, 1-butanol and 1-hexanol[4]	Cryptobiosis[14,18]
Ramazzottius varieornatus	Cryptobiosis: -196 °C – 90 °C[3]	Cryptobiosis: 4 kGy ^{4}He ions[3]			Cryptobiosis: 99.8 % acetonitrile[3]	
Milnesium Tardigradum	Cryptobiosis: 100 °C[2]	Cryptobiosis: 4.4 kGy γ- & 5.2 kGy Heavy ion radiation Active: 5 kGy γ- & 6.2 kGy Heavy ions[7]	Cryptobiosis: 7.5 GPa – regain motility; 20 GPa – regain metabolic activity[11]			Cryptobiosis[15,18]
Macrobiotus occidentalis			Cryptobiosis: 600 MPa Active: 100 MPa[10]			
Halobiotus crispae				Active: 0 – 2000 mOsm/kg[12]		
Paramacrobiotus richtersi	Both: 23.22 – 61.92 kJ/m^2 UV-B[6]					Cryptobiosis[16,17]
Ramazottius oberhaeuseri	Both: 23.22 – 61.92 kJ/m^2 UV-B[6]					Cryptobiosis[14-16]
Echiniscus testudo						Cryptobiosis[14,15]
Macrobiotus hufelandi	Cryptobiosis: 125 °C – If dried slowly[1]					

Different species have been used with different specific tolerances and low non-zero survival rates have been reported simply as 'survival' – leading to some conflation and overestimation of the abilities of "tardigrades" as such. However, the feats are nonetheless impressive and have been demonstrated to be relevant for biotechnological applications. One example of the potential applications of tardigrade research is the identification of genes that can be used for genetically modifying other organisms, including human cells, making them more tolerant to stress factors. For example, Hashimoto *et al.*, (2016) identified a tardigrade-unique gene encoding a protein they named 'damage suppressor' or Dsup. The protein was shown to associate with DNA and protect it from damage caused by oxidative stress. When transfected into human cells, it decreased the DNA-damage caused by X-ray radiation in those transgenic cells by approximately 40 % at 10 Gy – compared to unmodified cells. Additionally, transfected cells showed no change in proliferative activity after exposure to 4 Gy radiation, whereas unmodified cells lost all proliferative activity immediately. These effects were achieved by the transfection of only one tardigrade-unique gene into human cells, but the study identified more than 8000 other tardigrade-unique genes (Hashimoto *et al.*, 2016) that may serve as a reservoir for bioengineering studies.

Similarly, Boothby *et al.*, (2017) showed that yeast and bacterial cells transfected with genes coding for tardigrade cytosolic-abundant heat-soluble (CAHS) proteins increased their tolerance to desiccation 100-fold. The tardigrade CAHS proteins also preserved the function of lactate dehydrogenase (LDH) *in vitro*, allowing it to resume activity after rehydration. LDH activity normally falls to < 1 % after desiccation and rehydration. However, its activity post-rehydration increased as a function of the concentration of CAHS protein present during desiccation. This effect could be as high as 100 % of normal activity, given a sufficient CAHS protein concentration and achieves this more effectively than trehalose or BSA. Given the advent of the CRISPR/Cas9 technique, these types of studies will likely become increasingly relevant in years to come. Applications that have been suggested includes the stabilization and preservation of biological materials such as food, vaccines, pharmaceuticals, enzymes, lysosomes, blood, sperm and human organs under complete desiccation, freezing and high temperatures (Crowe, 1971; Rebecchi, Altiero and Guidetti, 2007; Møbjerg *et al.*, 2011), as well as the design of desiccation resistant crops (Boothby *et al.*, 2017), cryosurgery and suspended animation (Crowe, 1971). Furthermore, the fact that tardigrades are able to survive space conditions may suggest that such technologies could have applications for future space projects – perhaps even for genetically augmented astronauts if the ethical rulings shift.

Tardigrades and cryptobiotic organisms in general have been suggested as interesting model organisms for astrobiology as far back as 1964 (May, Maria and Guimard, 1964; Crowe and Clegg, 1973; Weronika and Kaczmarek, 2016). Studies like those seen in Table 1 where tardigrades were sent into space have included collaborations with three different space missions: The *Foton-M3* mission included the projects *TARSE*, *TARDIS* & *RoTaRad* (Jönsson *et al.*, 2008; D Persson *et al.*, 2011; Rebecchi *et al.*, 2011) and the *Endeavour* mission included the project *TARDIKISS* (Rizzo *et al.*, 2015). *The Phobos Life Project*, which unfortunately failed due to the spacecraft crashing, included selected species from all three domains of life – including three species of tardigrades (The Planetary Society, 2011; Weronika and Kaczmarek, 2016). These recent studies showing that tardigrades can survive exposure to low-earth orbit, along with the multiple Mars- and lunar missions currently being discussed, have led to renewed interest in this field (Jönsson, 2007; Horikawa *et al.*, 2008; Guidetti *et al.*, 2012; Weronika and Kaczmarek, 2016; Jönsson and Wojcik, 2017; Vasanthan *et al.*, 2017). Most astrobiological model organisms are unicellular. Tardigrades should be considered complementary to those, since they have lesser tolerance when compared, but the mechanisms protecting them are maintaining complicated organ-systems. The more complex structure of the organism also means it becomes relevant for a different category of questions regarding biomarkers and the origin of life elsewhere in the universe. Tardigrades and their metabolism are also important for ecology, where they may act as pioneer organisms of new environments (Nelson, 2002; Brown *et al.*, 2004; Nichols, 2005). This would be relevant both with regards to ecosystems here on earth and ultimately for astrobiology – if humans decide to terraform Mars.

To quote Brown *et al.*, (2004) in the paper *Toward a Metabolic Theory of Ecology*:

> "*Metabolism provides a basis for using first principles of physics, chemistry, and biology to link the biology of individual organisms to the ecology of populations, communities, and ecosystems. Metabolic rate, the rate at which organisms take up, transform, and expend energy and materials, is the most fundamental biological rate. […] metabolic rate, by setting the rates of resource uptake from the environment and resource allocation to survival, growth, and reproduction, controls ecological processes at all levels of organization from individuals to the biosphere.*"

2. The Tardigrade

2.1. Evolution and systematics

Tardigrades are small invertebrates of the animal kingdom and are thought to date back to the Cambrian period based on Orsten-type fossils that are approximately 520 million years old (Budd, 2001; Maas and Waloszek, 2001). Popularly, this has been used to argue that they are the only animals that have survived all 5 major extinction events in the history of the planet (Pope, 2014). This has been met with some critique, as the fossils from this period are not like any tardigrade species currently known to be alive – although they share many important characteristics. The oldest known fossils of tardigrades in the form they have today are preserved in amber and are approximately 90 million years old (Cooper, 1964). If these fossils are considered the earliest known tardigrades, then tardigrades can only be said to have survived one major extinction event – not all. Both fossils can be seen on figure 1.

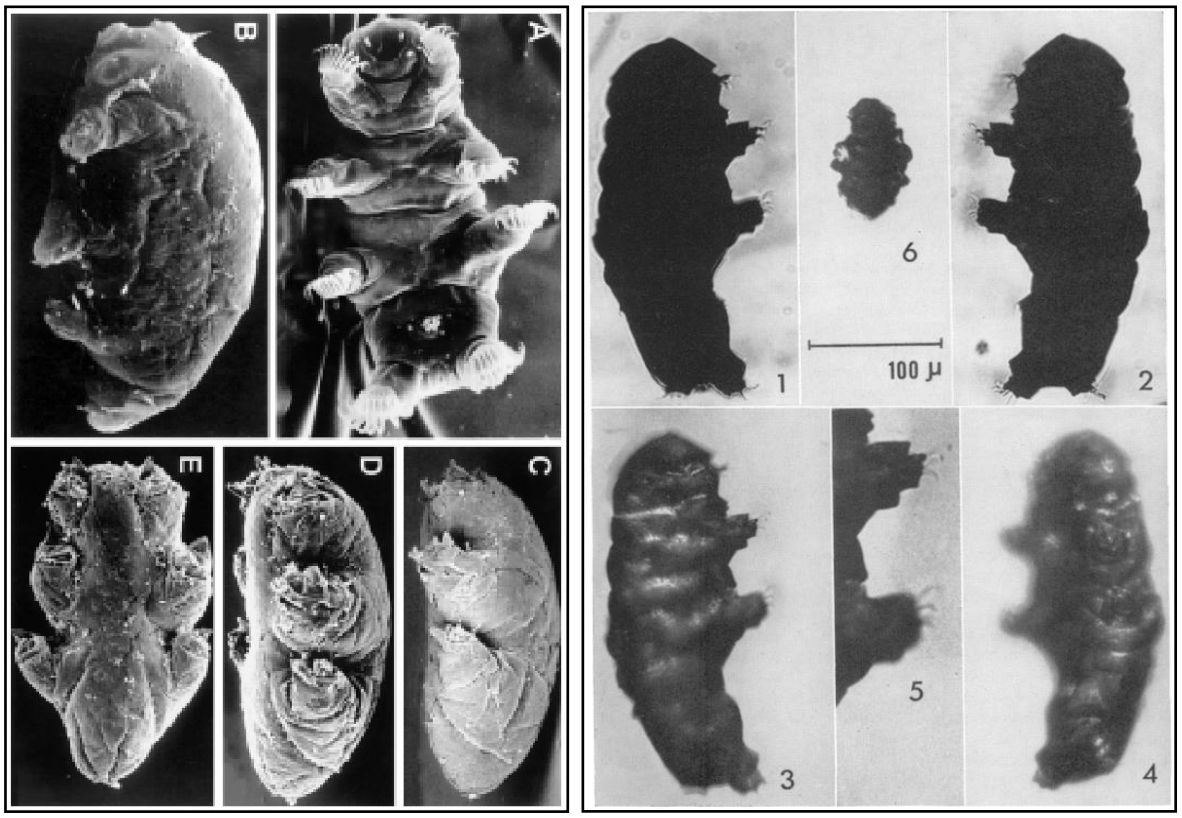

Figure 1: *Orsten-type fossils from approximately 530 million years ago (Left) (Maas and Waloszek, 2001) and amber preserved fossils from approximately 90 million years ago (Right) (Cooper, 1964).*

The question of how many extinction events tardigrades have survived remains debatable, but another popular description of tardigrades has been introduced and thoroughly rebutted in the last 3 years. Boothby *et al.*, (2015) reported to have found 17.5 % foreign DNA from bacteria, fungi, plants and Archaea in the genome of *Hypsibius dujardini* and concluded that this must be due to unprecedented levels of

horizontal gene transfer (HGT) in eukaryotes. They also speculated that this might explain how cryptobiosis evolved in tardigrades. However, subsequent studies have shown that HGT is at most responsible for 2 % of the *Hypsibius dujardini* genome and the results of Boothby *et al.*, (2015) are most likely due to undetected contamination of the samples (Arakawa, 2016; Bemm *et al.*, 2016; Hashimoto *et al.*, 2016; Koutsovoulos *et al.*, 2016; Tenlen *et al.*, 2016; Yoshida *et al.*, 2017). Despite this, the HGT misconception persists and has made its way to popular science (Osunsanmi, 2017).

Tardigrades belong to the Phylum Tardigrada, which contains more than 1000 different known species and can be further divided into subcategories of Hetero-, Eu- and Mesotardigrada. The last category contains only one known species and is not well documented (Romano, 2003; Møbjerg *et al.*, 2011). Because of this, most research has been focused on the two former groups. Heterotardigrades have plated cuticles that increase durability against mechanical stress, whereas Eutardigrades have smooth cuticles that give them a more elastic body type and a translucent appearance. Eutardigrades are also more likely to be sexually dimorphic – although some species of both classes are sexually monomorphic and reproduce through parthenogenesis. Most Heterotardigrades are adapted to limno-terrestrial or marine habitats, whereas Eutardigrades are adapted to limno-terrestrial or freshwater habitats (Romano, 2003; Weronika and Kaczmarek, 2016). The classification is primarily based on the morphological and anatomical difference. For Heterotardigrades, the main characteristics being considered are cephalic appendages, cuticular extensions, claws and patterns of the dorsal cuticular plates. For Eutardigrades, it is the claws, buccopharyngeal apparatus and structure of the cuticle (Romano, 2003). Both species used in this study, *R. coronifer* and *M. macrocalix*, are Eutardigrades. Examples of Hetero- and Eutardigrades from Wełnicz *et al.*, (2011) and Guidetti *et al.*, (2012) can be seen on figure 2.

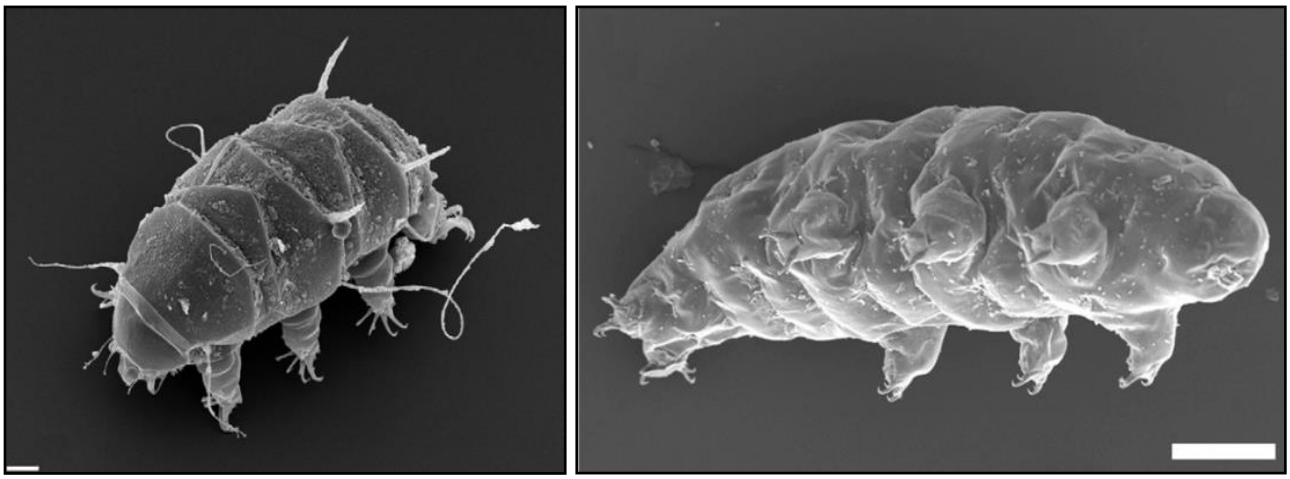

Figure 2: *SEM images of the Heterotardigrade Echiniscus granulatus – scale bar 20 µm (Left) (Wełnicz* et al.*, 2011) and the Eutardigrade R. coronifer – scale bar 50 µm (Guidetti* et al.*, 2012).*

The Phylum Tardigrada belongs to the superphylum Ecdysozoa – derived from the word Ecdysis, which is the process of cuticle moulting. The superphylum is thought to have branched into several Phyla approximately 530 million years ago during the Cambrian period or possibly even earlier (Budd, 2001; Maas and Waloszek, 2001). Despite significant morphological differences, the closest related Phylum is thought to be Arthropoda (Sands *et al.*, 2008). The two Phyla are considered together under the rubric Tactopoda and with Onychophora as Panarthropoda. Other Phyla of the Ecdysozoa superphylum include, Loricifera, Nematomorpha, Nematoda, Kinorhyncha and Priapulida (Budd, 2001). The systematics remain subject to revision and debate on whether morphological or molecular methodologies should be prioritized (Budd, 2001; Maas and Waloszek, 2001; Nelson, 2002; Romano, 2003; Sands *et al.*, 2008). Figure 3 shows one cladogram of the Ecdysozoa superphylum (Edgecombe *et al.*, 2011).

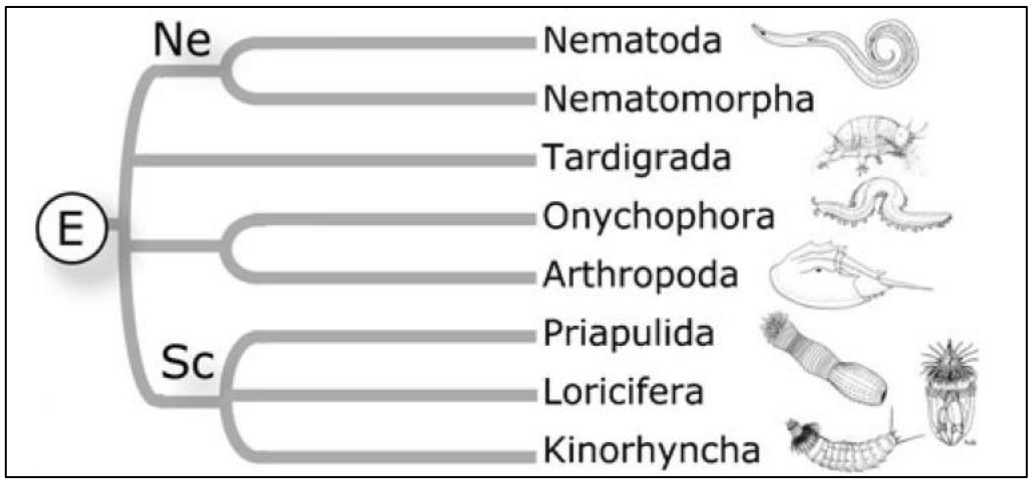

Figure 3: *Cladogram of the Ecdysozoa Superphylum branching off 525 million years ago. 'E' symbolizes Ecdysozoa, 'Ne' symbolizes Nematozoa and 'Sc' symbolizes Scalidophora (Edgecombe* et al.*, 2011).*

One reason for the evolution of the tardigrades extreme tolerance to stress and ability to enter cryptobiosis may be the inhabitation of a specific ecological niche. Because of these abilities, they can be found in environments that are relatively low in predators and competition for resources (Nelson, 2002). This allows for the expansion of their population sizes, which would otherwise be suppressed by predators and competitors (Hyvönen and Persson, 1996).

2.2. Morphology and physiology.

As mentioned, tardigrades are small invertebrates – meaning they do not have a spine. The body is defined by a cuticula that undergoes periodic moulting. The tardigrade cuticula has 4 layers, unlike most other Ecdysozoa – whose cuticula's only has 3 layers (Barnes, 1982). An average lifespan is approximately 3 – 30 months (Nelson, 2002), during which the tardigrade will undergo somewhere between 2 – 7 moultings. Sexual maturity is reached after the first 2 – 3 moultings (Weronika and Kaczmarek, 2016). In the case of sexually dimorphic tardigrades, fertilization can occur either internally – by deposit of sperm in the ovary or body cavity of the females or externally – by deposit in the cuticle, which is then shed by the female along with the unfertilized eggs. Apart from the cuticle, the eggs are protected by an additional layer of chorion. For many species, this layer is ornamented with spikes to deter other animals. Depending on species, tardigrades may eat some combination of bacteria, algae, fungal cells and small invertebrates – such as rotifers, nematodes and even other tardigrades (Weronika and Kaczmarek, 2016). Depending on species, the size can vary from 50 to 1500 μm in length although most species are within 300 to 600 μm. The tardigrade body can be segmented into 5 areas. One is the cephalic area – or head of the tardigrade. It includes a set of buccal stylets used to puncture food particles and the sensory organs – namely the papillae, eyes and chemoreceptors. The remaining 4 areas each end in a pair of unsegmented legs with tardigrade claws (Weronika and Kaczmarek, 2016). The largest internal structure is the digestive system, which can be divided into 3 areas: Foregut, midgut and hindgut. The foregut consists of the mouth, buccal tube, stylet, salivary glands, myoepithelial pharynx and esophagus. The midgut consists primarily of the stomach, but also the Malpighian tubule, which is where urine is produced. The Malpighian tubule is also important for secretion, excretion and osmoregulation. Finally, The hindgut consists of the rectum where reabsorption of water occurs and the cloaca where waste products are excreted (Dewel and Nelson, 1993; Halberg and Møbjerg, 2012).

The muscular system is made up of muscle bands that work off and are connected to the body wall. To achieve stability, the body wall maintains a hydrostatic pressure. It is reinforced with an extra thick exocuticle layer where the muscle bands are connected (Dewel and Nelson, 1993; Hickman *et al.*, 2008). In addition to the body wall, muscle bands also connect to the pharyngeal and stylet in the cephalic area to allow for coordination. This muscular structure consists of transverse muscles along with ventral, dorsal and lateral longitudinal fibers (Marchioro *et al.*, 2013). The intestinal movements are regulated by small visceral muscles (Dewel and Nelson, 1993). The nervous system includes a brain made up of nerve bundles

in the shape of a ring around the mouth area. An abdominal chain with 4 segmented ganglia spans the length of the tardigrade. Each ganglion is located near one of the 4 pairs of legs (Kinchin, 1994; Weronika and Kaczmarek, 2016). A schematic drawing of the tardigrades internal structures from Hickman *et al.*, (2008) can be seen on figure 4.

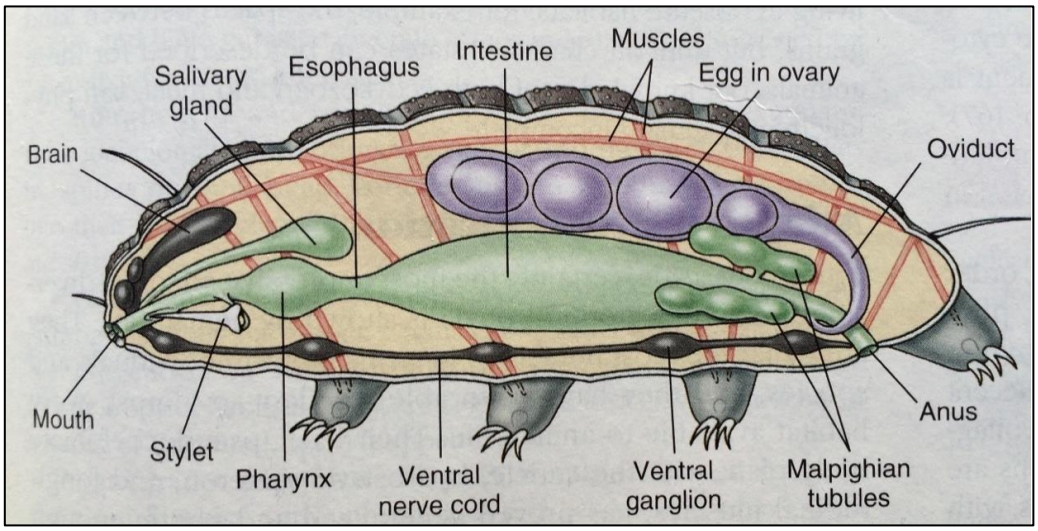

Figure 4: *The internal structures of the tardigrade. Purple represents the reproductive system, green is the digestive system, red is the muscular system and black is the nervous system (Hickman et al., 2008).*

The internal organization of reproductive, digestive, muscular and nervous systems is quite complex – relative to the small size of the tardigrades. They do however not have any respiratory or circulatory systems. Oxygen is absorbed by gas exchange across the cuticula and then pumped through the hemolymph by body movements (Miller, 1997).

Despite being able survive desiccation, all tardigrades are aquatic and must be surrounded by a film of water to maintain activity (Nelson, 2002). Although their most notable resistance to stress is in the cryptobiotic state, they have also developed strategies for coping with certain stress factors while maintaining activity. This is achieved by the process of cyclomorphosis (Halberg *et al.*, 2013), where the morphology and physiology of the tardigrade is altered in response to the environment. One example of this is supercooling. The tardigrade lowers its body temperature to – 20 °C while avoiding intracellular ice formation by excluding the presence of nucleating agents. This allows the tardigrade to remain active at sub-zero temperatures. Another example is the response to fluctuations in salinity. The internal osmolality of *R. coronifer* hemolymph in demineralized water is 168 mOsm/kg – similar to the osmotic concentrations in its natural habitats. Tardigrades employ a combination of osmoregulation and osmoconforming – meaning the body osmolality increases with the osmolality of the external

environment but is regulated so that the difference remains stable. In an external salinity of 200 mOsm/kg, the internal osmolality of *R. coronifer* is 350 mOsm/kg. This ability allows the species survive salinities up to 500 mOsm/kg. Other species may survive osmolalities as high as 2000 mOsm/kg (Møbjerg *et al.*, 2011). For NaCl solutions, 500 mOsm/kg is approximately 14 ppt and 2000 mOsm/kg approximately 56 ppt (Lenntech, 2018). The morphological consequence of such adjustments is a reversible change in body volume. In hypotonic solutions, the tardigrade may swell up to 160 % of its normal body volume. Conversely, it will shrink in hypertonic solutions (Halberg *et al.*, 2009; Møbjerg *et al.*, 2011).

2.3. Cryptobiosis and metabolism

Tardigrades contain large storage cells that serve as energy depots and supply the metabolism in the absence of food. Czernekova and Jönsson, (2016) found that these storage cells are consumed during repeated cycles of anhydrobiosis – the type of cryptobiosis that occurs in response to desiccation. Cryptobiosis is generally divided into anhydrobiosis, osmobiosis, cryobiosis, anoxybiosis and encystment (Crowe, 1975) – although a sixth type known as chemobiosis is sometimes referred to (Møbjerg *et al.*, 2011). These subtypes are defined from the type of stimuli they act as a response to. Anhydrobiosis is induced by desiccation, cryobiosis by freezing, osmobiosis by osmotic stress, anoxybiosis from a lack of oxygen and chemobiosis from environmental toxins. It is less clear what induces encystment, although starvation may play some role (Crowe, 1975; Møbjerg *et al.*, 2011). The most extensively researched type is anhydrobiosis followed by cryobiosis. Figure 5 shows an illustration of these subtypes.

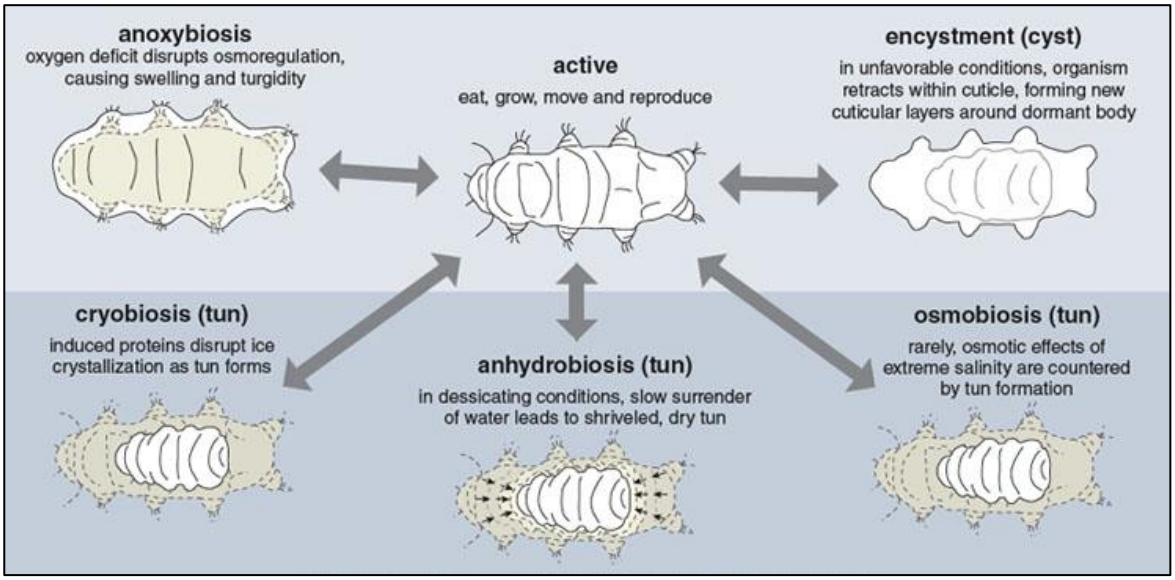

Figure 5: *Modified illustration of the different types of cryptobiosis (Randy and Miller, 2011).*

There has been some debate on whether they function by different mechanisms or not. Anoxybiosis is thought to involve an oxygen deficit disrupting the osmoregulation and leading to turgidity from water influx, whereas encystment involves the formation of an additional cuticle (Randy and Miller, 2011). Both of these appear distinct from the remaining types. However, anhydrobiosis, osmobiosis and cryobiosis all seem to involve the evacuation of 97 % of the tardigrades water content leading to tun formation. This requires muscular contractions and packing of organelles and internal organs, which leads to approximately a 3-fold decrease in size. It also requires the upregulation of bioprotectants that stabilize cellular structures and leads to vitrification of the tun (Crowe, Carpenter and Crowe, 1998). Several bioprotectants have been implicated in these processes, including trehalose, tardigrade intrinsically disordered proteins (TDPs), cytosolic-, secreted- and mitochondrial abundant heat soluble (CAHS/SAHS/MAHS) proteins, late-embryogenesis-abundant (LEA) proteins and heat-shock proteins (HSPs). Trehalose is thought to work by replacing the hydrogen bonds of the lost water. TDPs and CAHS/SAHS/MAHS proteins are able to envelope other proteins due to their intrinsic disorder and then vitrify during desiccation, thus maintaining the structure of those proteins. LEA proteins are thought to contribute primarily to the protection of membranes, while HSPs function as molecular chaperones (Wright, Westh and Ramløv, 1992; Clegg, 2001; Tanaka *et al.*, 2015; Boothby *et al.*, 2017). Hashimoto *et al.*, (2016) found that tardigrades of the species *Ramazzottius varieornatus* also have significantly expanded gene families of superoxide dismutase (SOD) compared to other metazoans. SODs are enzymes that detoxify superoxide radicals – a type of reactive oxygen species (ROS), which may protect tardigrades from oxidative stress induced by desiccation. They also found that the peroxisomal pathway of the metabolism had been eliminated, thus avoiding the production hydrogen peroxide from β-oxidation during fatty acid catabolism.

Biochemical processes such as metabolism tend to occur faster at higher temperatures. The rate of this change can be understood in terms of the temperature coefficient Q_{10} – defined by the following equation:

(1) $$Q_{10} = \left(\frac{R_2}{R_1}\right)^{\frac{10\,^{\circ}\mathrm{C}}{(T_2 - T_1)}}$$

Where R_1 and R_2 are the reaction rates of the process at two different temperatures and T_1 and T_2 are those temperatures in Celsius or Kelvin. Q_{10} is the factor by which the rate of a given process increases between two temperatures per hypothetical 10 °C increase in that temperature range. It is generally expected to increase exponentially with temperature and metabolism is typically considered stable when $Q_{10} \sim 2$ to 3

(Reyes, Pendergast and Yamazaki, 2008). Another way that metabolic rate relates to temperature is described by the Arrhenius equation:

$$k = Ae^{-\frac{E_a}{(RT)}} \tag{2}$$

Where k is the rate constant of the reaction, A is the pre-exponential factor, E_a is the activation energy, R is the universal gas-constant and T is the absolute temperature in Kelvin. Taking the natural logarithm of this equation and rearranging yields the following equation describing the straight line of an Arrhenius-plot:

$$\ln(k) = -\frac{E_a}{R} \cdot \frac{1}{T} + \ln(A) \tag{3}$$

Since the slope of the Arrhenius plot is $-\frac{E_a}{R}$ °K and $R = 8.3144598\ \frac{\text{J}}{\text{°K} \cdot \text{mole}}$, the activation energy of the reaction can be calculated by multiplying the slope of this curve with $-8.3144598\ \frac{\text{J}}{\text{°K} \cdot \text{mole}}$. The activation energy is the energy necessary to break the chemical bonds of reactants and form the bonds of the products in a reaction during collision. When calculated from the metabolic rate, it is the activation energy of the rate-limiting step in the metabolic pathway.

3. Microsensor Technology

Oxygen microsensors were first developed by Clark *et al.*, (1953) and have gone through several design-modifications since then (N. P. Revsbech, 1989; Oldham, 1994; Severinghaus, 2002). The sensors used in this study were designed by Revsbech, (1989) and manufactured by Unisense. A schematic drawing of the sensor tip and defined segments with corresponding oxygen-concentrations can be seen on figure 6.

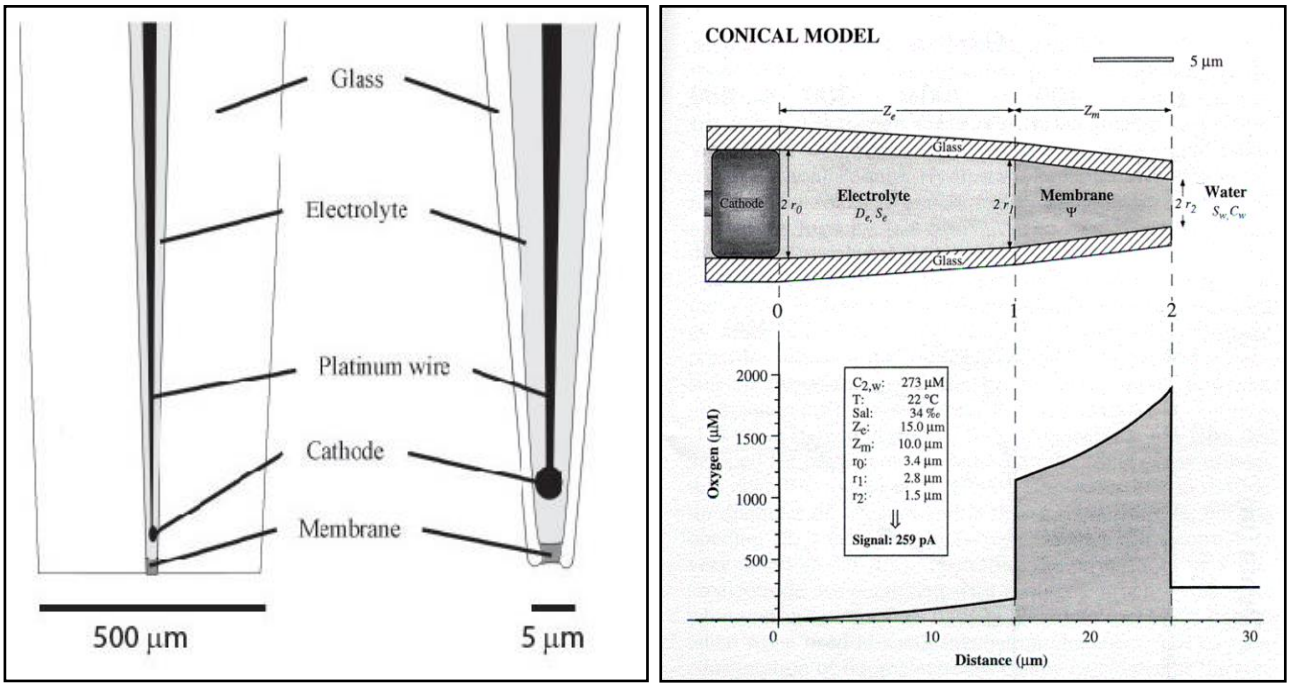

Figure 6: *(Left) Schematic drawing of oxygen-sensor tip with glass, electrolyte, platinum wire, cathode and membrane (http://www.unisense.com/O2/). (Right) A schematic drawing of the conical model for an oxygen-sensor tip with defined lengths and O_2-concentrations at the various segments. Copied from Gundersen, Ramsing and Glud, (1998).*

The sensor is composed of an Ag/AgCl cathode surrounded by electrolyte and encased by glass of varying thickness. The tip is covered by a silicone membrane – leaving some distance between the silver cathode and itself to only electrolyte. When immersed in water, oxygen will be distributed as seen to the right on figure 6. The concentration at the outward end of the membrane is equal to the concentration in the water itself and slightly less at the inner end of the membrane. Because oxygen solubility is significantly lower in electrolyte than in silicone, the concentration drops significantly between the two phases. The concentration continues to decrease toward the cathode – where it is effectively zero (Gundersen, Ramsing and Glud, 1998). The oxygen flux through the membrane can be expressed by the following equation:

(4) $$F_m = \Psi \frac{\Delta p_m}{Z_m}$$

Where F_m is the O_2-flux through the membrane, Ψ is the membrane transport coefficient – or permeability, Δp_m is the change in partial pressure of O_2 over the membrane and Z_m is the thickness of the membrane (Gundersen, Ramsing and Glud, 1998). Partial pressure is equal to concentration divided by solubility. Since the partial pressure is the same throughout the interface between membrane and liquid, the equation can be rewritten:

$$F_m = \Psi\left(\frac{C_{2,w}}{S_w} - \frac{C_{1,e}}{S_e}\right)\frac{1}{Z_m} \quad (5)$$

The oxygen flux through the electrolyte can be expressed by the following equation:

$$F_e = D_e \frac{C_{1,e}}{Z_e} \quad (6)$$

Where F_e is the O_2 flux through the electrolyte, D_e is the diffusion coefficient, $C_{1,e}$ is the oxygen concentration change in the electrolyte and Z_e is the distance of diffusion through electrolyte. The oxygen flux through the membrane and electrolyte must be the same, due to conservation of mass. According to Gundersen, Ramsing and Glud, (1998), $C_{1,e}$ can be isolated from the two previous equations, leading to the following expression of O_2-flux through the electrolyte:

$$F_e = p_{2,w}\left(\frac{Z_m}{\Psi} + \frac{Z_e}{D_e S_e}\right)^{-1} \quad (7)$$

The oxygen signal of the sensor can then be expressed by the following equation:

$$I = \varphi \pi r^2 F_e = \varphi \pi r^2 p_{2,w}\left(\frac{Z_m}{\Psi} + \frac{Z_e}{D_e S_e}\right)^{-1} \quad (8)$$

Where I is the signal, defined as output minus zero-current, φ is the current generated per mole oxygen reduced, πr^2 is the area the flux is passing and $p_{2,w}$ is the partial pressure of oxygen from water to membrane. The current generated per mole oxygen can be calculated as number of electrons reduced per oxygen molecule times the elementary charge per electron, times Avogadro's number (molecules oxygen per mole):

$$\varphi = (4\ electron\ molecule^{-1})(1.602189 \cdot 10^{-19} A\ electron^{-1})(6.023 \cdot 10^{23}\ molecule\ M^{-1})$$
$$= 3.86 \cdot 10^5\ A\ M^{-1}.$$

The model for calculation of signal seen on equation 8 is of an idealized cylindrical sensor. However, as seen on figure 6, the sensors used in this study are not perfectly cylindrical but rather conical. A slightly

different model can be made to describe the signal of conical sensors (Gundersen, Ramsing and Glud, 1998):

(9) $$I = \varphi\pi r_1 p_{2,w}\left(\frac{Z_m}{r_2\Psi} + \frac{Z_e}{r_0 D_e S_e}\right)^{-1}$$

This takes into account the changing area of diffusion for oxygen through the sensor. For a cylindrical sensor, the radius would be the same throughout the sensor – i.e. $r_0 = r_1 = r_2$ meaning equation 9 would be identical to equation 8. Since partial pressure is equal to concentration divided by solubility, this equation can be rewritten to describe the concentration of oxygen outside the sensor (Gundersen, Ramsing and Glud, 1998):

(10) $$C = I \cdot S_w\left(\frac{Z_m}{r_2\Psi} + \frac{Z_e}{r_0 D_e S_e}\right)(\varphi\pi r_1)^{-1}$$

In Gundersen, Ramsing and Glud, (1998), 23 O_2-sensors had their exact physical dimensions measured under a microscope. Experimental data was gathered and compared to the theoretical signals calculated from both models and the conical model (equation 9) clearly predicted the signal better. As mentioned, the signal (I) is the current generated in the water minus the zero-current – i.e. the current generated in oxygen free water. The zero-current is determined by calibrating in ascorbate before measurements. Typically, the zero-current is between 0 – 2 % of the current generated in atmosphere at room temperature but can be higher – either due to conductivity of or reducible constituents in the glass. This effect is exasperated at higher temperatures and calibration should therefore always be at the same temperature as measurements (Gundersen, Ramsing and Glud, 1998).

The signal is sensitive to changes in both temperature and salinity. When salinity changes, the only parameter of equation 9 that changes is the partial pressure of oxygen in water ($p_{2,w}$). Therefore, the signal increase is directly proportional to the salinity increase. When temperature increases, both the partial pressure and the transport coefficients of oxygen (D and Ψ) change, but the solubility of oxygen in electrolyte decreases (S_e). Gundersen, Ramsing and Glud, (1998) modelled the signal response to these changes and found that the signal increases ~ 4 % per °C increase at 20 °C and ~ 3 % at 0 °C. This increase is higher per °C for sensors with high relative thickness of membrane compared to the electrolyte phase ($Z_m/Z_e + Z_m$).

Because the signal relies on the partial pressure of oxygen through the membrane, turbulence in the water might affect the signal so that it does not accurately represent the passive diffusion through the membrane

at the given concentration. This effect can be minimized by increasing the diffusion path through the sensor ($Z_m + Z_e$) relative to the opening radius (r_2). A longer diffusion path also means a longer response time of the sensor, so this solution involves a trade-off between reducing sensitivity to turbulence and maintaining a short response-time. However, sensors can be constructed to have negligible sensitivity to turbulence (< 1 %) and a short enough response time for most applications (90 % of < 1 s) (N. P. Revsbech, 1989). Most sensors will decrease in signal over time due to decreasing permeability of the membrane. This could either be due to hardening of the silicone or precipitation of salt from the electrolyte (Gundersen, Ramsing and Glud, 1998). This issue can be avoided simply by not using old sensors with very low signals. A final concern may be that the oxygen consumption of the cathode itself will reduce the concentration outside the sensor. The small size of the cathode typically means that the amount of oxygen reduced is effectively zero compared to the environment, but it may become an issue when measuring in small incubation chambers – such as the ones used in this study (Gundersen, Ramsing and Glud, 1998).

This issue should be negated by the fact that the chambers of this study are an open system together with a much larger water bath containing the same solution as the chamber. Any reduction of the oxygen concentration in the chambers should be replaced by oxygen from the water bath. Furthermore, the sensor is never measuring the same space in the chamber for more than 10 s at a time, so the concern is negligible with regards to affecting the oxygen gradient. Even if this was not the case, the effect remains minimal. The average volume of capillary chambers is $8.6 \cdot 10^{-7}\ L$ – calculated from the average dimensions of 2.5x0.66 mm seen in appendix I. The typical sensor signal is ~ 79 pA leading to an oxygen consumption $1.7 \cdot 10^{-8} \frac{mmol}{day}$ (Gundersen, Ramsing and Glud, 1998). From this, the potential effect on oxygen concentrations by reduction under all conditions in this study were calculated. The consumption rate of the sensors ranges from 0.19 – 0.37 % of the total amount per hour. Depending on the conditions, it would take between 11.3 and 21.8 days for all the oxygen of a chamber to be depleted – without the oxygen supply from the surrounding water bath. The majority of experiments were done in the span of 1 – 3 hours, where oxygen consumption by the sensor is 0.2 – 1 % of the oxygen in the chamber. Some studies were done over 24 hours, where as much as 9 % of the oxygen in a chamber would have been reduced by the cathode – if not for the water baths.

The sensors described in this section have been used for a variety of applications. From measuring cerebral activity (Offenhauser *et al.*, 2005; Thompson, Peterson and Freeman, 2005; Caesar, Offenhauser and

Lauritzen, 2008; Lecoq *et al.*, 2009) and even single neurons (Mayhew, 2003; Thompson, Peterson and Freeman, 2003) to characterizing the oxygen consumption of microbial mats (Epping, Khalili and Thar, 1999). The application in this study is most reminiscent of their use in studies of the oxygen flux toward biofilms and through sediments by measuring oxygen micro-gradients (Niels Peter Revsbech, 1989; Nøhr Glud *et al.*, 1995; Gundersen and Jørgensen, 2012) and the determination of the respiration rate of subitaneous copepod eggs (Nielsen *et al.*, 2007). Similarly, the respiration rate of a tardigrade at the bottom of a capillary chamber can be determined – using Fick's first law of diffusion:

(11) $$J = -D \cdot \frac{d\varphi}{dx}$$

Where J is the oxygen flux through the chamber (nmol $O_2 \cdot cm^{-2} \cdot s^{-1}$), D is the diffusion coefficient of oxygen at the given conditions ($cm^2 \cdot s^{-1}$) and $\frac{d\varphi}{dx}$ is the change in oxygen concentration per distance through the chamber ($\mu M\ O_2 \cdot \mu m^{-1}$). If temperature and salinity of the solution is known, then D can be determined using the Unisense Seawater and Gases Tables seen in appendix II. By measuring an oxygen profile through the chamber, the expression $\frac{d\varphi}{dx}$ can be determined as the slope of the micro gradient in $\mu M\ O_2 \cdot \mu m^{-1}$. This can then be converted to nmol $O_2 \cdot cm^{-4}$ by multiplying with $10^4 \frac{\text{nmol } O_2 \cdot \text{cm}^{-4}}{\mu M\ O_2 \cdot \mu m^{-1}}$, since 1 μM = 1 nmol $\cdot$ cm^{-3} and 1 μm = 10^4 cm. Thus converted, the oxygen flux can be calculated from equation 11. Assuming the chamber is cylindrical along the diffusion distance measured, the diffusion area will be circular and can be calculated from the radius. The radius of each chamber used in this study can be seen in appendix I. The respiration rate (nmol $O_2 \cdot s^{-1}$) can be calculated by multiplying the oxygen flux with the diffusion area (cm^2):

(12) $$R = J \cdot A = J \cdot \pi r^2$$

In this study, the respiration rate is given as nmol $O_2 \cdot hour^{-1}$. The metabolic rate is defined as respiration rate divided by either weight (mg) or surface area (mm^2):

(13) $$MR_w = \frac{R}{w}; \qquad MR_A = \frac{R}{A}$$

Typically, the metabolic rate is calculated based on weight. Because oxygen is absorbed by diffusion across the surface area of the tardigrade, scaling may play a role in its consumption. This is evaluated in chapter 1 by comparing MR_w and MR_A. A cylindrical shape and a density of 1.04 g/mL can be assumed for the

tardigrades (Hallas and W, 1972; Jennings, 1975). Thus, their weight and surface area can be calculated from their length and width, using the following equations:

(14) $$V = \pi \left(\frac{w}{2}\right)^2 L$$

(15) $$W = V \cdot \rho = \pi(\frac{w}{2})^2 L \cdot \rho$$

(16) $$A = 2\pi \left(\frac{w}{2}\right) L + 2\pi(\frac{w}{2})^2$$

Where V is volume, w is width, L is length, W is weight, p is density and A is surface area. How this theory was applied practically will be elaborated on in Chapter 1 under Materials and Methods.

Chapter 1: Respiration and Metabolism

1. Materials and Methods

1.1. Tardigrades

Mosses containing a single population of the tardigrades were collected from a limestone fence in Öland, Sweden on July 9th, 2016 and kept dry in coffee filters under dry conditions at room temperature until use. The moss primarily contained tardigrades of the species *R. coronifer*, but also some of the species *M. macrocalix* and a few specimens of *M. tardigradum*. The species could be clearly distinguished from their size and appearance under a stereo microscope, during the extraction phase. To extract tardigrades, moss was ground through a parsley cutter into the upper fraction of a sieve system with decreasing pore size. The moss in the upper fraction was then flushed with demineralized water to facilitate the descend of the tardigrades through the pores and to remove possible particles from their bodies. The highest density of tardigrades was typically found in the second-lowest fraction (Fraction 120), so the material in this fraction was transferred to a petri-dish containing tap water.

28 live specimens of *R. coronifer* and 19 specimens of *M. macrocalix* species were hydrated and left in regular tap water with access to moss overnight (hereafter *ON*). Afterwards, they were transferred to and incubated in tap water without access to moss ON, before being placed in the capillary chambers. This procedure was followed to select only tardigrades that had not been damaged by the exit from cryptobiosis and to measure tardigrades with approximately the same gut content. As a control experiment, the respiration of 10 dead *R. coronifers* was also measured. These tardigrades were collected from the surface of the water and confirmed dead based on the lack of any movement under stereo-loop 24 hours before being measured. Transfer of tardigrades to chambers was done using customized Irwin Loops. All measurements in this section were done using MiliQ water that had been passed through a Q-Max PES 0.22 μm mesh. This was done both to minimize contamination and to reduce the risk of unknown substrates in the medium affecting the metabolism of the tardigrade.

1.2. Chambers

The capillary chambers used for measurements were constructed by heating 5 mm glass pipes under a Bunsen burner and pulling the glass apart to achieve an elongated segment at the centre of the pipe with a diameter of approximately 660 μm. This segment was then cut from the larger pipe with a glass cutter and further cut into fragments of approximately 2.5 mm in length. The fragments were then sealed in one end by raising them into a horizontal Bunsen burner flame using a pincer, until the glass at that end collapsed. The resulting capillary chambers were characterised under a microscope, and chambers of appropriate dimensions were transferred to a microtiter well and labelled according to the well. An example of the characterisation of the chamber labelled a1 can be seen on figure 7.

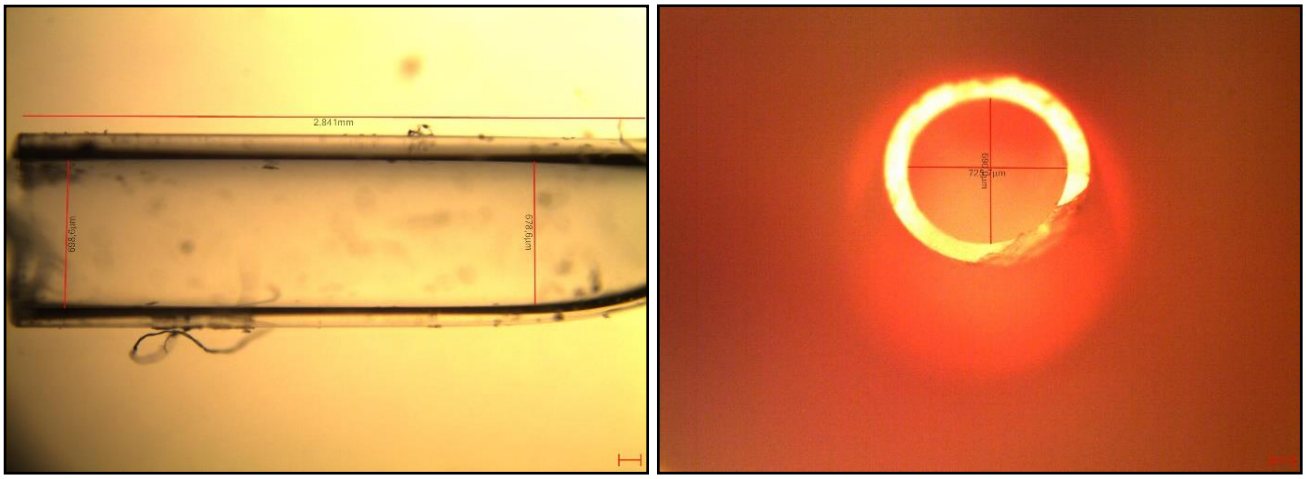

Figure 7: *Chamber a1 from the side (Left) and above (Right). Its dimensions correspond roughly to the desired, its sides are parallel, and the opening is not cracked. The diameter of the chamber was determined from the image on the right. Scale bars = 100 µm.*

Similar characterization of all chambers used can be seen in appendix I. The radius used in the Fick's equation for calculating oxygen flux through the chamber was calculated based on the mean diameter of the two cross-sections seen to the right on figure 7. Chambers were discarded if they deviated significantly from the standard dimensions of 2.5x0.66 mm, if the sides of the chamber were not parallel, thus leading to a change in diameter across the length of the chamber, or if the opening of the chamber was cracked and therefore distorted the assumed diffusion area. If the bottom was found to be incompletely sealed, further heating was done to collapse it and the chamber was studied again. To transfer medium to and from the chambers, pipettes were constructed in a similar fashion. 1 mL *Luer* plastic pipettes (Chirana, Stará Turá, Slovakia) were held into a Bunsen burner flame until they collapsed, then removed and held with the tip downward – letting gravity elongate it. Once the pipettes had cooled off, the elongated and shortened tips were cut with scissors to fit the capillary chambers. Each pipette was labelled according to the type of medium it should be used for and kept in a sealed plastic bag.

In order to avoid evaporation of the medium during measurements, an aquarium set-up was established. This set-up consisted of a large cuvette, constructed by gluing 5 cover-slides together. A smaller cuvette that had been modified with air-holes near the bottom was glued upside-down to the bottom of the larger cuvette with silicone. This aquarium was then filled with the same water as the capillary chambers. The chambers were fixated in small pieces of modelling wax and also filled with medium – using the customized pipettes. A single tardigrade was extracted using an Irwin Loop whilst being observed under a stereo microscope and released into the capillary chamber. The chamber was then placed on top of the small cuvette in the aquarium, using a pincer. The chamber was observed under a horizontal light microscope to make sure the tardigrade was still present and to make sure that any air bubbles were removed before measuring.

The entire system was then placed on an adjustable platform under a micro-sensor that was fixated to a clamp with motor-control. Next to the platform was a cold-lamp for illumination during preparations for the measurements and a thermometer, to keep track of the temperature during any given experiment. A picture of the set-up can be seen on figure 8:

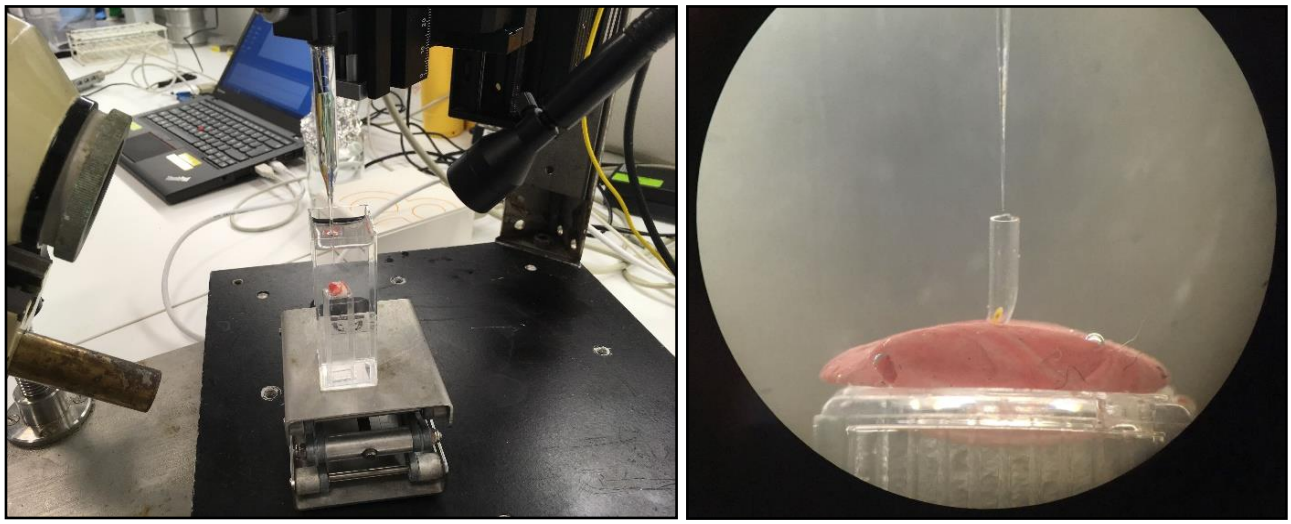

Figure 8: *The set-up including Aquarium, adjustable platform, lamp, microscope, suspended microsensor and computer (Left) and a picture of an R. coronifer in chamber a1 during oxygen profiling (Right). Taken through a microscope ocular with an iPhone SE camera.*

All individual elements of the set-up, except for the tardigrades, were washed with 70 % ethanol and then demineralized water, before being introduced to the rest of the system.

1.3. Sensors

The micro-sensors were connected to an Ampere-meter with an A/D-converter that transmitted the signal to a computer, through the programme *SensorTrace Pro* (Unisense, Aarhus, Denmark). The sensors were calibrated in oxygen saturated MiliQ water and oxygen-free ascorbic acid. The handling of sensors followed the *MicroRespiration System User Manual* (Unisense, 2016). Sensors were washed with MiliQ water between exposure to ascorbic acid and measurements. The sensor was observed under a horizontal microscope, whilst being lowered into the chamber. The lowest possible depth within the parallel-sided part of the chamber that did not risk interfering with the tardigrade was identified and set as depth of measurement in *SensorTrace Pro*. The step length was typically 100 μm, measure time was one second and the wait before each measurement was adjusted depending on sensor requirements. After the tardigrade was transferred, the system was left for 45 minutes so the tardigrade could establish an oxygen gradient in the chamber. Once it had done that, 5-10 oxygen profiles were measured. During profiling, details such as the exact temperature and time of transfer for the tardigrade were written under 'comments' in *SensorTrace Pro*.

After completion of the measurements, the chamber containing the tardigrade was imaged under a *Leitz Biomed* light microscope (Leica, Wetzlar, Germany) connected to a *Si CETi* camera (Medline Scientific, Chalgrove, United Kingdoms) to determine the length and width of the tardigrade. Finally, the tardigrade and medium were removed and discarded – using one of the customized pipettes. The chamber was studied under stereo-microscope to ensure it was empty, before being returned to its microtiter well or used in another measurement. Before measuring with tardigrades, 5-10 profiles of the empty chamber were measured to ensure that there was nothing else driving an oxygen gradient through the chamber – for example respiring microbes. Figure 9 shows examples of oxygen profiles through a chamber with or without a tardigrade at the bottom – as seen in *SensorTrace Pro*.

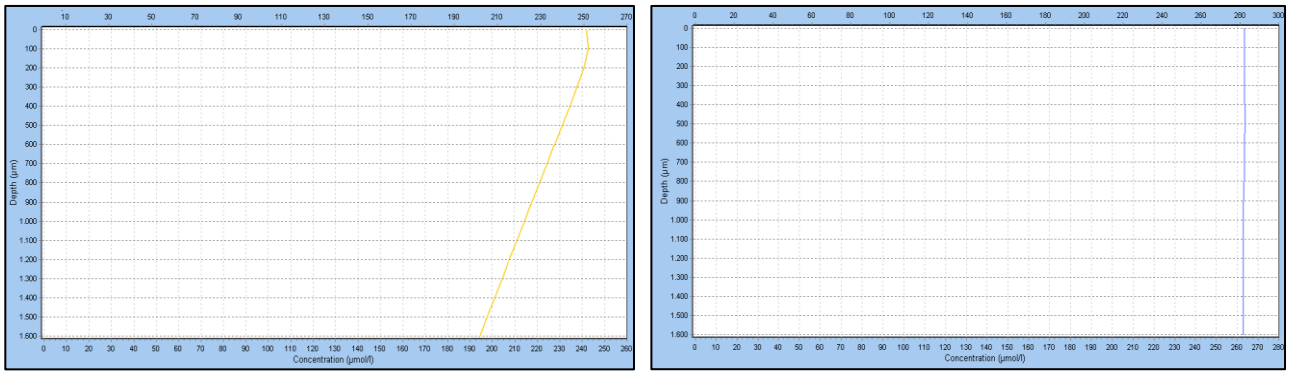

Figure 9: *Screenshots of the oxygen profile through a capillary chamber with a tardigrade at the bottom (Left) and a control measurement with no tardigrade in the chamber (Right). Profiles are displayed in SensorTrace Pro.*

1.4. Size determination

Many images were recorded of each tardigrade. The one that best showed its dimensions was selected based on several criterions. To minimize distortions of proportionality from the curvature of the glass, images where the tardigrade was centered along both axes of the chamber were preferred. Images where the tardigrades length extended perpendicular to the angle of the microscope were also preferred. Finally, to better match the cylindrical assumption, images where the tardigrade body was fully extended were selected above images where the body was in a crouched position. The chambers were dried with paper to ensure no water on the surface of the glass during imaging. An example of the images used for size determination can be seen on figure 10. The images were opened in the program *(Fiji is just) ImageJ* (Open Source). The scale in *Fiji* was set to fit the scale bar of the image. Dimensions were determined using the *measure* function. Due to the imperfect cylindrical shape of the animal, 5 measurements of width were done at various points of the body and a mean value determined, whereas only one measurement of length was required.

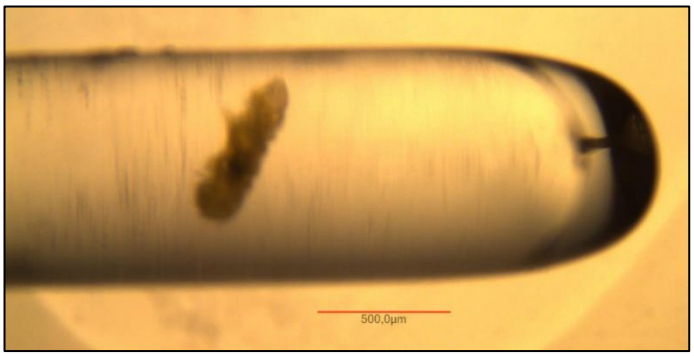

Figure 10: *Screenshot of R. coronifer during imaging, after profiles have been measured. The image is displayed in XLCam. Scale bar =*

1.5. Statistical Analysis

The oxygen microgradient was described by plotting concentration against depth. Each profile was subjected to regression analysis in excel and $r^2 > 0.99$ was confirmed before using the profile in further analysis. The slopes of these gradients were used to calculate the respiration rate as explained in the introduction. To this purpose, an algorithm was written in excel based on equations 11 & 12. The salinity was always 0, but temperature ranged between 21-24 °C during the experiments in this chapter. The mean temperature across experiments was 22.3 °C. Therefore, the temperature of the experiment is generally referenced as 22 °C, but the diffusion coefficient used in calculations was adjusted to match the specific temperature during each measurement. The specific radius of the relevant chamber was also used in the calculations – see appendix I. The respiration rate of tardigrades was normalized by subtracting the respiration rate calculated for the corresponding control. The respiration rate of controls ranged from 0.2 – 2 % of the tardigrade respiration. Additional algorithms were written based on equations 14 – 16 to

calculate the weight and surface area of the tardigrade from its length and width. The metabolic activity was calculated as MR_w and MR_A based on equation 13. The respiration was plotted against time to identify a steady-state and the mean respiration, MR_w and MR_A of each tardigrade was calculated from the profiles within that steady-state. These mean values for each individual tardigrade were copied to another Excel document, where they were organized into 3 tables – *R. coronifer*, Dead *R. coronifer* and *M. macrocalix.*

Two of the 19 tardigrades in the *M. macrocalix* table were excluded as outliers. Because of their much smaller size, it is possible that they were of a different and unidentified species. 4 out of 10 dead *R. coronifer* were also excluded as outliers. These showed 100-fold larger metabolic rates than the others. No outliers were identified for the active *R. coronifer*. After outliers had been eliminated, a mean value and population standard deviation was calculated for each category. A one-tailed heteroscedastic t-test was performed between all 3 categories to determine the significance of any differences. The average dimensions of the two species were determined. To increase the sample size, the *R. coronifers* studied in Chapter 2 were also included. The variations in temperature that these tardigrades were exposed to should have no effect on their size. The tardigrades studied in Chapters 3 & 4 were not included, because the specific conditions of those tardigrades – i.e. salinity and hydration state does affect their size. The mean surface to weight ratio (hereafter *A:w* ratio) was calculated for both species. Respiration and MR_w of all tardigrades from both species were plotted against weight to determine any effect of scaling.

To evaluate the reliability of the methods, 5 *R. coronifers* were randomly selected for case studies where multiple determinations of the size and MR_w were analysed. For the microsensor method, those multiple determinations were the 3 – 8 profiles in steady-state used to calculate its mean MR_w. The standard deviation in percentage of mean value (hereafter *SD%*) for each of the 5 case studies was calculated. In each case study, size determination was carried out as per protocol and the weight was calculated – but from 4-6 different images of the same tardigrade at varying angles or positions. A mean weight and *SD%* between the different images was calculated for each case study. Finally, the mean *SD%* and standard deviation of the 5 case studies was calculated for both MR_w and weight.

2. Results

2.1. Metabolic rate

Table 2 shows the mean *R*, MR_W and MR_A ± SD for both species – as well as the dead *R. coronifers*.

Table 2: *Mean values of Respiration, MR_W and MR_A ± SD for R. coronifer (n = 28), M. macrocalix (n = 17) and the dead R. coronifer controls (n = 6).*

Species	*Respiration* $\left(\frac{nmol\ O_2}{hour}\right)$	MR_W $\left(\frac{nmol\ O_2}{mg \cdot hour}\right)$	MR_A $\left(\frac{nmol\ O_2}{mm^2 \cdot hour}\right)$
R. coronifer	0.1540 ± 0.0466	10.8 ± 1.84	0.4277 ± 0.0842
M. macrocalix	0.1351 ± 0.0448	13.4 ± 2.19	0.4672 ± 0.0868
Dead R. coronifer	0.0030 ± 0.0011	0.21 ± 0.03	0.0081 ± 0.0016

Box-plots showing the distribution of *R*, MR_W and MR_A in the populations can be seen on figure 11.

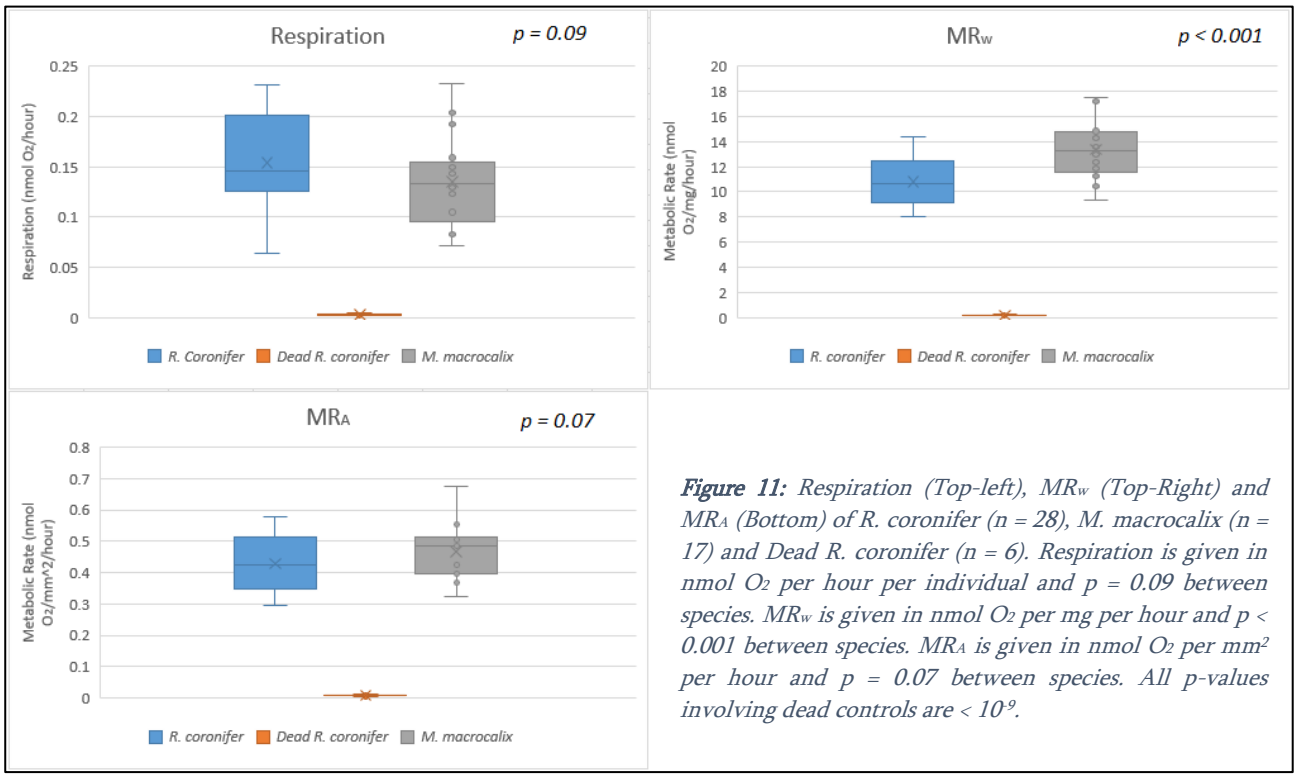

Figure 11: *Respiration (Top-left), MR_W (Top-Right) and MR_A (Bottom) of R. coronifer (n = 28), M. macrocalix (n = 17) and Dead R. coronifer (n = 6). Respiration is given in nmol O_2 per hour per individual and p = 0.09 between species. MR_W is given in nmol O_2 per mg per hour and p < 0.001 between species. MR_A is given in nmol O_2 per mm^2 per hour and p = 0.07 between species. All p-values involving dead controls are < 10^{-9}.*

Respiration is higher for *R. coronifers* than for *M. macrocalix*, but the metabolic rate is lower. The differences are insignificant ($p > 0.05$) for respiration rate and MR_A, but significant ($p < 0.001$) for MR_W. All 3 expressions differ significantly between active and dead tardigrades ($p < 10^{-9}$). When correcting respiration rate against weight or surface, the standard deviation decreases from ~ 33 % to ~ 18 %.

2.2. Scaling

Table 3 shows the average size of tardigrades from this study and from two separate studies by Ramløv & Westh, (1989) and Czernekova and Jönsson, (2016). Those studies only looked at *R. coronifer*.

Table 3: *The average length, width, weight and surface area of both R. coronifer (n = 54) and M. macrocalix (n = 17) ± sd in this study, as well as R. coronifers from two studies by Ramløv & Westh, (1989) (n = 75) and Czernekova and Jönsson, (2016) (n = 80). (*) indicates that the surface was calculated from length and width for this study.*

Species	*Length (µm)*	*Width (µm)*	*Weight (µg)*	*Surface (mm²)*
R. coronifer	565.7 ± 64.5	175.5 ± 17.0	14.30 ± 2.77	0.3601 ± 0.0467
M. macrocalix	498.6 ± 60.3	155.9 ± 18.1	10.16 ± 3.10	0.2846 ± 0.0572
Study				
Ramløv & Westh	570 ± 56	170 ± 23	16 ± 3.8	0.3498*
Czernekova & Jönsson	653	-	-	-

The values determined by Ramløv & Westh, (1989) are consistent with those of this study. However, the study by Czernekova and Jönsson, (2016) reported a much higher average length of 653 µm. The tardigrades described in this study varied significantly between species ($p < 0.001$) along all 4 measures of size. The *A:w* ratio of *M. macrocalix* is 12.6 % higher than that of *R. coronifer*. The difference in MR_w between the two species is 13.3 % higher than the difference in MR_A between them – leaving only 0.7 % of the difference unexplained by the *A:w* ratio. Figure 12 shows how respiration rate and MR_w relate to weight. Respiration increases linearly with weight ($R^2 \sim 0.7$), whereas MR_w appear to be independent of weight ($R^2 < 0.1$).

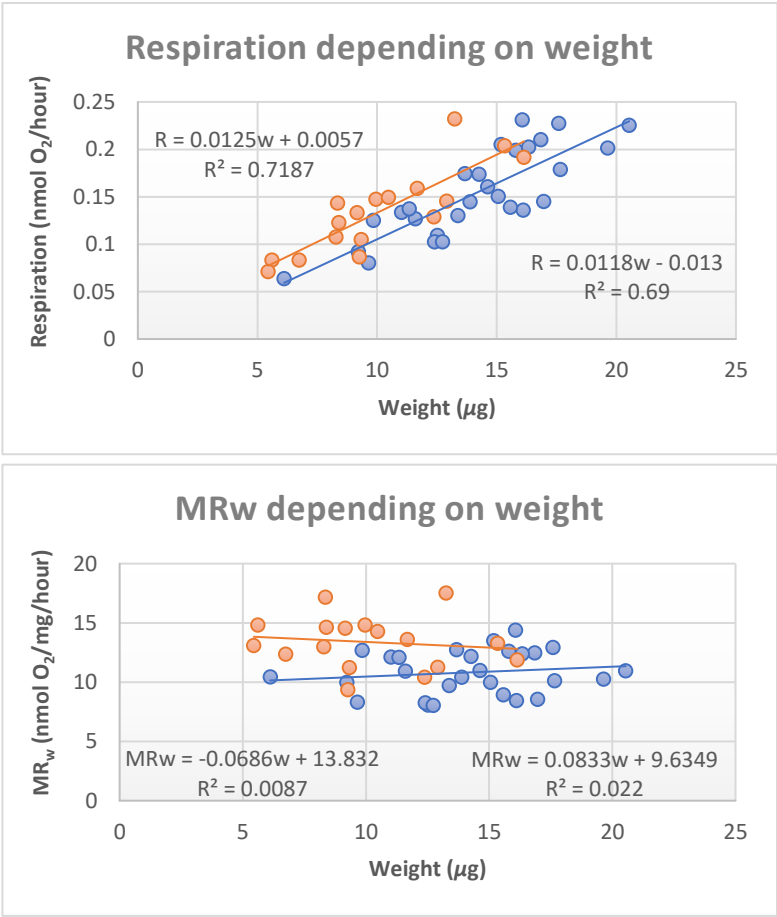

Figure 12: *The relationship of Respiration (Top) or MR_w (Bottom) to weight in µg. R. coronifers are marked with blue and M. macrocalix with orange. Linear regression of the plots shows the closest fitted equations and corresponding R^2-values. The equations to the left describe M. macrocalix and those to the right R. coronifer.*

2.3. Reliability

Figure 13 shows variation inherent in the population against the variation introduced by the measuring techniques. The blue and grey bars show the standard deviation in percentage of mean value (*SD%*) for *R. coronifer* as a population – with regards to MR_w and weight respectively. *SD%* within the population was 17 % for MR_w and 19 % for weight. The orange and yellow bars show the *SD%* of repeated measurements of the same individuals under similar conditions. The mean *SD%* of the 5 case studies was 1.4 % for MR_w and 8.7 % for weight. Error-bars represent the standard deviation of that mean *SD%* among the 5 case studies.

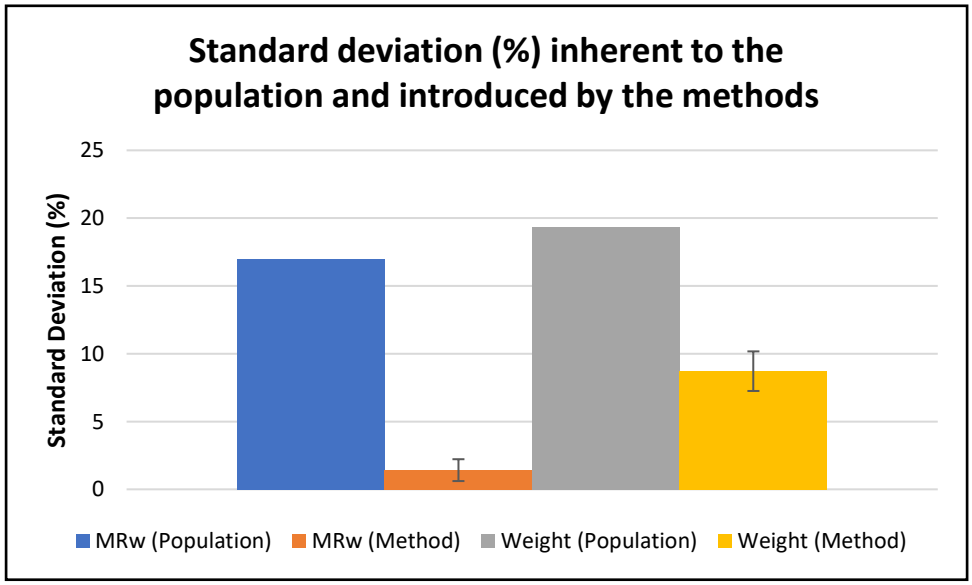

Figure 13: *The standard deviation (%) for MR_w of a population (blue, n = 28) vs. for MR_w measured in individual case studies (orange, n = 5) and the standard deviation (%) for the weight of a population (grey, n = 54) vs. the weight of individual case studies (yellow, n = 5). Only R. coronifer tardigrades were used for this figure. Error bars symbolize ± sd.*

3. Discussion

The metabolic rate of 10.8 ± 1.84 nmol $O_2 \cdot mg^{-1} \cdot hour^{-1}$ for active *R. coronifers* at 22 °C in MiliQ water will be used as a reference when interpreting the metabolic rate under different temperature, salinity or activity in Chapters 2 – 4. It was also found to be significantly lower than the metabolic rate of 13.4 ± 2.19 nmol $O_2 \cdot mg^{-1} \cdot hour^{-1}$ for the smaller and more rapidly moving *M. macrocalix* species. None of the cartesian diver experiments have been done at precisely 22 °C or on the same species, but the results of these studies fall roughly within the same order of magnitude as the results presented in this chapter (Pigon and Weglarska, 1953; Jennings, 1975; Klekowski and Opalinski, 1989). This suggests that although the method is impractical and was not reproducible, it was applied successfully in those studies. A more detailed comparison will be brought up in Chapter 2.

The fact that the active *R. coronifers* have metabolic rates 50 times higher than the dead controls demonstrate that it is indeed the activity of the living tardigrades that drive the measured oxygen consumption – at least 98 % of it. The relatively high number of outliers seen for dead *R. coronifer* is most likely due to issues with the sensor, which was subsequently replaced. It is unlikely that the high signal was due to a near death stress-response, as the tardigrades had been dead for at least 24 hours. Nor was it likely to be the result of residual cellular activity after organism death – as the signal was 2 to 3 times higher than that of active tardigrades. The phenomenon of residual cellular activity after organism death will be revisited in Chapter 3. Another possible explanation was colonization of the tardigrade body by respiring microbes. However, such colonization was studied in Chapter 4 and appeared to be lower than the signal of these outliers in tardigrades measured 1 – 8 days after death.

All mean-values have been determined using sample-sizes in the optimal range (Stec *et al.*, 2016). The fact that the standard deviation decreases when correcting for size is consistent with the expectation that the same cellular activity occurs in individuals of the same species, but on different scale depending on size. This is also supported by the fact that a linear relation to weight could be found for respiration, but not for MR_w. In the study by Czernekova and Jönsson, (2016), tardigrades were collected from Fraction 40 as opposed to the Fraction 120 used in this study. This suggests that the average of the whole species is different from that found in either study and that some bias toward larger or smaller specimens occurs when selecting which fraction to extract from. This will likely correlate with a bias toward older or younger specimens as well. In this study, that bias is toward smaller and thus likely younger tardigrades,

than a completely random selection would yield. However, no connection between size, and thus implicitly age and sexual maturity, and the metabolic rate could be shown in this study.

Seeing as metabolism occurs in all living cells of the organism, weight is generally a better metric to normalize respiration against than surface. After all, the surface only describes size in 2 dimensions. As was mentioned in the introduction, the tardigrade absorbs oxygen by passive diffusion across the cuticula – i.e. the surface area. This is the reason for the interest in scaling and MR_A as an expression of the metabolic rate. If the cuticula functions as either a limiting or actively facilitating factor in oxygen saturation of the tardigrade's cells, then the MR_A:MR_w ratio should differ from the *A:w* ratio itself. This does not appear to be the case. The 0.7 % difference between the two ratios is considered negligible. Because of this, there does not seem to be any regulatory mechanisms operating in the cuticula that either limit or facilitate oxygen saturation of the tardigrade's cells. Together with the fact that metabolic rate does not appear to vary with size for *R. coronifers*, this is taken to mean that scaling is not a relevant factor for interpreting the remaining results of the study. Chapters 2 – 4 will deal only with respiration and MR_w as the metabolic rate.

Comparing the *SD%* of case studies to the *SD%* of the population means – both with regards to MR_w and weight clearly shows that the variation introduced by the method is much smaller than that inherent to the population. The variation introduced by the sensors is so small as to be negligible. Although the variation introduced by size determination is significantly smaller than the inherent variation in size, it is still high enough to leave room for improvements. Other potential improvements include sterilizing the tardigrades e.g. with antibiotics to minimize the effects of bacterial respiration and measuring the same individual tardigrade under different conditions. Still, the study of reliability strongly suggests that the method is accurate, and the determined values are true.

Chapter 2: Temperature

1. Materials and Methods

To measure oxygen consumption at different temperatures, water baths of the appropriate size were filled with MiliQ water from a *Q-POD® Ultrapure Water Remote Dispenser* (Merck, Darmstadt, Germany, ZMQSP0D01). A cold-finger was placed in each bath – along with a thermometer, a grounding cable, a rotating magnet, calibration liquids and an aquarium like those from Chapter 1. The cold-finger was connected to a cooling and heating system by rubber tubes cycling cooling fluid through the cold-finger. The temperature of the cooling fluid, and thus the temperature of the cold-finger, was controlled manually through the thermostat of the cooling and heating system. For any given experiment, the exact temperature was noted from the thermometer in the water bath. The grounding cable was connected to the amperemeter and placed in the water bath to avoid noise in the measurements (Unisense, 2016). The water bath was placed on a magnetic disc and the magnet placed near the cold-finger to ensure the same temperature in the whole water bath by stirring. A piece of styrofoam was used to insulate the system against heat from the magnetic disc. The calibration liquids were kept at the same temperature as the rest of the system by suspending them in the surface of the water bath. This was done by fixating them to the clamp holding the sensor in place using twine. Aquariums were placed in the water baths to protect the capillary chambers containing the tardigrades and to achieve proper placement of the chamber relative to the sensor. The set-up can be seen on figure 14.

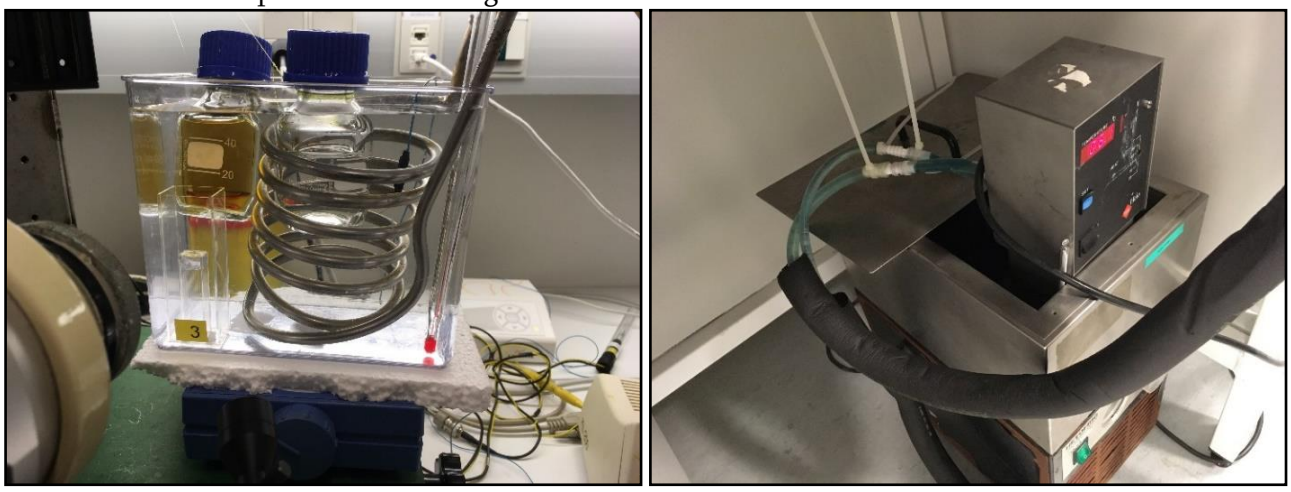

Figure 64: *(Left) A water bath containing a cold-finger, a thermometer, a grounding cable (blue), a magnet and an aquarium like those from Chapter 1. Calibration liquids are suspended in the surface and the water bath is placed on a magnetic disc – with a piece of styrofoam between them. (Right) Cooling and heating system regulating the temperature of the cold-finger. A reservoir of cooling fluid has its temperature regulated by the thermostat and is cycled through rubber tubes connected to the cold-finger.*

The tardigrades were handled identically to those in Chapter 1 – from collection in Öland until placing them in the water bath. Controls of empty chambers were measured for every experiment as described in Chapter 1. The temperature shift that occurred in the capillary chambers when placed in the water bath lead to a shift in solubility, which in turn created an oxygen gradient through the chambers – unrelated to the respiration of the tardigrade. This problem is addressed in more detail in Chapter 5. It was solved by carefully flushing the chambers with water from the water bath after they had been placed in it – using the customized pipettes. This removed the oxygen gradient caused by the solubility shift and allowed a new gradient to be established by the tardigrade respiration. Immediately after flushing, an oxygen profile was measured through the chamber to ensure a uniform oxygen distribution. Incubation time was at least 45 minutes after flushing. Controls were also flushed before incubation.

9 active *R. coronifers* were measured at 2 °C, 8 were measured at 33 °C and 6 were measured at 11 and 16 °C respectively. The correct D_{O_2} for each condition was used when calculating the respiration rate – based on the Unisense Seawater and Gases Table seen in appendix II. Respiration and metabolic rate were determined from the oxygen microgradients as described in Chapter 1 and organized in excel for further analysis. Two of the tardigrades measured at 33 °C were excluded as outliers, because they died during the experiment and one tardigrade measured at 2 °C was excluded, because it did not reach steady-state in the 1.5 hours it was measured. Mean values, population standard deviation and *p*-values were calculated for all conditions as described in Chapter 1. Additionally, the Q_{10} for every temperature range was calculated from the mean values of metabolic rate and respiration – using equation 1 from the introduction. An Arrhenius plot was also constructed based on equation 3 and described by linear regression analysis. The equation fitted to this plot was used to calculate the activation energy and pre-exponential factor for the rate-limiting step in the metabolic pathway.

For comparison, the metabolic rates determined in studies using the cartesian diver method were converted from $\frac{\mathrm{mm^3 \cdot 10^{-6}\ O_2}}{\mathrm{10^{-6}\ g \cdot hours}}$ to $\frac{\mathrm{nmol\ O_2}}{\mathrm{mg}}$ using the ideal gas law.

(17) $$pV = nRT$$

Where p is the pressure of the gas (atm), V is the volume (L), n is the amount of substance (mole), R is the gas constant ($\frac{\mathrm{L \cdot atm}}{\mathrm{mole \cdot °K}}$) and T is the absolute temperature (°K). Assuming a standard pressure of 1 atm in all the cartesian diver experiments, the amount of oxygen can be calculated from the volume and temperature by rearranging:

$$n = \frac{pV}{RT} = \frac{1\ \text{atm} \cdot V}{0.08205\ \frac{\text{L} \cdot \text{atm}}{\text{mole} \cdot °\text{K}} \cdot T}$$

V and T for all cartesian diver experiments are given in table 3 of Klekowski and Opalinski, (1989) with the units $\text{mm}^3 \cdot 10^{-3}$ and °C. Absolute temperature in °K is calculated from °C by adding 273.15 to that value. The proportionality of both $\text{mm}^3 \cdot 10^{-3}$ to L and nmol to mole are by a factor of 10^9. Therefore, by using the values given in Klekowski and Opalinski, (1989) as V, the calculated n is given in nmol. Finally, $\frac{\text{nmol O}_2}{10^{-6}\ \text{g} \cdot \text{hours}}$ is converted to $\frac{\text{nmol O}_2}{\text{mg} \cdot \text{hours}}$ by multiplying it with $10^3\ \frac{\text{mg}}{10^{-6}\ \text{g}}$.

2. Results

2.1. Metabolic rate

The mean values of metabolic rate, respiration and weight ± sd at the different temperatures can be seen on table 4. The data on *R. coronifer* at 22 °C from Chapter 1 is included.

Table 4: *Mean values of metabolic rate and respiration ± SD at the 5 temperatures investigated in this study. The sample size is n = 28 at 22 °C, n = 8 at 2 °C and n = 6 at 11, 16 and 33 °C.*

Temperature (°C)	*Metabolic Rate* ($\frac{nmol\ O_2}{mg \cdot hour}$)	*Respiration* ($\frac{nmol\ O_2}{hour}$)	*Weight (µg)*
2	2.28 ± 0.48	0.0348 ± 0.0072	15.3 ± 1.59
11	3.56 ± 0.59	0.0546 ± 0.0059	15.6 ± 2.28
16	8.42 ± 0.82	0.1147 ± 0.0121	13.7 ± 1.67
22	10.8 ± 1.84	0.1540 ± 0.0466	14.1 ± 3.22
33	19.5 ± 1.19	0.2556 ± 0.0471	13.1 ± 1.73

All standard deviations fall between 6 – 21 % – except for respiration at 22 °C where it is 30 %. Both respiration and metabolic rate increases significantly with every increase in temperature ($p < 0.001$). Additionally, the variation between individuals also appear to increase at higher temperatures. No significant difference of the average weights was found between any temperatures ($p > 0.05$). The tardigrades exposed to 2 °C seized all movement during oxygen profiling, but regained it during imaging at 22 °C. The movement of tardigrades exposed to temperatures from 11 to 33 °C showed no substantial

variation. Box-plots showing the distribution of metabolic rates and respiration at the different temperatures can be seen on figure 15.

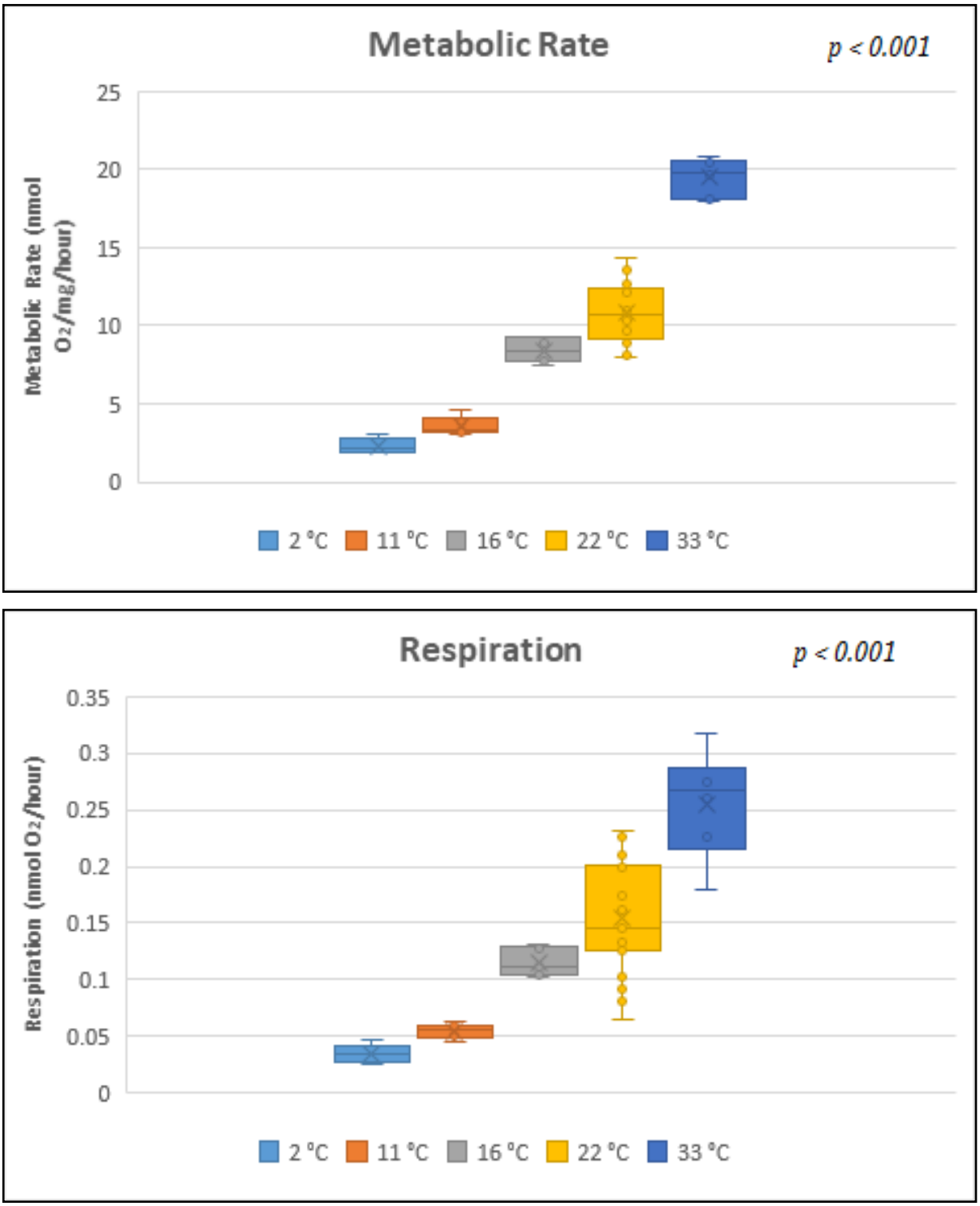

Figure 15: *Box-plot of metabolic rate (Top) and respiration (Bottom) for R. coronifer at 2 °C (n = 8), 11 °C (n = 6), 16 °C (n = 6), 22 °C (n = 28) and 33 °C (n = 6) respectively. p < 0.001 between all temperatures for both.*

2.2. Metabolic stability

The Q_{10} values for every temperature range can be seen in table 5 and figure 16.

Table 5: *Q_{10} between the mean values of metabolic rate and respiration at the 4 temperature ranges investigated in this study.*

Temperature range (°C)	*Metabolic Rate (Q_{10})*	*Respiration (Q_{10})*
2 – 11	1.64	1.65
11 – 16	5.58	4.42
16 – 22	1.52	1.63
22 – 33	1.71	1.59

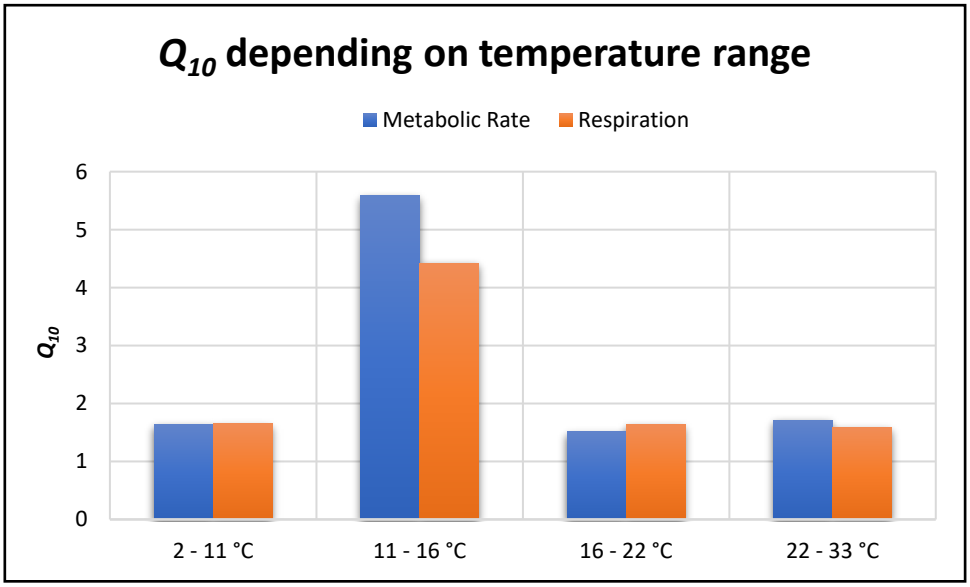

Figure 16: *Bar chart showing Q_{10} between the mean values of metabolic rate (blue) and respiration (orange) at the 4 temperature ranges investigated in this study.*

Q_{10} is ~ 1.5 for both metabolic rate and respiration in all temperature ranges except for 11 – 16 °C. In this specific range, it increases to 5.58 for metabolic rate and 4.42 for respiration.

2.3. Activation energy

Figure 17 shows the Arrhenius plot for metabolic rate (mole $O_2 \cdot \mu g^{-1} \cdot s^{-1}$) and respiration rate (mole $O_2 \cdot s^{-1}$). The equations fitted to both plots and their respective R^2 values can also be seen on the figure.

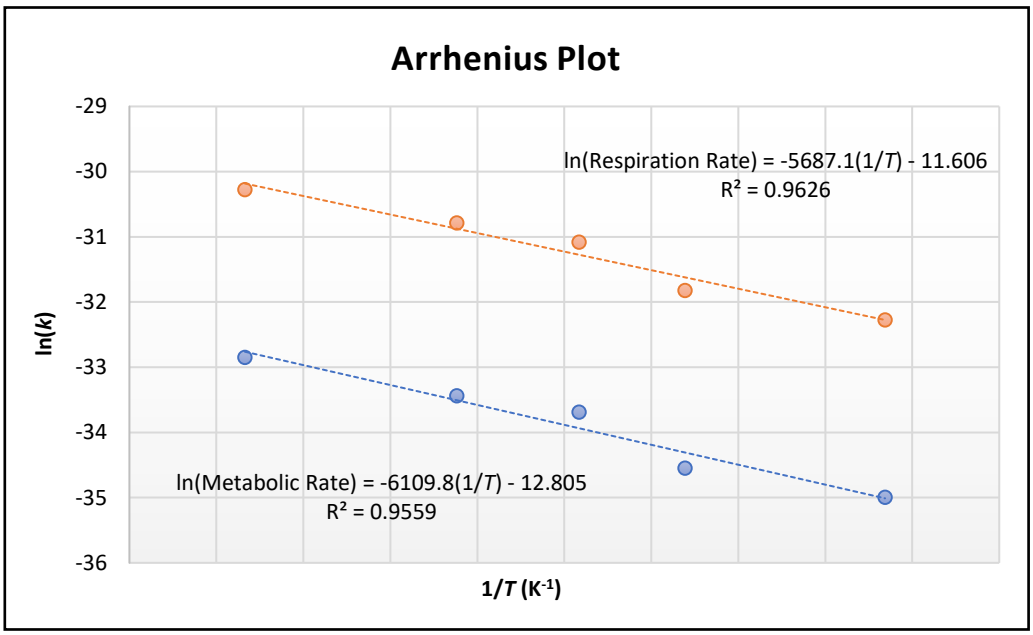

Figure 17: *Arrhenius plot of metabolic rate ($\frac{mole\ O_2}{\mu g \cdot s}$) in blue and respiration rate ($\frac{mole\ O_2}{s}$) in orange. Linear regression analysis shows the best fitted equations and R^2-values.*

As described in the introduction, the activation energy is the slope of the Arrhenius plot multiplied by $-8.3144598\ \frac{J}{°K \cdot mole}$. For metabolic rate and respiration, the activation energy was calculated as follows:

$$E_a(MR) = -6109.8\ °K^{-1} \cdot \left(-8.3144598\ \frac{J}{°K \cdot mole}\right) \approx 50.8\ \frac{kJ}{mole\ O_2}$$

$$E_a(R) = -5687.1\ °K^{-1} \cdot \left(-8.3144598\ \frac{J}{°K \cdot mole}\right) \approx 47.3\ \frac{kJ}{mole\ O_2}$$

Since the metabolic rate is respiration corrected for size, the difference is attributed to variance in size and the activation energy of the rate-limiting step in the metabolic pathway is understood to be 50.8 kJ/mole O_2. Because the intersection of the Arrhenius plot with the y-axes is equal to $\ln(A)$ (see equation 3), the pre-exponential factor can also be calculated:

$$A = e^{lnA} = e^{-12.805} \approx 2.75 \cdot 10^{-6}\ mole\ O_2 \cdot \mu g^{-1} \cdot s^{-1}$$

2.4. Cartesian Diver studies

A complete overview of the metabolic rate and Q_{10} values from the Cartesian Diver studies can be seen on table 6.

Table 6: *(Top) Modified version of Table 3 found in Klekowski & Opalanski, (1989). Units have been converted from* $\frac{mm^3 \cdot 10^{-3}\ O_2}{10^{-6}\ g \cdot hour}$ *to* $\frac{nmol\ O_2}{mg \cdot hour}$ *using the ideal gas law. (Bottom)* Q_{10} *of metabolic rates as determined by the Cartesian Diver studies. Mean values of metabolic rates and* Q_{10} *from the current study has been inserted in bold at the bottom of both tables.*

Table 3 from *Klekowski & Opalanski, (1989)* : Metabolic Rate (nmol O2/mg/hour) in Tardigrada at various temperatures									
Species	**Temperature (°C)**								**Locus / Author**
	2	**6**	**10**	**16**	**20**	**22**	**25**	**33**	
Doryphorybius smreczynskii	2.08	2.4	7.1						Arctic, Spitsbergen / *Klekowski & Opalinski, (1989)*
Diaphascon spitzbergensis	2.66								
Macrobiotus islandicus		3.97							
Macrobiotus echinogenitus		2.66							
Macrobiotus harmsworthi		4.41							
Macrobiotus spectabilis		3.89							
Macrobiotus dispar		3.19	5.55						
Macrobiotus dispar					1.08				Temperate zone, Poland / *Pigon & Weglarska, (1953)*
Macrobiotus hufelandi					8.15		9.24		
Macrobiotus furciger		5.98	11.15						Antarctic, Signy Island / *Jennings, (1975)*
Richtersius coronifer	**2.28**		**3.56**	**8.42**		**10.81**		**19.5**	**This Project**
Macrobiotus macrocalix						**13.43**			**This Project**
Q 10	**Temperature range (°C)**								**Locus / Author**
Species	**2 - 6**	**2 - 11**	**5 - 10**	**6 - 10**	**11 - 16**	**16 - 22**	**20 - 25**	**22 - 33**	
Macrobiotus hufelandi							1.3		Temperate zone, Poland / *Pigon & Weglarska, (1953)*
Macrobiotus dispar				4.2					Temperate zone, Poland / *Pigon & Weglarska, (1953)*
Macrobiotus furciger			3.46						Antarctic, Signy Island / *Jennings, (1975)*
Doryphoribius smreczynskii	1.5			15.6					Arctic, Spitsbergen / *Klekowski & Opalinski, (1989)*
Richtersius coronifer		**1.64**			**5.58**	**1.52**		**1.71**	**This Project**

The metabolic rates vary significantly based on species and temperature, but they all fall within the same order of magnitude as the results in this study. Q_{10} from these studies also do not deviate much from the range seen for *R. coronifer* – with the exception of *Doryphoribius smreczynskii* at 6 – 10 °C where it is almost 3 times higher than the extreme case in this study and 10 times higher than the other values.

3. Discussion

The temperature conditions in this study had no effect on the size or general morphology of tardigrades but did affect their movement. No changes were seen from 11 – 33 °C but when exposed to 2 °C, all movement seized within a few minutes – although respiration continued, and movement returned during imaging at 22 °C. The metabolic rate did not change substantially between unmoving tardigrades at 2 °C and moving tardigrades at 11 °C when compared to the 5-fold increase seen from 11 – 33 °C with no clear change in movement. This suggests that the energy required for muscle contractions is only a small fraction of the tardigrades overall energy expenditure. The consistency in morphology and behaviour also indicates that the tardigrades are not undergoing cyclomorphosis at any condition. If they were, then the most likely form of cyclomorphosis would be supercooling at 2 °C. Supercooling would primarily be expected to occur at sub-zero temperatures, since its purpose is to avoid intracellular ice formation. Depending on what nucleating agents are present, it may be relevant at near-zero temperatures as well (Halberg *et al.*, 2009). It would be interesting to investigate the change in movement from 2 – 11 °C in more detail – as well as its effect or lack thereof on the metabolic rate.

In the last of the cartesian diver studies, Klekowski and Opalinski, (1989) described the tardigrades *Macrobiotus hufelandi* and *Doryhoribius smreczynskii* as having adapted to their local temperature conditions by developing a Range of relative temperature independence (*RRTI*) regarding their metabolic rates. While the metabolic rate of *R. coronifer* determined in this study is not temperature independent in any of the studied ranges, it is stable in its temperature dependence for most of them – stable meaning $Q_{10} < 3$ as explained in the introduction. We might therefore consider the hypothesis with respect to a Range of relative temperature stability (*RRTS*). The climate at Öland where the population was collected fluctuates between 2 – 22 °C throughout the seasons (Meteoblue, 2018). According to the *RRTI* hypothesis, Q_{10} should be independent – or at least stable from 2 – 22 °C and unstable above that. However, this is not what happens.

The metabolic rate is as stable from 22 – 33 °C as it is from 2 – 11 °C. Furthermore, it is unstable in a 5 °C interval within its local climate – between those relative extremes. Because of this local peak in Q_{10}, the *RRTI* hypothesis cannot be true for *R. coronifer* with regards to any specific environment from its earlier evolutionary history either. Klekowski and Opalinski, (1989) did point out that no *RRTI* was found for the arctic tardigrade *Macrobiotus furciger*. However, *R. coronifer*s local environment is closer in temperature to *M. hufelandi and D. smreczynskii* than to *M. furciger*, so this is unlikely to be the

determining factor for developing an *RRTI*. The distinction between tardigrades with *RRTI* and not is also unlikely to be found by looking further back in the evolutionary history, as *M. hufelandi* and *M. furciger* are phylogenetically closer related to each other than to *D. smreczynskii* (Natural History Museum of Copenhagen, 2018). Compared to the current study, the margin of error was considerably larger for the cartesian diver experiments. This is most likely the reason for the confusion about a temperature independent range as opposed to a stably temperature dependent range. I suggest that this distinction would also reveal itself if *M. hufelandi* and *D. smreczynskii* were studied using oxygen microgradients. If adaptation to local environments have led to an *RRTS* in those species, it does not appear to be a generalizable phenomenon for tardigrades – arctic or otherwise.

This however does not address the reason for the metabolic instability observed in such a specific temperature range – experienced bi-annually in the local environment of the population. Bar any specific adaption to temperature, the default case for biological processes is for Q_{10} to increase exponentially with increasing temperature. The fact that the same $Q_{10} < 2$ is seen at 2 – 11 °C and 22 – 33 °C must therefore be the product of regulatory processes. The range of 11 – 16 °C where the increase in Q_{10} occurs approximately represent the months of May-June and September-October on Öland (Meteoblue, 2018). One possibility is that these seasons are the most favourable for reproduction – leading for example to differential hormone expression stimulated by temperature shifts. Another possibility may be that one or more key enzymes are switched on or off at some point between 11 – 16 °C, which fundamentally changes the metabolic pathway or energetic requirements of cells. The tardigrade metabolism may function bimodally depending on the presence of such enzymes or co-factors, with the high-temperature modality having a significantly higher rate but with both modalities having the same temperature stability while operating.

Another variant of this explanation could be the need for certain heat shock proteins arising in this temperature range to act as chaperones by ensuring correct protein folding and avoiding aggregation. This additional workload of the cell would increase the energy requirements. It has already been documented that *R. coronifer* show strong upregulation of the heat shock protein HSP70 in response to heating from 21 – 37 °C, as well as initiation and termination of cryptobiosis – both being transition phases for the *R. coronifer* metabolism (Ramløv and Westh, 2001; Schill, Steinbrück and Köhler, 2004; Jönsson and Schill, 2007). Although HSP70 has not been implicated in the metabolic transition seen from 11 – 16 °C in this study, it has been implicated in regulation of metabolic transitions in *R. coronifer* under different

conditions and a shared principle may exist with other similar proteins. It would be interesting to investigate the change in metabolic rate from 11 – 16 °C, at higher resolution. If the bimodal metabolism hypothesis is true, the shift may be narrowed down to a single critical temperature. If the change is instead due to increased energy requirements – e.g. from a heat shock response, then the change in rate may be more gradual. It would also be interesting to study how fast the response occurs by monitoring individuals during temperature changes in this range, rather than comparing metabolic rates of different individuals in steady state at the different conditions – as was done in this study. That would require some modifications to the set-up, as the system used in this study is highly sensitive to changes in temperature during measurements. The fact that the Q_{10} of respiration and metabolic rate appear to be almost identical in the temperature stable ranges but differ specifically in the 11 – 16 °C range is unlikely to hold any significance. No relationship was found between temperature and weight of tardigrades but the largest difference in mean weight was between 11 and 16 °C – the most likely explanation for the difference. Despite the focus on Q_{10} in this particular range so far, it is not the only range worth consideration. Most stable biological processes have Q_{10} values between 2 – 3. The fact that all 3 stable ranges for *R. coronifer* from 2 – 33 °C show $Q_{10} \sim 1.5$ suggests that the metabolism is highly regulated with respect to temperature.

Assuming that one unified metabolic pathway drives the measured oxygen microgradients, the activation energy for the rate-limiting step of this pathway is 50.8 kJ/mole O_2. Given enough information about the metabolic pathway, this may reveal the biochemical mechanisms underlying the rate-limiting step – and thus which metabolites and catalysts are most crucial for energy production in tardigrades. Generally, the activation energy necessary to break weak interactions are approximately 4 – 30 kJ/mole and for covalent bonds it is 60 – 100 kJ/mole. However, the chemical activation energy of the reaction step is certain to be much higher *in vitro* than the 50.8 kJ/mole O_2 determined *in vivo* – where enzymes are catalyzing the reaction by lowering its activation energy substantially (Nelson and Cox, 2013). The pre-exponential factor A was experimentally determined to be $2.75 \cdot 10^{-6}$ mole $O_2 \cdot \mu g^{-1} \cdot s^{-1}$, which is 9 orders of magnitude above the metabolic rates of this study. According to collision theory, this is the frequency of collisions between the reactants of the reaction. However, it is thought to be unfeasible to establish the pre-exponential factor based on temperature studies of rate constants, due to its relatively weak temperature dependence (Connors, 1990). The interpretation is further complicated by the fact that the reactants of the rate-limiting step are unknown, and its rate constant is measured indirectly by the

consumption of oxygen – which may not be part of that specific reaction step. Because of this, the experimentally determined value is unlikely to be useful for future interpretations of the metabolism.

The studies using Cartesian Divers were done at different temperatures and with different species adapted to very different climates. Therefore, the metabolic rates are not necessarily going to be the same as those of *R. coronifer* in this study. The fact that they still fall within the same order of magnitude despite this, gives some indication of the validity of those studies – although they are not all perfectly consistent. Klekowski and Opalinski, (1989) found the metabolic rate of *Macrobiotus dispar* to be 5.55 nmol $O_2 \cdot mg^{-1} \cdot hour^{-1}$ at 10 °C, whereas Pigon and Weglarska, (1953) found it to be 1.08 nmol $O_2 \cdot mg^{-1} \cdot hour^{-1}$ at 20 °C. That inconsistency combined with the results in this study suggest that the results from Pigon and Weglarska, (1953) may be less reliable – unless *M. dispar* tardigrades simply die at 20 °C. The only other tardigrade studied by Pigon and Weglarska, (1953) also showed lower metabolic rates at similar temperatures when compared to the *R. coronifer* in this study. The populations from that study were collected in a temperate zone in Poland with climate warmer than Öland. Conversely, the population studied by Jennings, (1975) was collected in the Antarctic environment of Signy Island and all of the populations studied by Klekowski and Opalinski, (1989) were collected in the Arctic environment of Svalbard – both significantly colder than Öland. With the exceptions of *D. smreczynskii* and *Macrobiotus echinogenitus*, all of those populations showed metabolic rates higher than *R. coronifer* at similar temperatures. This shows a consistent trend that tardigrades adapted to colder environments tend to develop faster metabolisms and vice versa.

Moving forward, the microgradient method is preferable to the cartesian diver method for this type of studies across the board. It is more accurate and allows for more reproducibility and data acquisitions due to computational solutions to steps that would require human judgements for the cartesian diver method. This also allows for high resolution descriptions of the metabolic response in real time over both very short and very long time-frames – as will be elaborated on in Chapters 3 and 4. It can measure much smaller and faster changes in oxygen consumption rates – more so than was utilized in the current study if given the right expertise. This allows for strong signals of single, well characterized tardigrades – whereas some divers rely on the overall signal from 5 – 200 tardigrades at once to get an average (Pigon and Weglarska, 1953; Jennings, 1975). Tardigrades can be easily extracted from and returned to the set-up for combination with other experiments or evaluation techniques – such as imaging, which can also be done in parallel with the respiration measurements. Due to the relative simplicity of the set-up, it is also

easier to repurpose it for studies of a vast array of interesting conditions. The experimental set-up described in this chapter could be replaced with the much simpler set-up from Chapter 1 – if conducted in temperature-controlled rooms. This would eliminate the concern about fluctuations in temperature, which required careful monitoring of the temperature in water baths throughout the experiments. It would also eliminate the need for a flushing step, which risks ejecting or damaging the tardigrade if done too forcefully.

Chapter 3: Salinity

1. Materials & Methods

1.1. Preparation of salt solutions

To test the effect of a Mars-analogue condition on the metabolic rate of tardigrades, two different types of salt solutions were made. One was a simple NaCl solution and the other was a mixture of perchlorate salts – as found on Mars. To also study the effects of osmotic pressure, multiple dilutions of both types of solutions were prepared. To make the NaCl solutions, 15 and 30 gram of *Pro Analysis (PA)* NaCl (Sigma Aldrich, St. Louis, Missouri, United States) were weighed out on a *DeltaRange®* weight (Mettler Toledo, Columbus, Ohio, United States) and transferred to two 1 L volumetric flasks before being dissolved in 1 L MiliQ water. A dilution series was prepared from the 15 g NaCl stock solution by transferring 250 mL to a 500 mL volumetric flask and filling with MiliQ water, then repeating to get a 4 times dilution. The Mars-analogue perchlorate solution was prepared based on the average composition of Martian soil reported in Hecht *et al.*, (2009) from the Phoenix mission in 2007-08. For simplicity, the solution was prepared by dissolving only perchlorate salts in MiliQ water. Those salts were $NaClO_4 \cdot H_2O$, $KClO_4$, and $Ca(ClO_4)_2 \cdot 4\ H_2O$ (PA, Sigma Aldrich) and $Mg(ClO_4)_2$ (Sercon Ltd., Crewe, United Kingdoms). Figure 18 shows the weighing of 15 g NaCl – as well as the perchlorate salts used for the Mars-analogue solution.

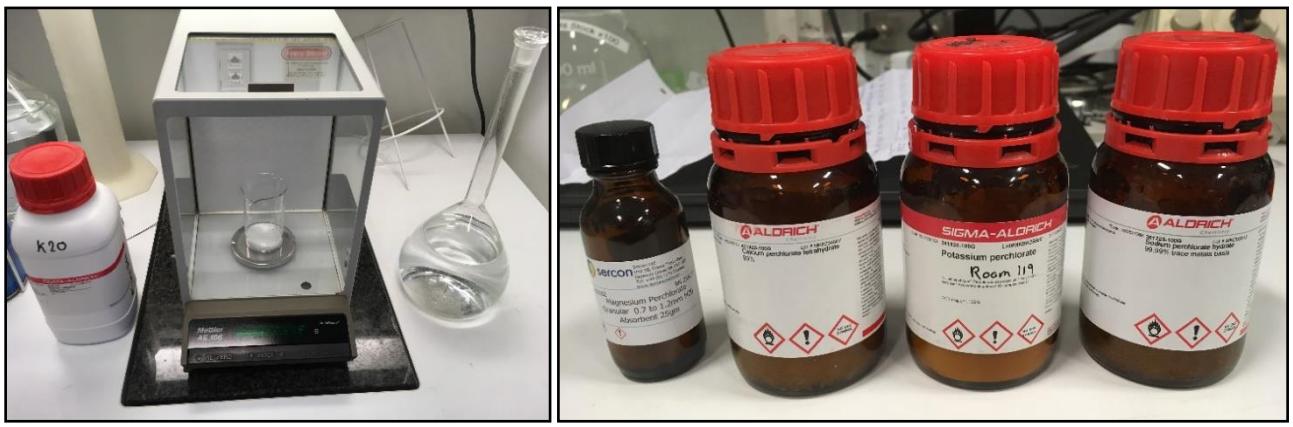

Figure 78: *The weighing of 15 g Sigma Aldrich pa NaCl before transfer to a 1 L volumetric flask and (Left) and the perchlorate salts used for the Mars-analogue solution (Right).*

However, the amount of cations found in Hecht *et al.*, (2009) exceeded what can be stoichiometrically paired with perchlorate anions. As perchlorates and not the cations were expected to affect the metabolism of tardigrades, the solution was designed to have the reported perchlorate concentration and a ratio

between cations matching that reported in Hecht *et al.*, (2009). The following calculation is for the amount of perchlorate needed for 1 L of Mars-analogue solution:

$$2.4 \text{ mmol } ClO_4^- + 0.54 \text{ mmol } Cl^- = 2.94 \text{ mmol } ClO_4^-$$

The chloride found in Martian soil was included in this calculation, because perchlorate was the only source of Cl in these solutions and will be in equilibrium with chloride once dissolved. The reported concentrations of the 4 different types of cations can be seen in column 2 of table 7.

Table 7: The reported concentrations of cations in Martian soil, concentration times valence, the fraction of perchlorate that must be transferred with the given type of salt, the amount of perchlorate transferred for the total amount to be 2.94 mmol and the amount of each type of salt that must be dissolved in 1 L MiliQ water to achieve the correct n(ClO_4) and ratio between cations according to Hecht et al., (2009).

Cation	Reported C (mM)	Times Valence (mM)	% ClO_4	n(ClO_4) (mmol)	n(salt) (mmol)
Na^+	1.4	1.4	14.7	0.43	0.43
K^+	0.38	0.38	3.90	0.12	0.12
Ca^{2+}	0.58	1.16	12.2	0.36	0.18
Mg^{2+}	3.3	6.6	69.2	2.03	1.02
Sum:	**5.66**	**9.54**	**100**	**2.94**	**1.75**

The reported concentrations of cations were multiplied by valence to get the stoichiometrically corresponding concentrations of perchlorate – seen in column 3. If the reported concentrations of cations were used, the total concentration of perchlorate would be 9.54 mM – rather than the reported 2.94 mM. The following calculation is an example of how the fraction of perchlorates transferred with a given salt is calculated – in this case with $NaClO_4 \cdot H_2O$:

$$\%\ ClO_4^-\ transferred\ with\ NaClO_4^- \cdot H_2O = \frac{1.4\ mM\ ClO_4^-\ transferred\ with\ NaClO_4^- \cdot H_2O}{9.54\ mM\ ClO_4^-} \approx 14.7\ \%$$

Column 4 shows the results of this calculation for each salt. By taking that fraction of the total 2.94 mmol perchlorate, the amount that should be transferred with the given salt is calculated as seen in column 5. That amount is then divided with the number of perchlorates per salt molecule to get the amount of each salt that should be transferred for a 1 L solution. Those amounts can be seen in column 6. The corresponding mass of salt is calculated from the equation $m = n \cdot M$:

$$m(NaClO_4 \cdot H_2O) = 0.43 \text{ mmol} \cdot 140.436 \frac{\text{mg}}{\text{mmol}} \approx 60.59 \text{ mg}$$

$$m(KClO_4) = 0.12\ \text{mmol} \cdot 138.544 \frac{\text{mg}}{\text{mmol}} \approx 16.22\ \text{mg}$$

$$m(Ca(ClO_4)_2 \cdot 4\,H_2O) = 0.18\ \text{mmol} \cdot 310.97 \frac{\text{mg}}{\text{mmol}} \approx 55.58\ \text{mg}$$

$$m(Mg(ClO_4)_2) = 1.02\ \text{mmol} \cdot 223.197 \frac{\text{mg}}{\text{mmol}} \approx 227.0\ \text{mg}$$

Because these amounts would be difficult to weigh out precisely, a stock solution with 100 times higher concentration of solutes was prepared. The following amounts were weighed out: 6.0693 g $NaClO_4 \cdot H_2O$, 1.6169 g $KClO_4$, 5.5515 g $Ca(ClO_4)_2 \cdot 4\ H_2O$ and 22.7187 g $Mg(ClO_4)_2$. Deviations from the calculated amounts were < 0.5 %. The salts were transferred to a 1 L volumetric flask that was then filled to the 1 L mark with MiliQ water. To obtain the Mars-analogue concentrations, 5 mL of the stock solution were transferred to a 500 mL volumetric flask that was then filled with MiliQ water. A separate dilution series was made from the stock by transferring 250 mL stock to a 500 mL volumetric flask, filling with MiliQ water and repeating to get a 4 times dilution.

All perchlorate salts are hydroscopic. To avoid absorption of water, a slight excess of each salt compared to the desired mass was placed in glass petri dishes and dried at 100 °C for 2.5 hours. Then $KClO_4$, $Mg(ClO_4)_2$ and $NaClO_4$ were taken out of the incubator and placed in a desiccator, where they were shielded from atmospheric water. However, $Ca(ClO_4)_2 \cdot 4\ H_2O$ had not been dehydrated, but rather dissolved in water and was therefore dried at 180 °C. After ~ 18 hours, $Ca(ClO_4)_2 \cdot 4\ H_2O$ was still wet and was therefore dried at 210 °C. After another ~ 18 hours the $Ca(ClO_4)_2 \cdot 4\ H_2O$ had lost excess water and solidified. It was placed in the desiccator with the other salts and taken to the weight – where it was fragmented using a spatula before being weighed. All salts were weighed and transferred to the volumetric flask within less than 3 minutes after being removed from the desiccator to avoid rehydration. Figure 19 shows the perchlorates in both the incubator and desiccator.

Figure 19: *The perchlorate salts in glass petri dishes being placed in the incubator (Left) and desiccator (Right).*

1.2. Measuring salinity

In addition to the salt solutions, regular tap water was also used as one of the conditions in this chapter. To ensure that the water was saturated with oxygen, it was bubbled using an atmosphere pump connected to a *Unisense* gas stone for 4 – 5 minutes. The salinity of every tested condition was measured using a *SevenGo* Conductivity-meter (Mettler Toledo) with inbuilt thermometer. The electrode was first calibrated in a conductivity standard and then washed with demineralized water, before it was placed in the plastic cup containing the solution. The salinity at the electrode in demineralized water was 0.01 ppt. It was washed between measurements. The conductivity-meter automatically corrected for temperature using the inbuilt thermometer – meaning the values determined are the true salinity of the solutions. All solutions were passed through a 0.22 μm mesh filter before measurement to mirror the conditions during oxygen profiling. Figure 20 shows pictures of the conductivity-meter, the display during measurement of the 100x Mars-analogue stock solution and the conductivity standards used for calibration.

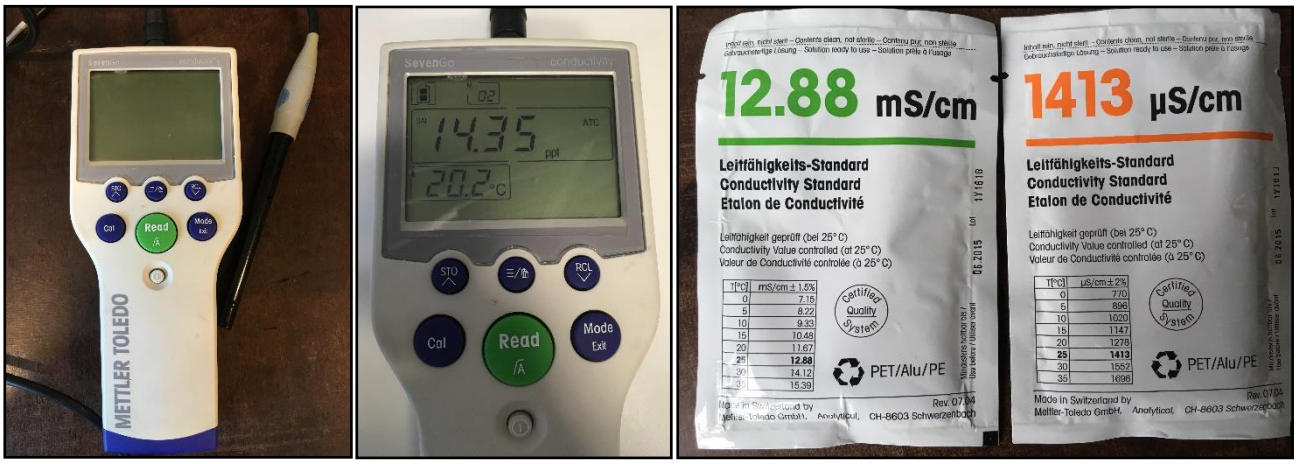

Figure 20: *Pictures of the conductivity-meter (Left), the display after measuring salinity of the 100x Mars stock solution of perchlorates (Middle) and unopened calibration fluid envelopes (Right). All pictures were taken with an iPhone SE camera.*

The conductivity standards were chosen based on the *Envco Conversion Table for Changing Conductivity into Salinity* – seen in appendix III. For the 0.16 ppt Mars-analogue solution, as well as MiliQ and oxygen saturated tap water, the 1413 μS/cm conductivity standard was used. The rest of the solutions were measured after calibration in the 12.88 ms/cm conductivity standard. These were the measured salinities:

$$MiliQ\ water: 0.01\ ppt; Tap\ water: 0.32\ ppt$$

$$NaCl: 3.85\ ppt, 7.87\ ppt, 16.0\ ppt\ and\ 31.5\ ppt$$

$$Mars\ Perchlorates: 0.16\ ppt, 3.40\ ppt, 7.12\ ppt\ and\ 14.4\ ppt$$

All measured salinities were close to the calculated values. The salinity of the Mars-analogue 0.16 ppt perchlorate solution is also consistent with the 1400 µS/cm described in Hecht *et al.* (2009). When calibrating the microsensors in *SensorTrace Pro*, the salinities had to be rounded off to whole numbers – i.e. 0 ppt for MiliQ and tap water, 4, 16 and 32 ppt for NaCl solutions and 0, 3 and 14 ppt for ClO_4^- solutions. The 8 ppt NaCl and 7 ppt ClO_4^- solutions were not used because of time constraints.

1.3. Statistical analysis

Mean values of the metabolic rate in steady-state under each condition was determined as described in Chapter 1. Sensors were calibrated in the given salt solution instead of in MiliQ water and D_{O_2} was adjusted for salinity – see appendix II. The metabolic rate in MiliQ water from Chapter 1 was plotted together with tap water and perchlorate solutions, whereas metabolic rates in NaCl solutions were plotted separately. The tardigrades measured in 14.4 ppt perchlorate solution was excluded from these plots, because it was unclear if any of them were in steady-state during the experiments.

To understand how the metabolic rate changes in response to the salt solutions outside of steady-state, $MR_{(t)}$ plots were constructed for every tardigrade measured. The time it takes for an oxygen microgradient to be established in a chamber and the narrowing of chamber a1 specifically (see appendix I) led to some complications for this part of the study. The issues are addressed in more detail in Chapter 5. As a result, the ultimate values of metabolic rate seen on $MR_{(t)}$ plots are not as accurate as those of steady-state studies. However, the trends they show are still correct and is what will be focused on. Regression analysis was used to determine the best fitted equations describing the trends seen on $MR_{(t)}$ for one tardigrade exposed to 14.4 ppt perchlorates. Because of time constraints, this was only done for the most interesting $MR_{(t)}$ of the study.

2. Results

2.1. Steady-state metabolism

The mean values of metabolic rate and weight ± sd at the different conditions can be seen on table 8. The data on MiliQ water from Chapter 1 is included.

Table 8: *Mean values of the metabolic rate and weight ± sd of R. coronifer in 0.01 ppt MiliQ water (n = 28), 0.32 ppt tap water (n = 4), Mars-analogue 0.16 ppt perchlorates (n = 8), 3.40 ppt perchlorates (n = 6), as well as NaCl solutions with salinities of 3.85 ppt (n = 6), 16.0 ppt (n = 3) and 31.5 ppt (n = 3).*

Salinity (water)	*Metabolic Rate* ($\frac{nmol\ O_2}{mg \cdot hour}$)	*Weight (µg)*
0.01	10.8 ± 1.84	15.3 ± 1.59
0.32	14.4 ± 1.56	14.8 ± 3.00
Salinity (ClO_4)		
0.16	13.4 ± 2.22	12.6 ± 2.16
3.40	17.4 ± 1.52	12.2 ± 1.83
Salinity (NaCl)		
3.85	17.7 ± 2.07	10.9 ± 3.39
16.0	8.79 ± 1.10	11.2 ± 3.96
31.5	4.86 ± 0.20	8.28 ± 2.18

All tardigrades exposed to 31.5 ppt & 16.0 NaCl solutions died from dehydration within the first 3 & 10 minutes respectively. Death was determined from the complete cessation of movement and shrivelling of the cuticle observed in real time through the horizontal microscopes. When exposed to 3.40 & 3.85 ppt solutions, most coordinated movement seized after 10 – 50 minutes of exposure but the cuticle remained intact. Only 3 of the 6 tardigrades exposed to 14.4 ppt perchlorates died within 10 minutes – same as those in 16 ppt NaCl solution. However, all 6 were dead during imaging after 1 – 2.5 hours. The metabolic rate of tardigrades decreases significantly with higher salinity for the NaCl solutions.

There was no change in movement or cuticle for tardigrades in the Mars-analogue solution or those in regular tap water. The metabolic rates between these two conditions were also similar. Both were higher than for MiliQ water, but lower than in the 3.40 ppt perchlorates and 3.85 ppt NaCl solutions. There was no significant difference in metabolic rate between 3.40 ppt perchlorates and 3.85 NaCl or between MiliQ water and 16 ppt NaCl – although there were morphological differences for the latter. For all other

conditions, the metabolic rate differed significantly. With the exception of 31.5 ppt NaCl, no relationship between size and salinity was found. Box-plots showing the distribution of metabolic rates at the different conditions can be seen on figure 21. Significance is marked as *ns* for $p > 0.05$ (not significant), * for $p < 0.05$, ** for $p < 0.01$ and *** for $p < 0.001$.

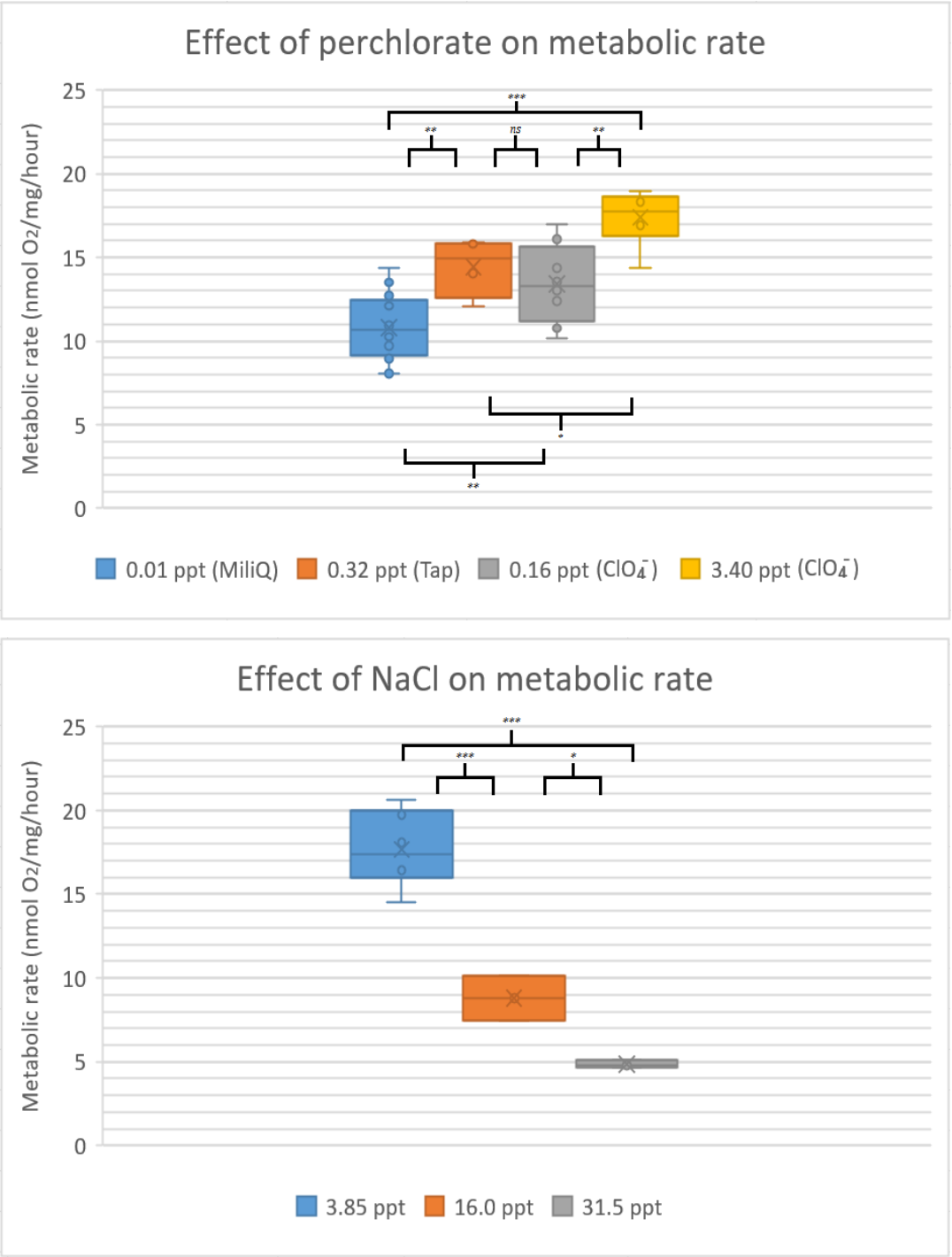

Figure 21: *Box-plots of the metabolic rate of R. coronifer in MiliQ water (n = 28), tap water (n = 4), Mars-analogue 0.16 ppt perchlorates (n = 8) and 3.40 ppt perchlorates (n = 6) (Top), as well as NaCl solutions with salinities of 3.85 ppt (n = 6), 16.0 ppt (n = 3) and 31.5 ppt (n = 3) (Bottom). Significance is marked as 'ns' for $p > 0.05$ (not significant), * for $p < 0.05$, ** for $p < 0.01$ and *** for $p < 0.001$.*

2.2 Metabolic response to salt solutions

The change in metabolic rate during exposure to perchlorates can be seen on figure 22.

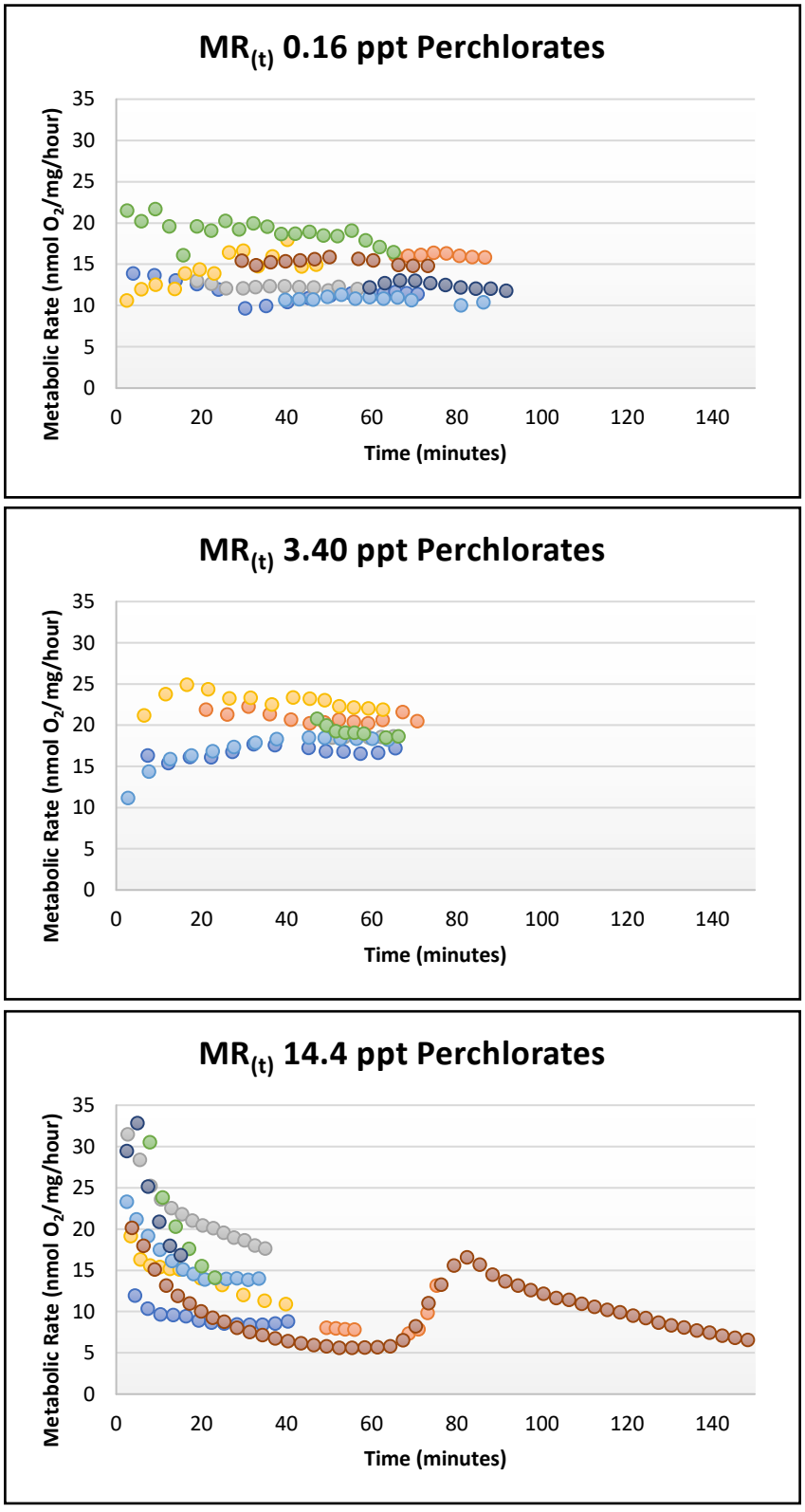

Figure 22: *$MR_{(t)}$ plots of tardigrades after transfer to perchlorate solution with salinity of 0.16 ppt (Top), 3.40 ppt (Middle) and 14.4 ppt (Bottom).*

At the Mars-analogue 0.16 ppt perchlorate, the metabolic rate seems to stabilize after ~ 30 minutes. Only 3 of 6 tardigrades were measured for the first 30 minutes after transfer. Two of those show a slight decline in metabolic rate in this period, whereas one increases ~ 50 % from 10 to 15 nmol O_2/mg/hour. At 3.40 ppt, metabolic rate stabilizes after ~ 40 minutes. 3 different trends are seen for the metabolic rates of the 3 tardigrades measured before then. One increases 25 % over the first 20 minutes from 20 to 25 nmol O_2/mg/hour and then decrease to 23 nmol O_2/mg/hour over the next 20 minutes before stabilizing; Another is stable for the first 20 minutes and then increase slightly during the next 20 minutes; The last one increases by 50 % over the first 20 minutes from 10 to 15 nmol O_2/mg/hour and then 20 % over the next 20 minutes from 15 to 18 nmol O_2/mg/hour – before reaching a steady-state.

The response to the 14.4 ppt perchlorate solution is the most complex of any condition studied. One tardigrade was measured for 2.5 hours from immediately after transfer and showed significant and sudden spikes and falls in its metabolic rate. For the first hour after transfer, it was decreasing exponentially. After 50 minutes it had decreased by 72 % from 20.1 to 5.6 nmol O_2/mg/hour. This was followed by 10 minutes of metabolic stability and then a sudden linear spike in metabolic rate of 286 % over the next 18 minutes from 5.8 to 16.6 nmol O_2/mg/hour. Immediately after this spike, the metabolic rate started to decrease again – this time linearly. The rate of decrease dropped to a third after the first 10 minutes and then remained constant. The initial steep decrease led to a drop in metabolic rate of 17.7 % over 10 minutes from 17 to 14 nmol O_2/mg/hour. The final decrease meant a 50 % drop in metabolic rate over one hour from 14 to 7 nmol O_2/mg/hour. Figure 23 shows this $MR_{(t)}$ with equations describing all 4 modes of change.

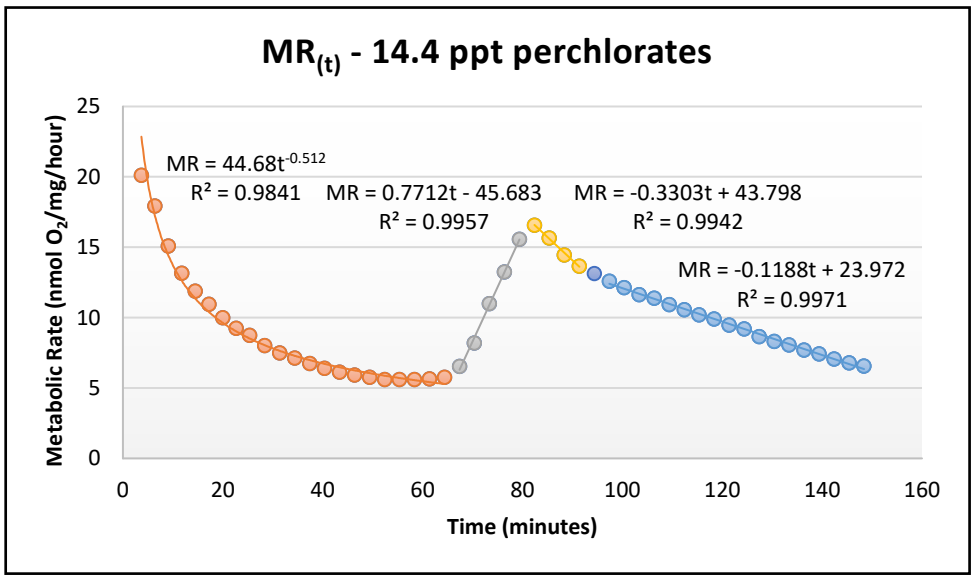

Figure 23: *$MR_{(t)}$ of one tardigrade in 14.4 ppt perchlorate solution with equations fitted to the 4 different modes of change in metabolic rate observed over 2.5 hours.*

Because the other tardigrades in 14.4 ppt perchlorate solution were only measured for ~ 40 minutes, it is difficult to say if their metabolic rates would follow the same pattern over 2.5 hours of exposure. 6 of them were measured for the first 40 minutes after transfer. 4 of those 6 tardigrades showed exponential decreases similar to that of figure 23 for the duration of the experiments. The other 2 also decreased exponentially for the first 10 minutes, but then started decreasing linearly instead. One tardigrade was measured from 45 – 75 minutes after transfer. Remarkably, its metabolic rate was stable in the same interval and then spiked at near-identical rate within 2 minutes of the spike seen on figure 23. The spike meant a 179 % increase in metabolic rate over 6.5 minutes from 7.3 to 13.15 nmol O_2/mg/hour. Unfortunately, profiling was seized before the spike had concluded, so it is unknown if the change in metabolic rate would have continued to mirror that of figure 23.

Figure 24 shows the $MR_{(t)}$ plots of tardigrades exposed to NaCl solutions. The change in metabolic rate over time is somewhat simpler for the NaCl solutions. At 3.85 ppt, all 4 tardigrades that were measured immediately after transfer show a 20 – 40 % increase in metabolic rate over the first 25 minutes. 3 of them become stable after those 25 minutes. The remaining one showed a linear decrease followed by a sudden spike and then another slower linear decrease in metabolic rate. This was also the case for the two tardigrades measured from 37 and 60 minutes after transfer respectively.

At 16.0 ppt NaCl, only one tardigrade was measured immediately after transfer. During the first 35 minutes, its metabolic rate decreased exponentially by 42.3 % from 21.3 – 12.3 nmol O_2/mg/hour. After that, it was in steady-state for 20 minutes followed by a linear decrease of 23.7 % over the remaining hour of the experiment from 13.5 to 10.3 nmol O_2/mg/hour. The two other tardigrades exposed to 16.0 ppt NaCl were measured from 60 – 80 and 40 – 100 minutes after transfer respectively. The first showed a slight linear decrease of 8 % over 20 minutes and the other a linear increase of 31.3 % over one hour.

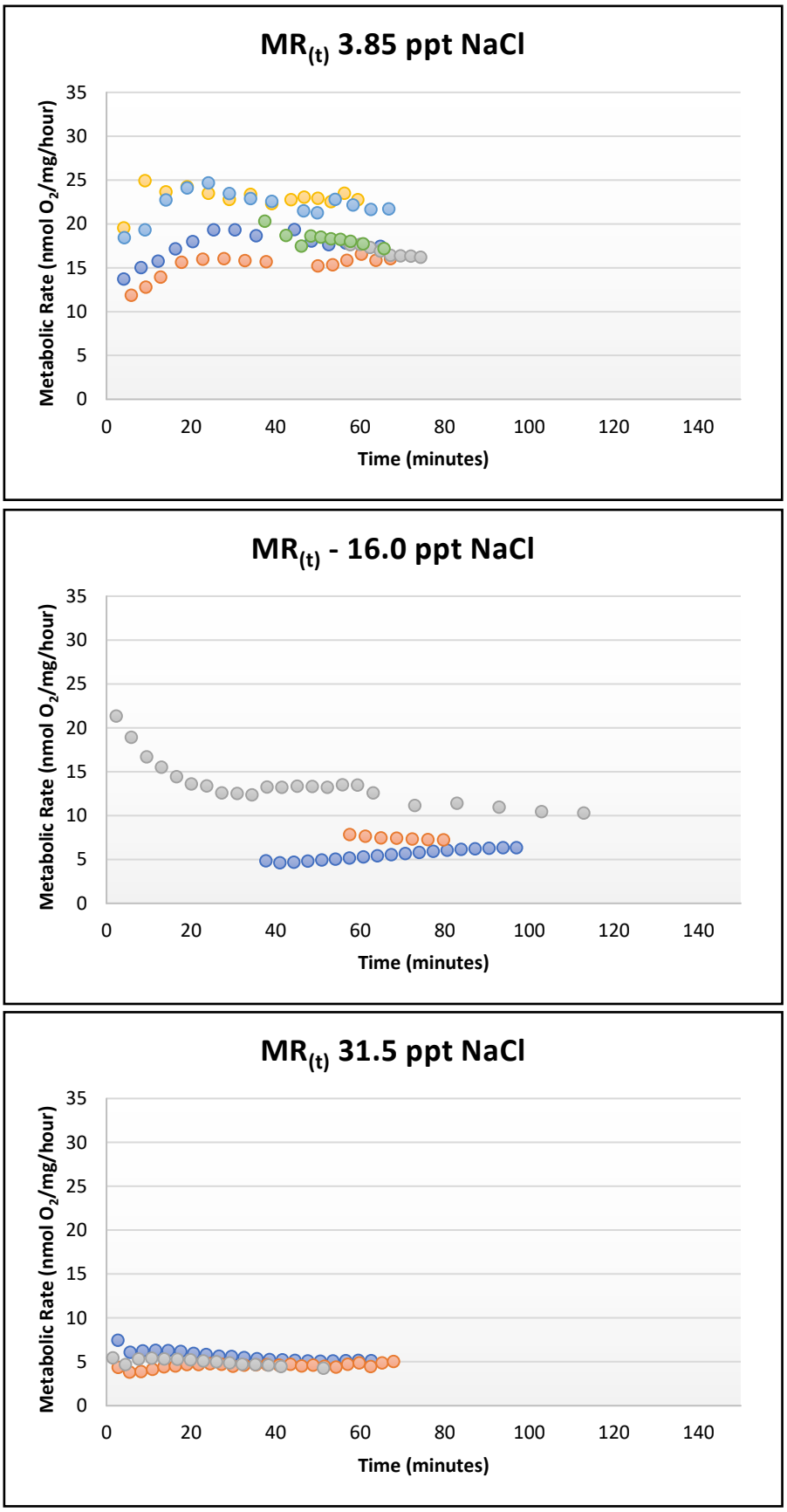

Figure 24: *$MR_{(t)}$ of tardigrades after transfer to NaCl solution with a salinity of 3.85 ppt (Top), 16.0 ppt (Middle) or 31.5 ppt (Bottom).*

By comparison, the tardigrades exposed to 31.5 ppt NaCl all appear to have stable metabolic rates just 5 minutes after transfer – although at substantially lower rates than for any other condition. The first two profiles of each tardigrade suggest that a decrease in metabolic rate has taken place in those 5 minutes – faster than the $MR_{(t)}$ plots can describe. However, the metabolic rate is not entirely stable after 5 minutes. Figure 25 shows how shortening the y-axes reveals different trends between the 3 tardigrades measured.

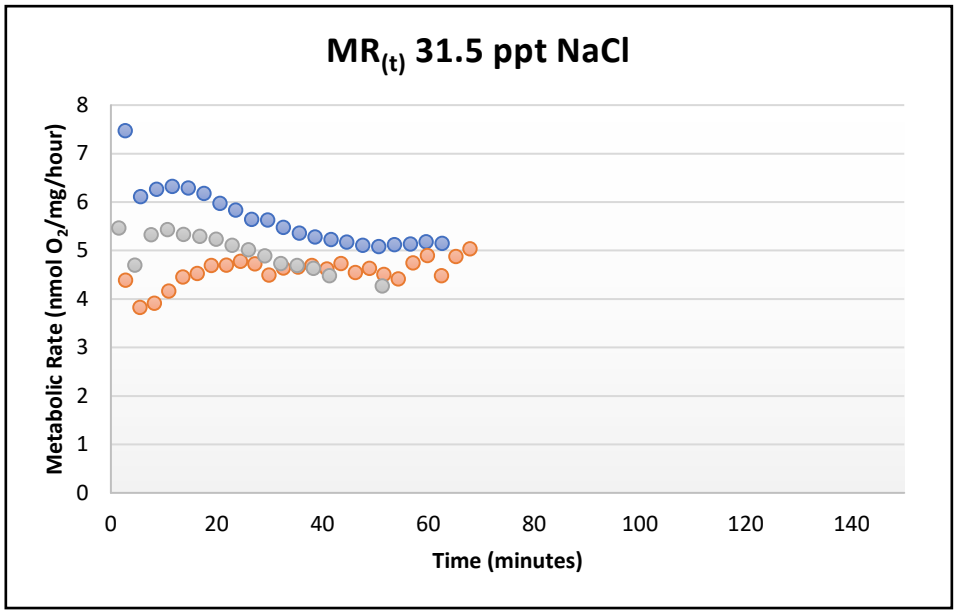

Figure 25: *$MR_{(t)}$ of the 3 tardigrades exposed to 31.5 ppt NaCl solution.*

One tardigrade showed a linear increase in metabolic rate of 26 % over 20 minutes from 3.8 to 5.0 nmol O_2/mg/hour, followed by steady-state. Another showed an increase of 14 % over 5 minutes from 4.7 to 5.4 nmol O_2/mg/hour, followed by a linear decrease of 21 % over the remaining 40 minutes from 5.4 to 4.3 nmol O_2/mg/hour. The final tardigrade showed a 2 % increase over 5 minutes from 6.1 to 6.3 nmol O_2/mg/hour. This was followed by an exponential decrease of 19 % over the next 40 minutes from 6.3 to 5.1 nmol O_2/mg/hour and then steady-state.

3. Discussion

The effects of osmotic pressure on metabolic rate can be determined by comparing solutions with the same solutes at different concentrations, whereas the effects of the solutes themselves can be determined by comparing solutions with similar salinities but different solutes. Metabolic rate clearly increases with salinity from 0 – 4 ppt regardless of solutes – most likely because of an osmoregulatory response that requires energy. The metabolic rate of tardigrades in Mars-analogue solution and regular tap water are similar – despite tap water having twice as high a salinity. This would suggest that the specific solutes do make a difference. Halberg *et al.*, (2013) found that the small ions Na^+, K^+, Ca^{2+}, Mg^{2+} and Cl^- were all present in *R. coronifer*, meaning it most likely has transport mechanisms for their uptake. The study did not find any ClO_4^- in *R. coronifer*, although it did leave 50.8 % of organic osmolytes unidentified. If no transport mechanism exists for the larger ClO_4^- anion, then that would increase the osmotic pressure and consequently dehydration in perchlorate solutions compared to NaCl solutions. This would affect osmoregulatory requirements and might explain why the metabolic rate is as high in the Mars-analogue solution as it is in tap water even though salinity is lower. The fact that ClO_4^- is the only ion from the salt solutions that is not known to be a part of the normal *R. coronifer* physiology also mean that it could have unique biochemical effects on the metabolism.

It may also be the case that the specific solutes do not affect metabolism, but that a 2x increase in salinity is simply not a big enough difference to require a stronger osmoregulatory response. In contrast, the increase in salinity between these conditions and the 3.40 ppt perchlorate solution are 11x & 22x respectively. Furthermore, the salinities are at least 16x and 32x higher than for MiliQ water, since the 0.01 ppt measured for this was the lowest value the conductivity meter could display. The tardigrades in Chapters 1 & 2 were measured in MiliQ water to keep the conditions as simple as possible. Using tap water would have better approximated the natural habitat of *R. coronifer* (Halberg *et al.*, 2013) but it would also have introduced unknown solutes that could affect the metabolism – as illustrated by the results in this chapter. Furthermore, since the composition of tap water varies significantly depending on area, results from tardigrades in tap water are less comparable across studies. The fact that movement, morphology and metabolic rate are all similar for tardigrades in the Mars-analogue solution and regular tap water suggests that perchlorates would not pose a problem for tardigrades under Martian conditions. However, synergistic effects of perchlorates and UV-radiation analogous to that on Mars have been shown to be deadly for certain extremophilic microorganisms (Wadsworth and Cockell, 2017).

The highest metabolic rates in this chapter were for tardigrades in 3.40 and 3.85 ppt solutions. There was no significant difference between the two solutions, which further suggest that the increase is due to an osmoregulatory response rather than any specific effects of perchlorate. All tardigrades in these solutions showed almost complete cessation of movement. As was the case in Chapter 2, cessation of movement did not correlate with any significant decrease in metabolic rate. In fact, these unmoving tardigrades had the highest metabolic rates found in this chapter – further indicating that muscle contractions are not a major factor for energy expenditure in the tardigrade. The decrease in metabolic rate for tardigrades in 16 and 31.5 ppt NaCl solutions is almost certainly due to death from dehydration. The remaining activity is from residual cellular respiration after the organism has died. It is lower in 31.5 ppt than in 16.0 ppt NaCl because cells dehydrate and die faster. If left ON, all metabolic rates at these conditions would most likely be the same as those of dead *R. coronifers* from Chapter 1. Møbjerg *et al.*, (2011) showed that *R. coronifer* have an upper lethal limit of ~ 500 mOsm/kg for NaCl solutions – roughly corresponding to a salinity of 14 ppt (Lenntech, 2018), whereas other species may survive as much as 2000 mOsm/kg. This means both solutions were above the upper lethal limit for salinity. The conditions were tested due to an error in unit conversion but are still useful for demonstrating the different effects on oxygen consumption between organism death and cellular death. No relationship between the volume of tardigrades and salinity was observed from 0 – 16 ppt, meaning that the tardigrades are not undergoing the type of cyclomorphosis described in Halberg *et al.*, (2009) & Møbjerg *et al.*, (2011). The volume was significantly lower for tardigrades in 31.5 ppt NaCl solution than for any other condition. It is possible that this is due to osmoconforming, but since all 3 tardigrades appear to die within 5 minutes of exposure, no effect of osmoconforming on metabolic rate could be established.

The $MR_{(t)}$ plots of tardigrades in the Mars-analogue solution do not reveal any consistent trends outside of steady-state. For tardigrades in 3.40 & 3.85 ppt solutions, it takes ~ 20 minutes to reach steady state at significantly higher metabolic rates – most likely due to a stronger osmoregulatory response. The most interesting $MR_{(t)}$ plots are those of tardigrades exposed to 14.4 ppt perchlorates and 16 ppt NaCl – near the upper lethal limit of salinity for *R. coronifer*. Although salinity is relatively similar, the $MR_{(t)}$ plots are very different. This could be related to the larger size and likely lack of transport mechanisms for the ClO_4^- anion or alternatively some unresolved biochemical protective functions of perchlorate. However, the simplest explanation is that 14.4 ppt is close enough to the lethal limit of 14 ppt for some tardigrades to survive at least briefly, whereas 16 ppt is not. Whether it is caused by specific effects of perchlorate or the

difference in salinity, it may be the case that some of the tardigrades in the 14.4 ppt perchlorate solution are attempting to enter cryptobiosis – specifically osmobiosis. It would typically not be possible to measure the metabolic rate during entry into cryptobiosis – since most studies focus on anhydrobiosis, which requires desiccation, and the method requires a liquid phase to measure the microgradient across.

Only one of the tardigrades was measured for long enough to see more than two different modes of change in the metabolic rate during exposure. However, almost all tardigrades at 14.4 ppt perchlorate showed the same mode of action as that specific tardigrade in the measured time-frames. Because of this, it seems likely that they would follow the same pattern over longer periods – although further experimentation is required to confirm this. The $MR_{(t)}$ can be interpreted as 5 distinct phases. In Phase 1, the dangerous conditions are registered and preparation for cryptobiosis begins. This causes an exponential decrease in metabolic rate as unnecessary processes are eliminated over ~ 50 minutes. Phase 2 consists of ~ 10 minutes where the metabolic rate is constant and equivalent to that of dead tardigrades in 16 ppt NaCl. This phase may involve settling into the new physiological conditions and ensuring that the tardigrade is ready for Phase 3. Phase 3 is the sudden spike in metabolic rate and could be a preparatory phase where the necessary modifications for cryptobiosis are undertaken – e.g. organ packing, muscle contractions, changes to gene-expression, trehalose synthesis and vitrification (Crowe, 1975; Ramløv and Westh, 1992; Crowe, Carpenter and Crowe, 1998; Hashimoto *et al.*, 2016; Boothby *et al.*, 2017). Phase 4 is a short but steep linear decline in metabolic rate and Phase 5 is the much longer but less steep decline that follows. These phases would be the abrupt cessation of some preparatory modifications and the more gradual cessation of other modifications respectively. One of the tardigrades in 16 ppt NaCl appear to have attempted the same regulation of metabolic rate for the first 60 minutes of exposure. It spends 10 minutes less in Phase 1 and 10 minutes more in Phase 2 compared to those in 14.4 ppt perchlorates. Within the same 2-minute interval where Phase 3 begins for the tardigrades in 14.4 ppt perchlorates, the $MR_{(t)}$ instead goes from steady-state to linear decrease. This supports the idea that Phase 1 & 2 was controlled by the same underlying mechanisms. It also suggests that this tardigrade attempted to initiate the same processes that underlie Phase 3 but failed and died because of it. Likewise, the change from exponential to linear decrease for two of the tardigrades in 14.4 ppt perchlorates during Phase 1 may indicate that they died from elimination of processes that were unnecessary for cryptobiosis.

All tardigrades exposed to 14.4 ppt perchlorates appeared dead during imaging and there was no tun formation. This means that if they did attempt to enter cryptobiosis, it was not successful. In light of this,

it may be the case that Phase 3 was not completed for any of them due to excessive damage and that the decline in metabolic rate seen in Phase 4 & 5 was caused by death rather than a controlled cessation of specific processes. It is also possible that none of these phases are related to cryptobiosis, but they are almost certainly caused by some type of physiological regulation. If the spike in oxygen consumption was simply caused by mechanical or chemical degradation, then it should not be occurring within the same 2 minute-interval regardless of the size of the tardigrade. Furthermore, if the physiological condition of the tardigrades were irrelevant, then the tardigrade in 16 ppt NaCl following the same pattern should spike as well – instead of changing to a linear decline. The highest metabolic rates for tardigrades in the 14.4 & 16 ppt solutions were seen at the first profiles measured 2 – 5 minutes after transfer. In this brief time span, the mean metabolic rates were ~ 22 nmol O_2/mg/hour. This is significantly higher than for tardigrades in 3.40 & 3.85 ppt solutions – even after 20 minutes when steady-state had been reached. This means that the osmoregulatory response can continue to drive up metabolic rate to match the salinity for the entire range of survivable salinities. The limit to this effect appear to be approximately 3 times that of active tardigrades in MiliQ water. It also means that the speed of the response can be increased – at least under critical conditions. The response does not occur faster at 3.4 & 3.85 ppt solutions than in the 0.16 ppt perchlorate solution. In fact, the opposite appears to be the case – although this may be because the magnitude of the response is smaller. No consistent relationship between salinity and osmoregulatory response-time could be concluded from this. $MR_{(t)}$ plots for tardigrades in 8 ppt solutions would be interesting in this regard. If the 3 tardigrades in 31.5 ppt NaCl mounted any osmoregulatory response, its effects on metabolic rate were eliminated in less than 2 minutes before $MR_{(t)}$ plots began. Most likely, they died too quickly for any increase in metabolic rate to occur. The fact that all 3 tardigrades show different non-steady-state trends means no generally valid interpretations can be made for them.

To better understand the effects on metabolic rate from osmoregulatory responses and potentially osmobiosis, more replications at the conditions of this study are required – as well as experiments at other salinities below the lethal limit. To better understand the effects of specific solutes, large molecules such as PEG or glucose could be used. The $MR_{(t)}$ plots should span at least 3 hours and if possible, describe the first 5 minutes of exposure in more detail. This is complicated by the need for an oxygen microgradient to be established first but measuring in shorter chambers and at shorter distances might be sufficient to solve this problem. Step-size should be lowered to calculate the slope of gradients from more data and most importantly, chambers should be perfectly cylindrical to avoid any overestimation of the ultimate values.

Chapter 4: Cryptobiosis

1. Materials and Methods

1.1. Desiccation

The metabolic rate of 9 desiccated *R. coronifer* tuns were measured during rehydration and termination of cryptobiosis. To prepare these tuns, various techniques for desiccation were employed. The first 6 tuns were desiccated using a customized desiccation tube set-up. The tubes were constructed by cutting the lid and the bottom end of a standard 1.5 mL Eppendorf tube off. A fitting piece of micro-pore net was cut and placed around the top of the e. tube – where it was fixated by an elastic. The tube was then placed net-first into 50 – 70 mesh sand (SiO_2, Sigma-Aldrich). Once a sufficient number of active tardigrades had been collected, they were transferred into the tube using a Pasteur pipette to avoid damaging them. The pipette was wetted before transfer to avoid tardigrades sticking to its interior. After transfer, the top of the tube was covered with tin foil to ensure that water evacuated unidirectionally. The tardigrades were left to desiccate for 2 – 4 days. The micro-pore net was then removed and inspected under a stereo loop to ensure that they had successfully formed tuns. Pictures showing this process can be seen on figure 26.

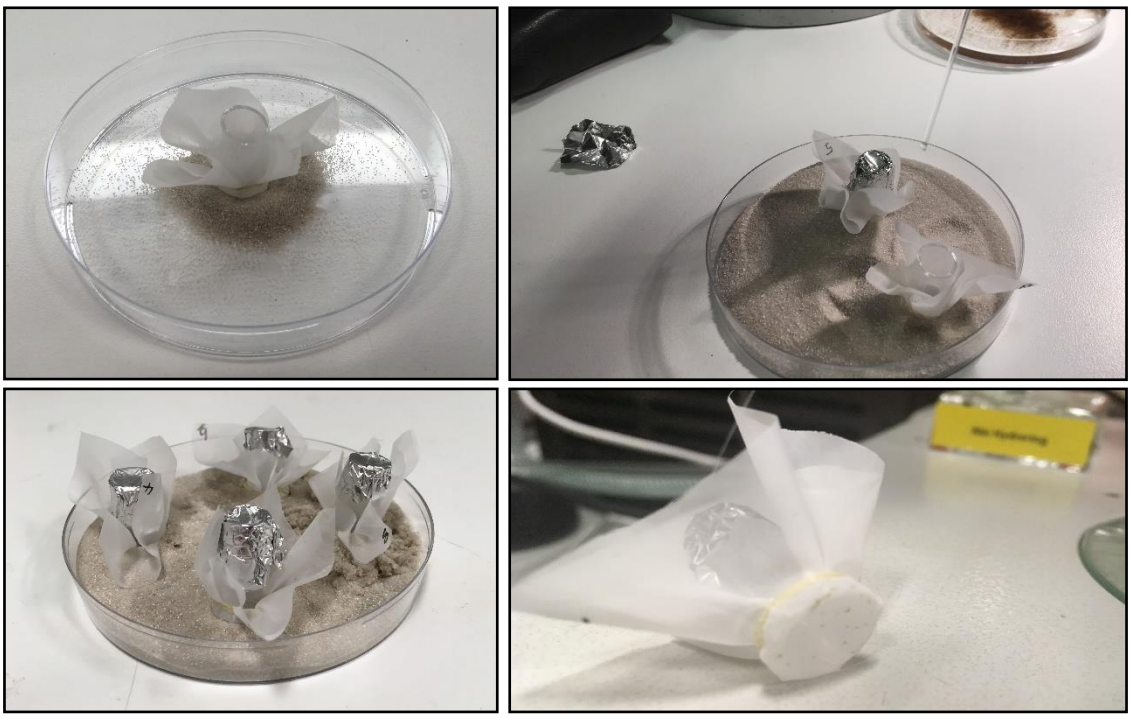

Figure 26: *Desiccation tubes before transfer of tardigrades (Top-left), during transfer (Top-Right), after transfer (Bottom-left) and after desiccation is complete (Bottom-Right). Pictures were taken with iPhone SE.*

Tuns 1 – 4 were desiccated on Net 3, December 2nd 2017 – meaning tuns 1 – 2 had been in cryptobiosis for 70 days and tuns 3 – 4 for 74 days prior to rehydration. Tuns 5 – 6 were desiccated on Net 4, February 13th 2018 – meaning they were only in cryptobiosis for ~ 24 hours before rehydration. However, none of these tardigrades appeared to regain their activity upon rehydration. The viability of tardigrades desiccated on micro-pore net was found to be low in a series of side-experiments described in Chapter 5. Because of this, different desiccation techniques were used for the remaining tuns.

Tuns 7 – 8 were collected directly from the moss, by grinding it through the parsley cutter and sorting through the fragments found in Fraction 250 under a stereo loop without water. This eliminated the need for a desiccation step, simplifying the process and reducing the risk of damage from handling. It also allowed tardigrades that had been desiccated for more than a year to be measured during termination of cryptobiosis. However, it is impossible to know exactly how long these tardigrades had been in cryptobiosis. Although it avoids the potential damage from a desiccation step, the tuns may be less viable because of accumulated damage during the time spent in cryptobiosis. The addition of a hydration and subsequent desiccation step may risk damaging the tardigrades, but it also selects for those that do regain full activity after their longest period of cryptobiosis – in this study > 1.5 years. Another issue with transferring tuns directly from moss is the difficulty of determining the species in this state. Tun 7 was found to be a rotifer of unknown species from the imaging done after rehydration.

Tuns 9 – 10 both regained activity during the viability tests described in Chapter 5. Afterwards, they were transferred to *Whatman 3* filter paper to be desiccated again. The paper was fitted to an empty petri dish and the tardigrades were transferred with the wetted Pasteur pipette. The petri dish was left on the laboratory bench ON with no lid on. Figure 27 shows a picture taken through a stereo loop ocular of still active tardigrades immediately after transfer to the *Whatman 3* filter paper.

Figure 87: *Picture of active tardigrades transferred to Whatman 3 paper under stereo loop.*

1.2. Hydration

Tuns 1 – 6 were each scraped off the micro-pore net using the Irwin Loop, transferred to a chamber with MiliQ water and then placed in an aquarium. Tuns 7 – 8 were also transferred with the loop in dry state but did not have to be released from any surface first. For tuns 9 – 10, adding a few drops of water was found to release them from the filter paper and make transfer with the loop easier. This was done very quickly to minimize the time spent rehydrating without being measured. The exact moment of exposure to water was noted for each tun and set as $t = 0$, so $R_{(t)}$ plots would accurately depict the rehydration process. Tuns 7 – 10 were all rehydrated in oxygen saturated tap water. This was done to try and solve the viability issue – since the tardigrades used in Chapters 1 – 3 were all rehydrated in tap water rather than MiliQ water. During rehydration, chamber a1 was removed from the set-up with tun 7 and inspected for issues that might contribute to the low viability of tuns. Tun 8 got stuck in a hole at the bottom of chamber a4 and had to be released from it with the loop. Afterwards, profiling was resumed for both tuns which led to an interruption in their $R_{(t)}$ plots. All capillary chambers were examined for potential contributions to the low viability. Chambers a1 and a2 were disqualified because the narrowing near the bottom caused the tuns to be almost surrounded by glass – potentially exerting resistance toward the growth and subsequent extension of the tardigrades body. Chamber a3 was inconvenient for observations during profiling, as the glass droplet below the chamber blocked the view from the horizontal microscope. Chambers b1–4 and c1 showed no potential issues and tuns 9 – 10 were rehydrated in chambers c1 & b2 respectively – see appendix I. Both became fully active upon hydration.

1.3. Follow-up

The tardigrades from tuns 1 – 4 & 9 were left in the capillary chambers after rehydration to see how the oxygen consumption would change over longer periods. Tuns 1 – 2 were measured on day 4 after rehydration, tuns 3 – 4 were measured on day 2 and tun 9 on day 8. After tuns 1 – 2 had been removed, the chambers were washed with 70 % ethanol and measured again. After being measured on day 2, tuns 3 – 4 were removed from the chambers with the loop, dipped in ethanol for 3x 10 seconds then placed back into their respective chambers and measured again. This was done to test for any biofilm formation on the surface of tardigrades that might interfere with the successful termination of cryptobiosis. For comparison, the same was done to tuns 5 – 6 immediately after rehydration.

1.4. Statistical Analysis

$R_{(t)}$ plots describing the termination of cryptobiosis were constructed based on the same criteria as the $MR_{(t)}$ plots in Chapter 3 – from the bottom 400 – 1200 μm of the oxygen profiles. The issue of narrowing toward the bottom of chamber a1 is described in Chapter 5 – using the rotifer as an example. Due to the positioning of the sensor, the issue is more pronounced for the oxygen profiles of the rotifer than for any of the tardigrades. Because of this, the respiration of the rotifer was only calculated from the microgradient across the parallel part of the chamber. This meant the first 6 profiles had to be excluded and the plot begins 32 minutes after transfer – when the gradient has been fully established. Tuns 1, 4 & 5 were also profiled in chamber a1 – meaning the values are slightly overestimated. However, after the first 30 minutes, all *R. coronifer* tuns showed < 4 % change to respiration – depending on whether it was calculated from the full gradient or from the bottom 400 – 1200 μm. Tun 3 was lost before it was imaged, and its metabolic rate could therefore not be calculated. As in Chapter 3, finding consistent trends over time are more important than comparing the ultimate values for different tardigrades. Because of this, $R_{(t)}$ plots were constructed instead of $MR_{(t)}$ to maximize the number of plots that were compared. Metabolic rate was still calculated for the other tuns. However, these values may be misleading – since the weight of the tuns change during rehydration. The weight of the rotifer was calculated the same way as that of tardigrades.

$R_{(t)}$ plots were also constructed for the follow-up studies and mean values we calculated for steady-states as in Chapter 1 – 3. To evaluate the hypothesis that the respiration seen in follow-up studies from day 2 – 8 after rehydration were due to biofilm, the thickness necessary for a biofilm to account for this respiration was calculated. Based on the description of *K-12 e. coli* in table 4 of Riedel *et al.*, (2013), the average surface and oxygen consumption of single microbes were assumed to be 1 μm^2 and $4 \cdot 10^{-10}$ μmol O_2/day ≈ $1.67 \cdot 10^{-8}$ nmol O_2/hour. By dividing the total respiration with the respiration of a single microbe, the number of microbes required to account for the microgradient was found. By dividing their combined surface with the surface of the given tardigrade, the layers of biofilm necessary to account for the oxygen consumption was calculated. The surface of tardigrades was calculated as described in Chapter 1.

2. Results

2.1. Termination of cryptobiosis

Respiration appears to increase immediately after transfer but starts to decrease within the 30 minutes it takes for the gradient to fully establish throughout the chambers. Figure 28 shows this for profiling of tun 3 in *SensorTrace Pro* over 1.7 hours.

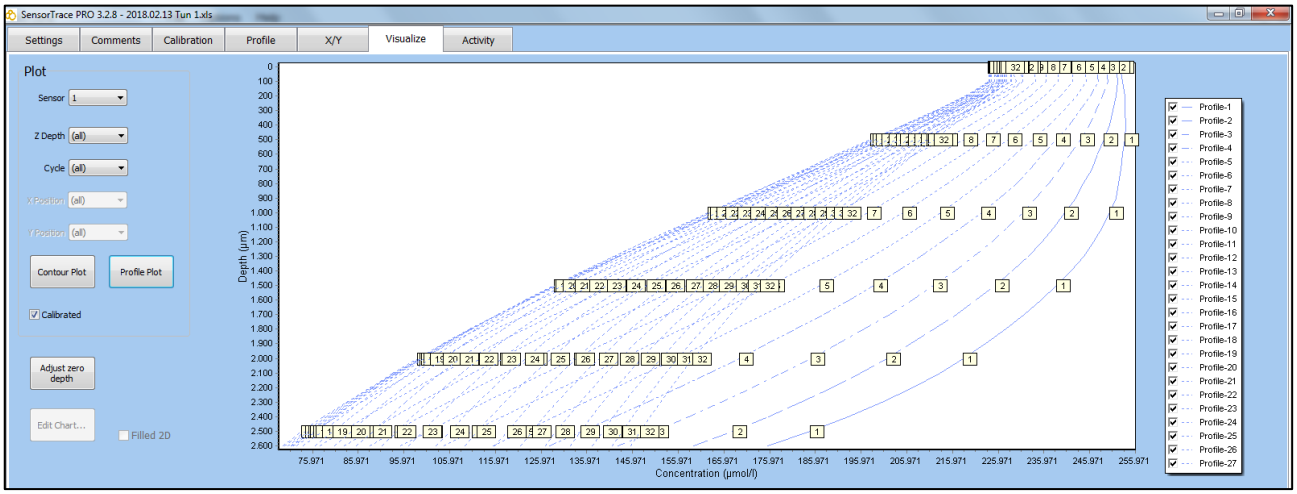

Figure 28: *Screenshot of hydration for tun 3 in chamber a3. Profiles are numbered chronologically with 3 minutes interval*

Tun 1 hydrated to a damaged tardigrade and showed no coordinated activity at any point in the process. Tuns 2 – 6 all hydrated to intact tardigrades and showed weak movement during profiling but appeared dead during imaging. Tun 8 appeared to go through moulding during or immediately after rehydration but showed no signs of movement. Tuns 9 – 10 both hydrated to intact and clearly active tardigrades during profiling. They continued to show coordinated movement during imaging the next day – although less than the tardigrades from Chapter 1. Figure 29 shows the $R_{(t)}$ plots of all tardigrades during rehydration. The tardigrades have been divided into separate plots based on maximum respiration. Tuns 1 – 4 & 6 have maximum respirations below 0.2 nmol O_2/hour whereas tuns 5 & 8 – 10 have maximum respirations of 0.3 – 0.4 nmol O_2/hour. Furthermore, tuns 8 – 10 were measured ON, so their $R_{(t)}$ plots are shown at two different time frames – 6 hours and 24 hours.

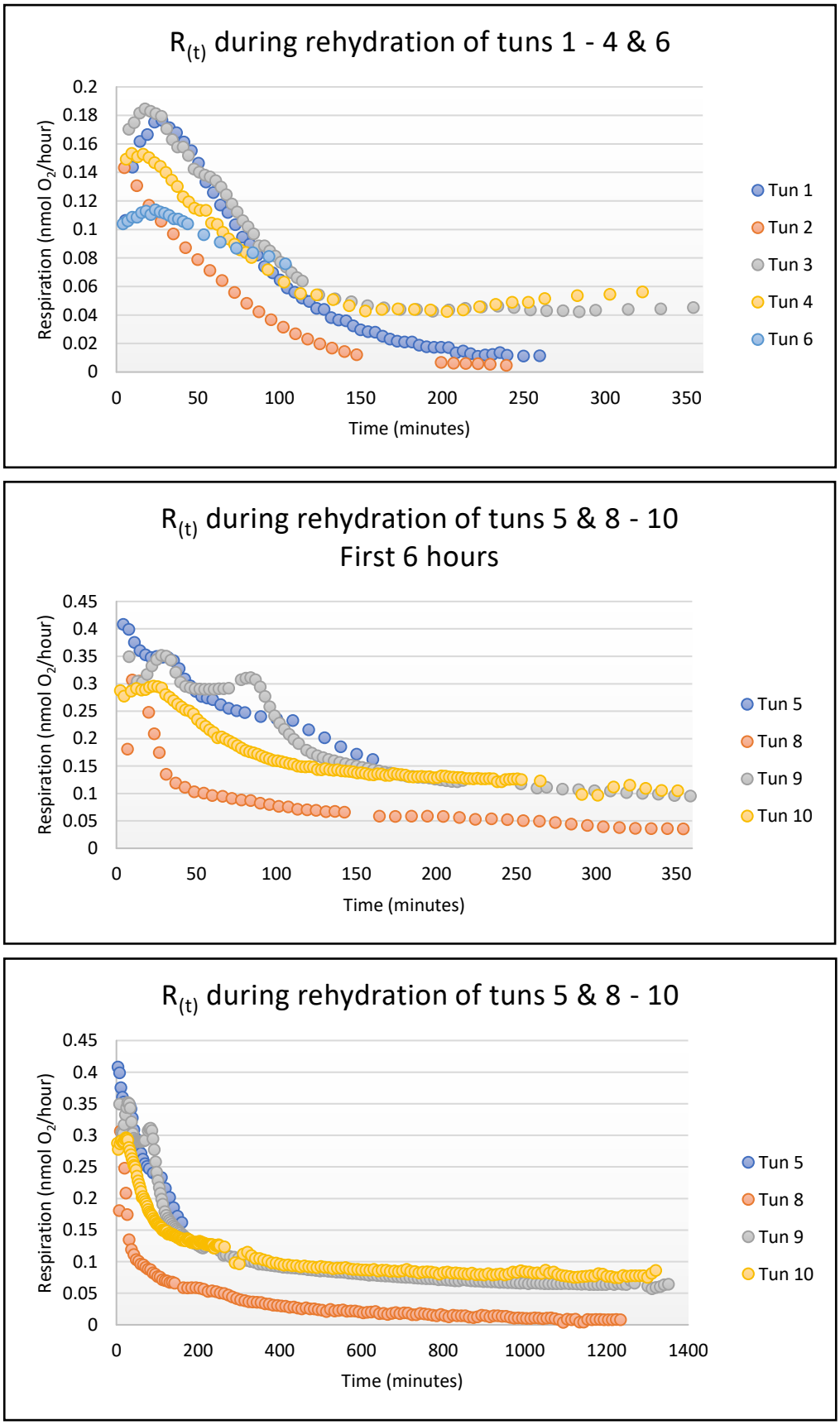

Figure 29: *$R_{(t)}$ plots of tuns 1 – 4 & 6 for 6 hours after transfer to water (Top) and tuns 5 & 8 – 10 for 6 hours (Middle) and 24 hours (Bottom) after transfer respectively.*

Respiration during termination of cryptobiosis can be meaningfully divided into 3 zones. Zone 1 is the initial stability and local peaks in respiration. Zone 2 is the exponential decrease where most of the respiration disappears. In this study, it is defined as the period where 95 % of the total decrease occurs. Zone 3 is the much longer period where the last 5 % of the decrease occurs. Table 9 shows the duration, respiration and metabolic rate in each of the three zones for every tardigrade – including details about the method of desiccation, time spent in cryptobiosis and the state of the tardigrade after hydration. The state is categorized as either damaged, intact or active – based on the condition of the cuticula and the mobility of the tardigrade.

Table 9: Time, respiration and metabolic rate of every tardigrade during zones 1 – 3. Details specify the method of desiccation, time spent in cryptobiosis before rehydration and state of the tardigrade during imaging after hydration.

Tun 1	*Time (min)*	*Respiration* ($\frac{nmol\ O_2}{hour}$)	*Metabolic Rate* ($\frac{nmol\ O_2}{mg \cdot hour}$)	*Details*
Zone 1	0 – 30	0.1063 – 0.1766	11.4 – 19.0	Desiccated on: Net
Zone 2	30 – 190	0.1766 – 0.0192	19.0 – 2.03	Cryptobiosis: 70 days
Zone 3	190 +	0.0192 – 0.0113	2.03 – 1.21	After Hydration: Damaged

Tun 2	*Time (min)*	*Respiration* ($\frac{nmol\ O_2}{hour}$)	*Metabolic Rate* ($\frac{nmol\ O_2}{mg \cdot hour}$)	*Details*
Zone 1	None	X	X	Desiccated on: Net
Zone 2	0 – 150	0.1433 – 0.0115	22.5 – 1.89	Cryptobiosis: 70 days
Zone 3	150 +	0.0115 – 0.0046	1.89 – 0.71	After Hydration: Intact

Tun 3	*Time (min)*	*Respiration* ($\frac{nmol\ O_2}{hour}$)	*Metabolic Rate* ($\frac{nmol\ O_2}{mg \cdot hour}$)	*Details*
Zone 1	0 – 20	0.1702 – 0.1846	X	Desiccated on: Net
Zone 2	20 – 140	0.1846 – 0.0496	X	Cryptobiosis: 74 days
Zone 3	140 +	0.0496 – 0.0425	X	After Hydration: Damaged

Tun 4	*Time (min)*	*Respiration* ($\frac{nmol\ O_2}{hour}$)	*Metabolic Rate* ($\frac{nmol\ O_2}{mg \cdot hour}$)	*Details*
Zone 1	0 – 20	0.1491 – 0.1503	15.7 – 15.8	Desiccated on: Net
Zone 2	20 – 140	0.1503 – 0.0481	15.8 – 4.89	Cryptobiosis: 74 days
Zone 3	140 +	0.0481 – 0.0561	4.89 – 5.90	After Hydration: Intact

Tun 5	*Time (min)*	*Respiration* ($\frac{nmol\ O_2}{hour}$)	*Metabolic Rate* ($\frac{nmol\ O_2}{mg \cdot hour}$)	*Details*
Zone 1	0 – 35	0.4084 – 0.3422	23.9 – 20.0	Desiccated on: Net
Zone 2	35 – 160	0.3422 – 0.1621	20.0 – 9.49	Cryptobiosis: 24 hours
Zone 3	Unknown	X	X	After Hydration: Intact

Tun 6	*Time (min)*	*Respiration* ($\frac{nmol\ O_2}{hour}$)	*Metabolic Rate* ($\frac{nmol\ O_2}{mg \cdot hour}$)	*Details*
Zone 1	0 – 25	0.1039 – 0.1138	13.5 – 14.8	Desiccated on: Net
Zone 2	25 – 105	0.1138 – 0.0757	14.8 – 9.82	Cryptobiosis: 24 hours
Zone 3	Unknown	X	X	After Hydration: Intact

Tun 8	*Time (min)*	*Respiration* ($\frac{nmol\ O_2}{hour}$)	*Metabolic Rate* ($\frac{nmol\ O_2}{mg \cdot hour}$)	*Details*
Zone 1	0 – 10	0.1809 – 0.3068	17.1 – 29.0	Desiccated on: Moss
Zone 2	10 – 505	0.3068 – 0.0230	29.0 – 2.17	Cryptobiosis: > 1.5 years
Zone 3	505 +	0.0230 – 0.0081	2.17 – 0.76	After Hydration: Damaged

Tun 9	*Time (min)*	*Respiration* ($\frac{nmol\ O_2}{hour}$)	*Metabolic Rate* ($\frac{nmol\ O_2}{mg \cdot hour}$)	*Details*
Zone 1	0 – 90	0.3493 – 0.2947	25.0 – 21.1	Desiccated on: Whatman 3
Zone 2	90 – 900	0.2947 – 0.0688	21.1 – 4.91	Cryptobiosis: 18 hours
Zone 3	900 +	0. 0688 – 0.0571	4.91 – 4.09	After Hydration: Active

Tun 10	*Time (min)*	*Respiration* ($\frac{nmol\ O_2}{hour}$)	*Metabolic Rate* ($\frac{nmol\ O_2}{mg \cdot hour}$)	*Details*
Zone 1	0 – 30	0.2876 – 0.2806	22.2 – 21.6	Desiccated on: Whatman 3
Zone 2	30 – 720	0.2806 – 0.0849	21.6 – 6.54	Cryptobiosis: 18 hours
Zone 3	720 +	0. 0849 – 0.0746	6.54 – 5.75	After Hydration: Active

2.2. Comparison with rotifer

Figure 30 shows an image of the rotifer after hydration and its $R_{(t)}$ plot during termination of cryptobiosis.

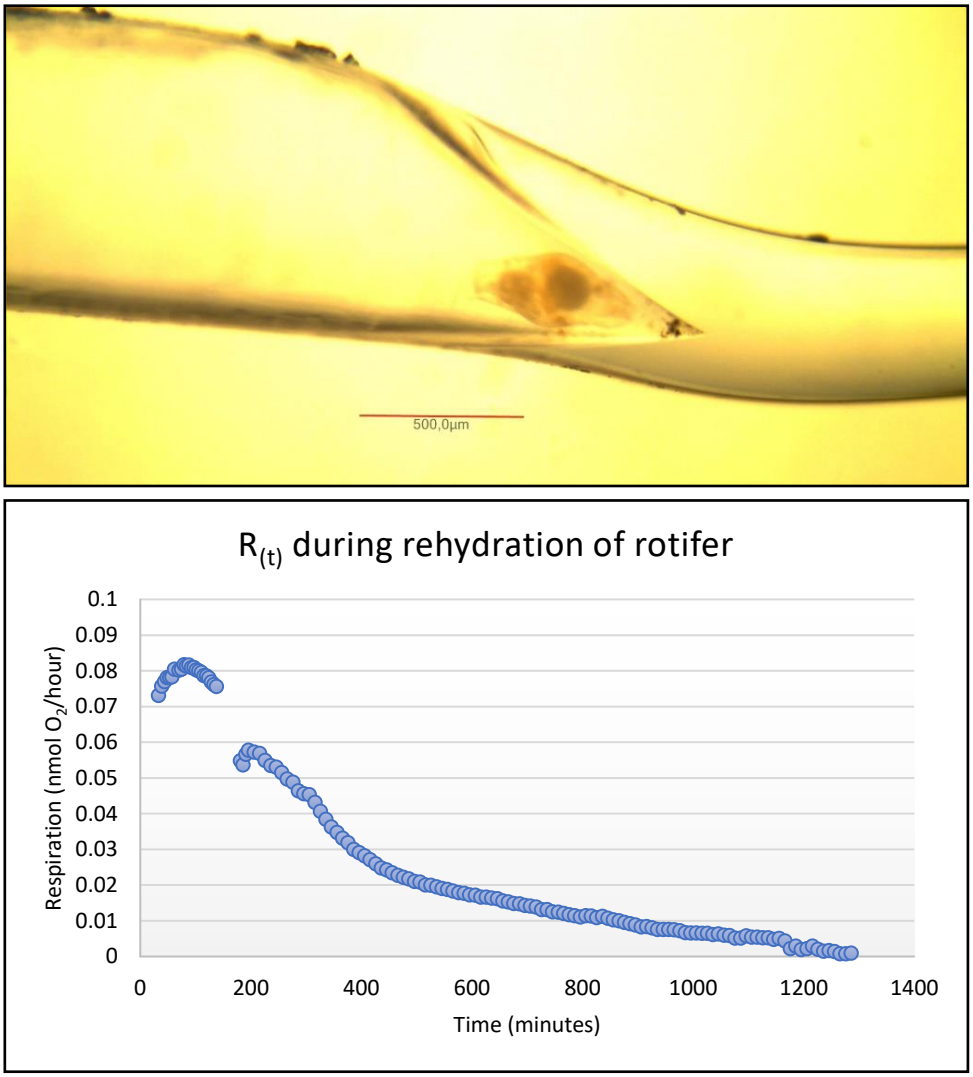

Figure 30: *Image of rotifer after rehydration (Top) and $R_{(t)}$ plot of its respiration during*

Table 10 describes the three zones of the rotifer and details regarding the method of desiccation, time spent in cryptobiosis and state of the rotifer after hydration.

Table 10: *Time, respiration and metabolic rate of the rotifer during zones 1 – 3, as well as relevant details.*

Tun 7	*Time (min)*	*Respiration* ($\frac{nmol\ O_2}{hour}$)	*Metabolic Rate* ($\frac{nmol\ O_2}{mg \cdot hour}$)	*Details*
Zone 1	0 – 90	0.0731 – 0.0816	5.82 – 6.50	Desiccated on: Moss
Zone 2	90 – 1140	0.0816 – 0.0049	6.50 – 0.38	Cryptobiosis: > 1.5 years
Zone 3	1140 +	0.0049 – 0.0009	0.38 – 0.07	After Hydration: Intact

2.3. Follow-up

Table 11 shows mean values for respiration and metabolic rate of the tardigrades during follow-up studies. The metabolic rate is simply to correct for size and should not be attributed to the dead tardigrades. The table also shows the calculated layers of biofilm necessary to account for the respiration and details regarding the tardigrade.

Table 11: *The mean respiration and metabolic rate ± SD for follow-up of tuns 1 – 6 & 9, the calculated layers of biofilm necessary to account for the respiration, time spent in cryptobiosis from last desiccation step until rehydration and the condition of the tardigrade during imaging.*

	Respiration ($\frac{nmol\ O_2}{hour}$)	*Metabolic Rate* ($\frac{nmol\ O_2}{mg \cdot hour}$)	*Biofilm*	*Cryptobiosis*	*After hydration*
Day 1	T5: 0.0563 ± 0.0031	3.29 ± 0.18	7.92	24 hours	Intact
	T6: 0.0243 ± 0.0048	3.15 ± 0.62	6.09	24 hours	Intact
Day 2	T3: 0.1549 ± 0.0075	X	X	74 days	Damaged
	T4: 0.0518 ± 0.0016	5.45 ± 0.17	10.9	74 days	Intact
Day 4	T1: 0.2261 ± 0.0018	24.3 ± 0.19	43.3	70 days	Damaged
	T2: 0.1453 ± 0.0018	22.8 ± 0.28	40.6	70 days	Intact
Day 8	T9: 0.2034 ± 0.0026	14.6 ± 0.17	33.2	18 hours	Active

The respiration increases from day 1 – 4 but remains the same from day 4 – 8. When correcting for the size of tardigrades, the increase is the same but from day 4 – 8 it decreases. The respiration is higher for damaged than for intact tardigrades measured after the same number of days. Because of the low sample size and different conditions of these follow-ups, the results are not interpreted beyond their implication for the importance of biofilm in the low viability of tuns. Figure 31 shows the $R_{(t)}$ plots of follow-ups from day 2 – 8 and the change in respiration for tuns 3 – 4 ON.

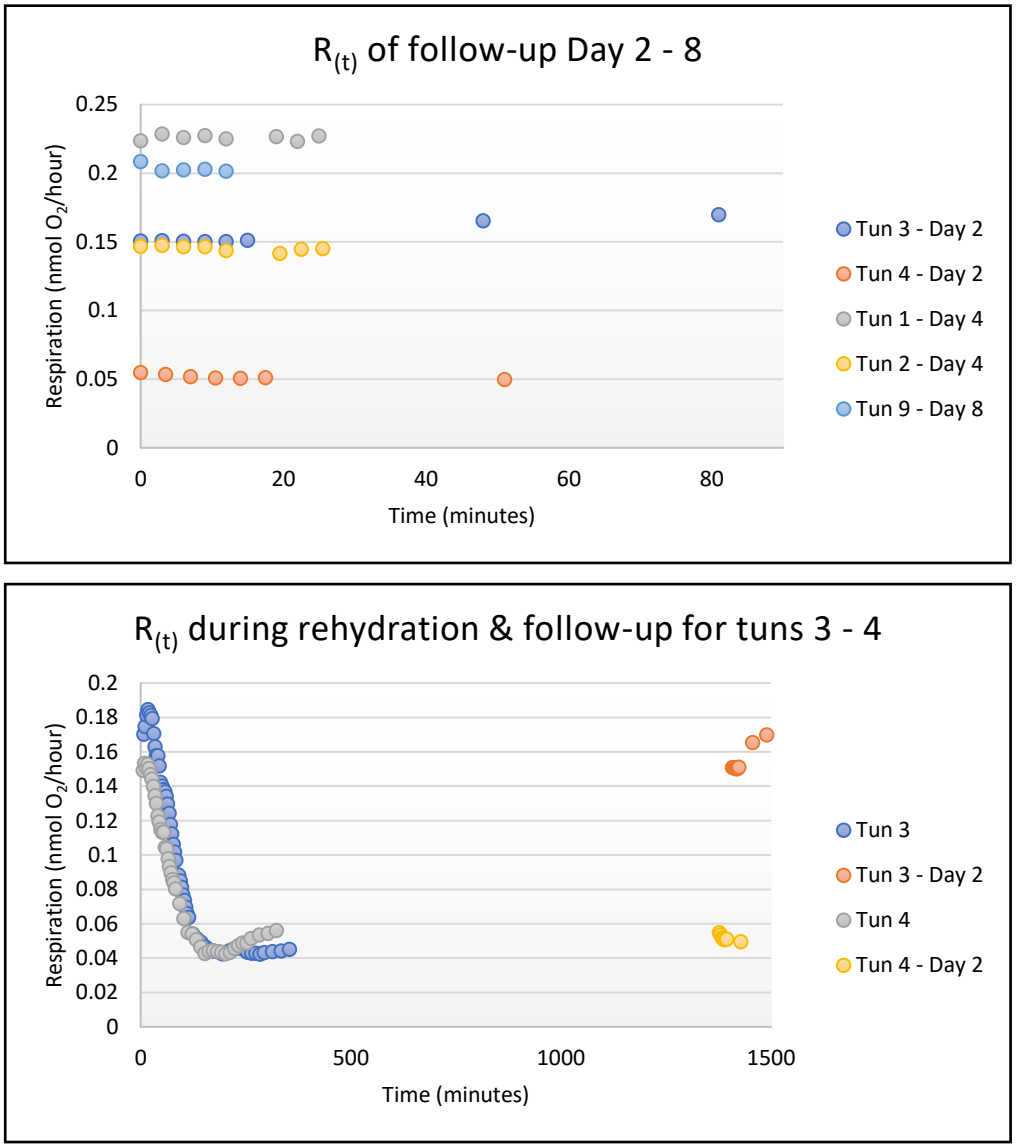

Figure 31: *$R_{(t)}$ for follow-up of tuns 1 – 4 & 9 on day 2 – 8 (Top) and for tuns 3 – 4 on day 1 & 2*

The respiration increases to zone 1 levels for the damaged tun 3 but remains at zone 3 levels for the intact tun 4. Figure 32 shows the $R_{(t)}$ plots for tuns 3 – 6 before and after treatment with ethanol on day 1 for tuns 5 – 6 and day 2 for tuns 3 – 4.

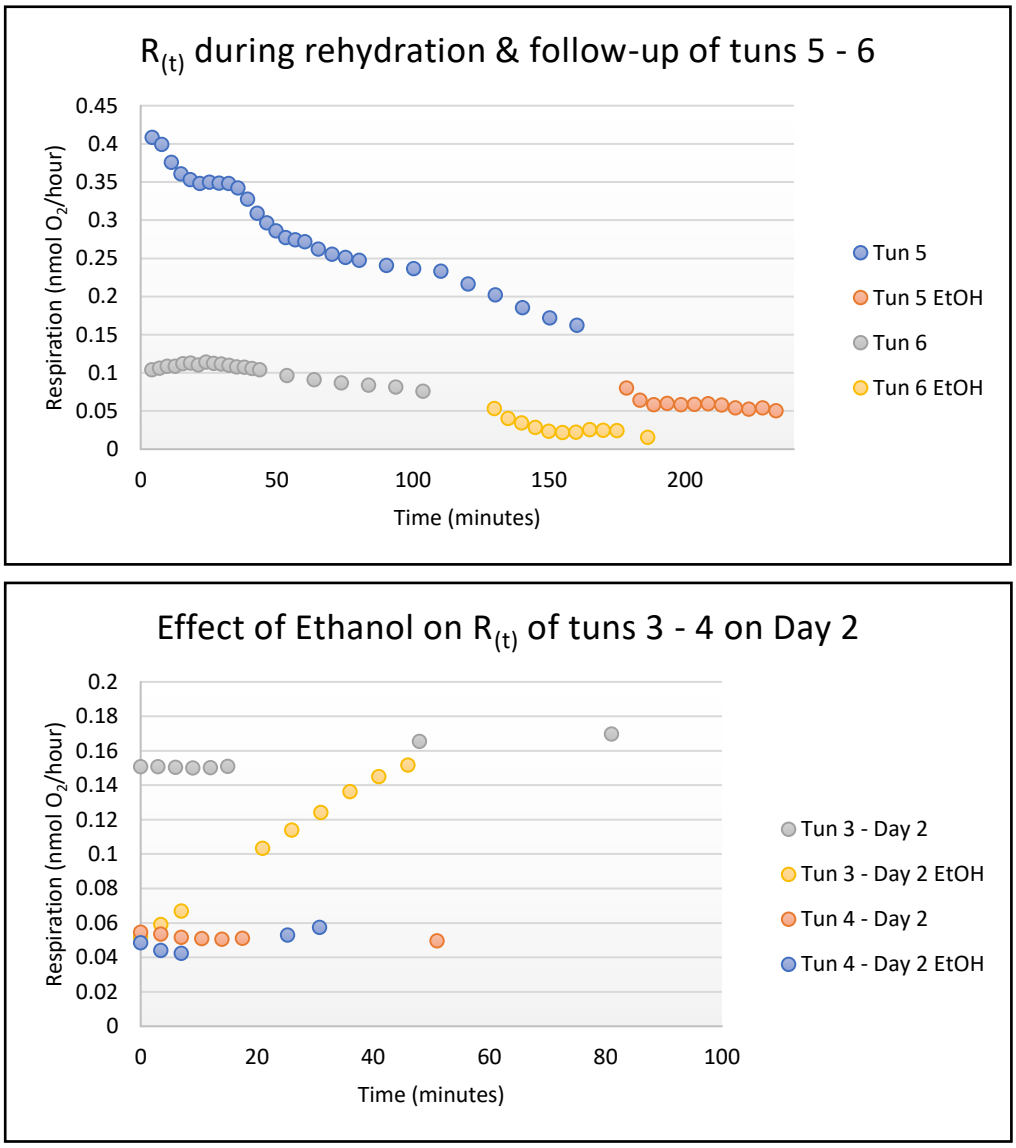

Figure 32: *$R_{(t)}$ before and after treatment with ethanol for tuns 5 – 6 on day 1 (Top) and for tuns 3 – 4 on day 2 (Bottom).*

No clear effect was seen from treatment with ethanol on the respiration of tuns 5 – 6 on day 1 or tun 4 on day 2. For tun 3, the respiration immediately decreased by 68.5 % but then returned to the same levels within 50 minutes.

3. Discussion

Because of time constraints and the viability issue, the results in this chapter are all limited to a sample size of two for any condition and should therefore be considered preliminary. However, the $R_{(t)}$ plots of tuns 9 – 10 give the first ever description of oxygen consumption during successful termination of cryptobiosis. Because of this, they will be used to evaluate some of the existing hypotheses on the mechanisms regulating this process – specifically with respect to anhydrobiosis. To validate the results, the experiment should be repeated with a larger sample size of tuns that reliably become fully active. This may require that the critical factors for successful termination of anhydrobiosis are identified. The follow-up studies suggest that biofilm formation is unlikely to be a major issue. First, it would require an implausibly thick biofilm to account for the respiration seen in those studies. Secondly, it did not appear to reduce respiration significantly when tardigrades were dipped in ethanol immediately after hydration. One of the tardigrades treated with ethanol on day 2 showed a significant decrease in respiration, which suggests that most of the growth was localized near the tardigrade – but this could be because that tardigrade was damaged and so the growth was not limited to its surface. There did seem to be some growth in the chambers after the tardigrades died, since respiration increased for follow-ups from day 1 – 4. The fact that it did not increase from day 4 – 8 could be because the microbes had reached the stationary phase – or it could be because tun 9 survived rehydration and had not been dead for 8 days. Additionally, some of the respiration remained after tardigrades had been removed but disappeared completely when the empty chambers were washed with ethanol.

Because the issue of viability was not tested in a systematic way due to time constraints, it is not clear which of the modifications in this study were instrumental for allowing tuns 9 – 10 to regain full activity – or if it was just random variance. The most likely explanation for tuns 1 – 6 is too rapid desiccation. This is because all the desiccation tubes were moved to dry areas of sand immediately after tardigrades had been transferred, which increased the desiccation rate substantially. The optimal conditions for desiccation may require a relative humidity as high as 95 % (Crowe, 1975; Czernekova and Jönsson, 2016). Another explanation is that the MiliQ water used to rehydrate tuns 1 – 6 forces a too rapid water influx due to osmosis and the tardigrades cannot cope with this hydration rate. As mentioned in Chapter 3, the tap water better imitates the conditions of the natural habitat (Halberg *et al.*, 2013) and was shown to alter the metabolic rate of active tardigrades. It was also the condition used to rehydrate all the tardigrades from Chapters 1 – 3. Regarding tuns 7 – 8, the explanation could simply be that viability decreases with time

spent in anhydrobiosis (Guidetti, Altiero and Rebecchi, 2011) and more than two tuns are required to reliably get successful termination at this condition. Given the success of tuns 9 – 10 and because it simplifies the set-up, future experiments should use *Whatman 3* filter paper for desiccation and oxygenated tap water for rehydration. Furthermore, the oxygen profiling should be complemented with time-lapse imaging of the rehydration process, so any atypical respiration might be linked to specific morphological or behavioural changes.

Another concern regarding viability was that the oxygen concentration in the water was too low to meet the requirements of the initially high respiration rate. This would not be an issue in a petri dish where oxygen is supplied from all directions but could become one when it can only be supplied unidirectionally through the long capillary chamber. The relatively narrow width of the chamber combined with the high respiration rate may also lead to autotoxicity from the accumulation of metabolic waste such as CO_2. This could be determined by sensors that measure microgradients of CO_2 or pH instead of oxygen. Both of these potential problems might be solved by changing the dimensions of the capillary chambers. Shorter chambers would allow for a faster oxygen supply from the aquarium and better dispersal of metabolic waste. It would also improve the resolution of $R_{(t)}$ plots immediately after transfer – as described in Chapter 3. Broader chambers would have the same effects, but also reduce the slope of the oxygen microgradient and consequently make the calculated respiration less reliable. The length-to-width of chambers should be at least 3:1 for the microgradient to be accurate (L. R. Damgaard, personal communication, March 6th, 2018).

The two main factors to investigate in future studies would be the effect of time spent in anhydrobiosis and the effect of repeated entry and exit from anhydrobiosis on the metabolic rate. It has been demonstrated that time spent in anhydrobiosis correlates with the time it takes to regain activity, which is thought to be due to accumulated damages to e.g. DNA and lipid membranes that first must be repaired (Neumann *et al.*, 2009; Rebecchi *et al.*, 2009). How the metabolic rate changes with time spent in anhydrobiosis may therefore reveal the energetic requirements of this repair and help to understand the underlying mechanism. According to Czernekova and Jönsson, (2016), repeated cycles of anhydrobiosis are associated not just with a decline in survival rate, but also a decline in the number of storage cells in surviving tardigrades. Since storage cells function as the tardigrades energy depot, this would almost certainly impact the metabolic rate. How the metabolic rate changes with repeated cycles of anhydrobiosis – both successful and unsuccessful, may therefore help to understand the role of storage cells in the

termination of anhydrobiosis. This is also relevant to the results of tuns 9 – 10 in this study, which were measured during their third rehydration in the laboratory due to being part of the viability studies described in Chapter 5. This meant a cycle of more than 1.5 years in anhydrobiosis followed by 2 days of activity, then 10 days of anhydrobiosis followed by 32 hours of activity and finally 18 hours of anhydrobiosis before being measured during rehydration. Those repeated cycles of anhydrobiosis may have affected the number of storage cells and thus metabolic rate.

The 3 zones seen on the $R_{(t)}$ plots of tuns 9 – 10 are very similar to those of tuns 1 – 8, except for tun 2 where respiration is already in zone 2 from the start. The only reason zone 3 was not described for tuns 5 – 6 was that they were removed before then to test the effects of ethanol. They do however appear to reach zone 3 in the follow-up. This similarity suggests that tuns 1 – 8 attempted to undergo the same process despite ultimately failing. The respiration of most tuns peaked during zone 1. Because of the way $R_{(t)}$ plots were constructed from the bottom of the oxygen microgradient, this is not an artefact caused by the gradual establishment of the gradient. The peak seen for tun 8 was short enough to be random, but the others are too persistent over time for this to be the explanation. Interestingly, tun 9 shows two peaks in zone 1 and the first two profiles suggest that it may have more – which the $R_{(t)}$ plot begins too late and at too low resolution to reveal. This could be the case with all the tuns, but especially tun 5 appears to have at least one more peak before the $R_{(t)}$ plot. The most likely explanation for the peaks seen in zone 1 is that as certain enzymes become active or structures get repaired, they begin to contribute to the reactivation process and thus the metabolic rate. Another possibility is that the tuns actively regulate oxygen influx in bursts during the early stages in termination of anhydrobiosis. This could be to ensure that necessary reactivation processes such as DNA-repair, transcriptional regulation, degradation of trehalose and other bioprotectants occur in a specific order and with limited overlap. If so, it might explain why the tuns that die hydrate faster than tuns 9 – 10 in this study. Regulating the hydration rate may be one way to control which processes can be initiated during a given oxygen burst. This could also explain why MiliQ water leading to a more rapid water influx due to osmosis would negatively affect viability.

The respiration of tuns 9 – 10 in zone 1 is significantly higher than for active tardigrades – whether in MiliQ or tap water. The same is true for most of tuns 1 – 8. This means one of two things. For the reactivation processes in zone 1 to only require a metabolic rate slightly higher than during normal activity, almost all the cells in the tardigrade must be hydrated enough to regain full metabolic capacity within the first 5 minutes of exposure to water. This seems unlikely based on the morphological state of

the tardigrades during zone 1. Alternatively, if only a minority of cells have hydrated enough to drive oxygen consumption within the first 5 minutes, then the metabolic rate in those cells must be many times higher than during normal activity. This suggests that the energy requirements of the reactivation processes are extremely high. A possible reason for this may be that those cells must also initiate the reactivation process in the other systems of the tardigrade – similar to the idea of a recursive-hierarchical structure proposed by Neuman, (2006) with respect to metabolism during termination of cryptobiosis. Neuman, (2006) claims that such a structure would require a minimal level of metabolic activity to maintain the organization of metabolic networks. It is unclear where this metabolism would occur given the absence of water, but some form of maintenance of the metabolic networks might explain how the oxygen consumption can increase so rapidly after exposure to water.

The exponential decrease in respiration during zone 2 is most likely caused by the cessation of reactivation processes that have been completed, although it is difficult to say how much of it is simply due to cell death for tuns 1 – 8. However, the metabolic rate reached in zone 3 for tuns 9 – 10 is only ~ 50 % that of normal activity in MiliQ, despite being fully mobile in tap water where the metabolic rate should be higher. This suggests that successful termination of cryptobiosis is followed by a recuperation period between 1 – 2 days long, where energy is preserved. It is also possible that the lack of food in capillary chambers might play a role. Naturally, the metabolic rate of tuns 1 – 8 in zone 3 is significantly lower than tuns 9 – 10, although it is still higher than for the dead *R. coronifer* from Chapter 1. As with the dead tardigrades in Chapter 3, this is most likely due to residual cellular respiration that will expire over another 24 hours. The fact that the duration of zone 2 increased with the overall duration of the $R_{(t)}$ shows that the way it was defined was not optimal. Perhaps a better cut-off would be after 90 % of the decrease instead of 95 % – or perhaps it should be until total respiration had decreased by 80 %. Another possibility is to define it as the period from zone 1 until full hydration of the tardigrade has occurred. However it is defined, the purpose of zone 2 is to capture the period where most of the oxygen consumption disappears.

The $R_{(t)}$ of the rotifer of unknown species shows the same 3 zones as the tardigrades. However, both respiration and metabolic rate in zone 1 is significantly lower than for any of the *R. coronifer* tuns. This is unlikely to be caused by overestimation from narrowing – as overestimation of respiration after 30 minutes was less than 4 % for all tuns and the $R_{(t)}$ plot of the rotifer only includes profiles from after 32 minutes. The most likely explanation is that the rotifer does not have as complex organ systems as the tardigrade and so it might not need to undergo as extensive processes of modification and repair during

termination of anhydrobiosis. The exponential decrease of zone 2 also occurred much slower than for any of the tardigrades. This included those that were measured for 24 hours and meant that after 2 – 3 hours of hydration, its respiration was higher than that of tuns 1 – 4 & 6. Of course, the $R_{(t)}$ of a single rotifer that failed to survive termination of anhydrobiosis is not enough to say something general about the differences between the two species. As with all of the results in this chapter, the experiment would have to be repeated with a larger sample size of tardigrades and rotifers that reliably survived rehydration.

As mentioned at the beginning of this discussion, the results for tuns 9 – 10 is the first description of respiration during termination of anhydrobiosis and would be interesting to consider with respect to existing hypotheses on the underlying mechanisms – despite being preliminary and requiring further experimentation. On the topic of metabolism during anhydrobiosis, Crowe, (1971) suggests 4 different hypotheses as important lines of inquiry. The first was that the animals may gradually attain a greater degree of dehydration with time spent in anhydrobiosis. Unlike the other three hypotheses, this does not directly pertain to the mechanisms required for successful termination of anhydrobiosis. Another hypothesis was that certain labile structures may be destroyed during dehydration and require resynthesis. This is consistent with the high energy requirements observed for zone 1 in this study. The successful resynthesis of such structures and their subsequent contributions to the termination process might also contribute to the bursts of oxygen influx seen as peaks in zone 1.

The final two hypothesis both pertain to the restriction of metabolism. One was that intermediate metabolites may be utilized during anhydrobiosis and require resynthesis before full activity can be resumed. Crowe, (1971) points out that that this would require enzymatic activity at low water potentials and suggests that some crystalline enzymes and substrates may interact at high humidities in anhydrobiotic organisms. The other hypothesis was that there could be a build-up of metabolic inhibitors that must be metabolized or excreted before full activity can be resumed. For either of these hypotheses to be true, the processes of metabolite resynthesis or inhibitor excretion would most likely have to be completed within the first 5 minutes of exposure to water – since the metabolic pathway is what drives the high oxygen consumption seen in zone 1. If either hypothesis is true, then oxygen consumption should be expected to increase exponentially as metabolites are resynthesized or inhibitors removed. A more detailed description of the $R_{(t)}$ plot during the first 5 minutes of exposure might reveal the dynamics of such processes. Crowe, (1971) also points out that the time required for anhydrobiotic nematodes to attain maximum oxygen consumption during termination of anhydrobiosis directly correlates with the time

spent in anhydrobiosis and suggests that this might explain why time spent in anhydrobiosis correlates with the time it takes to become active for tardigrades. Experiments like those in this chapter with a larger sample size and more systematic approach to conditions should be able to determine if the same correlation seen for nematodes also exists for tardigrades.

Clegg, (1964) suggested that artemia cysts cover all energy-requirements during termination of anhydrobiosis by oxidation of trehalose. He also describes how their metabolism during this process depends on the water content in a series of publications under the common title "Interrelationship between Water and Cellular Metabolism in Artemia cysts". At 7 % hydration, there are no enzymatic reactions and not even enough water to form monomolecular hydration shells around ribosomes. From 20 – 45 % hydration, the metabolism is restricted to specific enzymatic reactions in isolated hydration shells large enough to allow for enzyme activity and the diffusion of substrates and products. This is thought to be limited to the metabolization of small molecules such as amino acids, nucleotides and Krebs' Cycle intermediates. At 45 % hydration, all metabolic processes become possible due to the formation of water channels in the cell that connect the isolated hydration shells and allow for exchange between them. This is where respiration and protein synthesis are thought to begin. Further hydration is thought to have no effect on the qualitative nature of the metabolism, but only increase the metabolic rate due to water channel formation (Clegg, 1976, 1977; Clegg and Cavagnaro, 1976; Clegg and Lovallo, 1977; Westh, 1990).

This description does not seem to describe the *R. coronifer* tuns in this study. If it did, then $R_{(t)}$ would be expected to start low and increase as the tardigrade hydrates. Instead, the respiration of all tuns is at its highest in zone 1 – when no morphological changes can be seen. In fact, $R_{(t)}$ decreases exponentially with hydration – at least of the organism as a whole. If Clegg's description of rehydration does apply to *R. coronifer* tuns on a cellular level, then this would further indicate that only a small fraction of cells in the tardigrade is driving the high respiration seen in zone 1. It would also mean that the metabolic activity of those cells would be even more extreme than previously suggested. Not only would they have to consume significantly more oxygen than the totality of cells in fully active tardigrades, but the oxygen consumption of those initial processes would have to be so high that their cessation led to an exponential decrease in $R_{(t)}$ for the tardigrade – despite more cells hydrating and contributing to respiration. This seems unlikely – although if true then the peaks seen in zone 1 might be explained by the formation of water channels in different types of cells.

Chapter 5: Developing the method

This chapter will present no results, as it concerns the various modifications that were done to the experimental designs during the process of the study. Instead, the purpose is to highlight potential problems that may arise when employing the techniques described in previous chapters and what strategies were used to avoid or minimize such problems in this study. Therefore, this chapter will be divided into 3 sections regarding the process of developing the methods used in Chapters 1, 2 & 3 – 4 respectively. Each section will be further broken down by specific problems that were solved.

1. Respiration and Metabolism

1.1. Evaporation from chambers

Evaporation was a concern for several reasons. Most importantly, it would create a temperature gradient in the water column. When the water molecules with the highest kinetic energy in the surface layer of the water column evaporates, the average kinetic energy – i.e. temperature of that surface layer decreases, whereas it stays the same at the bottom of the water column. Temperature affects both the solubility and diffusion speed of oxygen in water, thus distorting the oxygen microgradient generated by the respiration of the tardigrade. Evaporation also put a narrow time limit on how long experiments could be run and led to much shorter distances being profiled for later measurements due to the decreasing volume.

In the original experimental design, the chamber and modelling wax was simply placed directly on the platform underneath the suspended microsensor, to keep the set-up as simple as possible. The platform was covered with soaked paper to increase the humidity around the chamber and thus reduce evaporation. A picture of this set-up can be seen on figure 33.

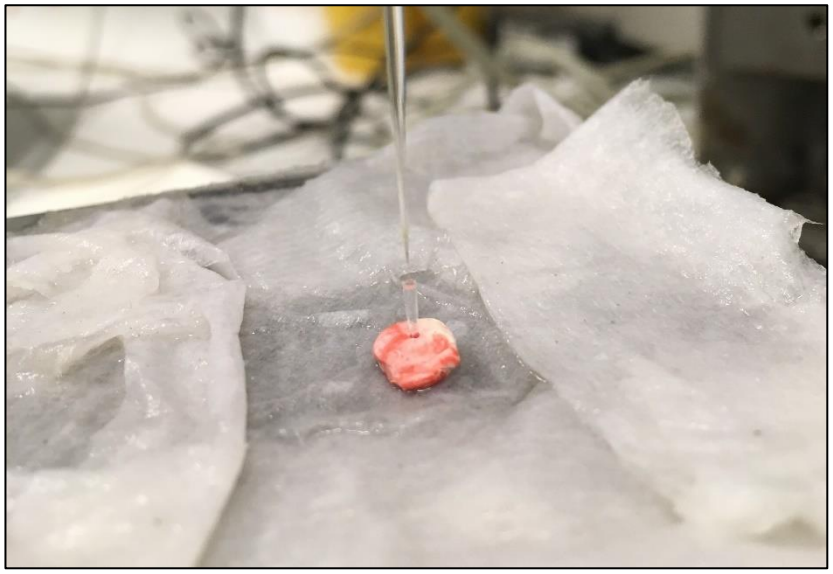

Figure 33: *A capillary chamber containing a tardigrade, fixated in modelling wax and placed on a platform covered with soaked paper underneath a microsensor.*

However, this strategy turned out to be ineffective for reducing evaporation. To eliminate this source of error, aquariums were constructed to keep the chamber submerged in a larger reservoir where evaporation from the surface of the aquarium would have no effect on the temperature of water in the chamber. Aquariums were constructed by gluing together 5 plastic cover slides. To make handling of the chambers easier, a cuvette was placed upside down in the middle of the aquarium as a platform. Holes were bored in the cuvette to allow for it to be filled with water as the reservoir was filled, thus preventing it from rising to the surface. However, this proved insufficient and so the cuvettes were further fixated in the aquarium by gluing them to its bottom, using customized pipettes with *Dow Corning 734 Clear* silicone. The fixation was completed by leaving the cuvette and silicone in the aquarium covered with water in an incubator at 53 °C for 2 hours. Aquariums were left *ON* filled with water to make sure they were not leaking. The aquarium set-up can be seen in Chapter 1.

1.2. Determining incubation time

10 tardigrades were measured in pilot experiments not included under results to find out what the optimal protocol would be. For the first of those experiments, profiles were measured continuously from as soon as the tardigrade had been transferred to the chamber. A linear concentration gradient through the chamber with an $R^2 > 0.99$ would be reached after ~ 20 minutes. However, the respiration would continue to increase until reaching a steady-state ~ 35 minutes after transfer for most tardigrades. To ensure that measurements were done during steady-state, incubation time was set to be minimum 45 minutes. For consistency, controls were also incubated for 45 minutes. The first profile of all controls was consistently different from all the others and were therefore omitted from calculation of the mean respirations. Only profiles in steady state were used for calculating the mean values described in Chapters 1 – 3. Figure 34 shows oxygen profiles of tardigrades both before and during steady-state – as seen in *SensorTracePro*.

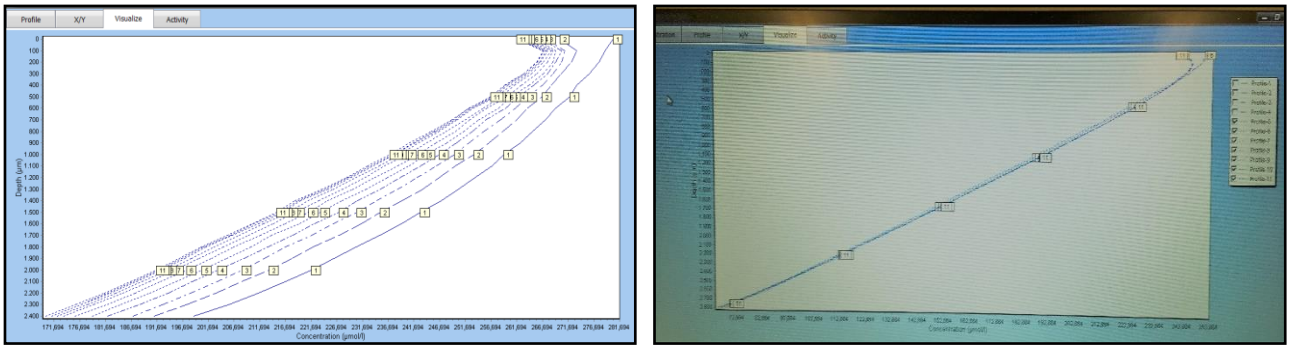

Figure 34: *Profiles of two different tardigrades – one which is pre-steady-state for profile 1-8 and then steady-state for profile 9-11 (Left) and one which is clearly in steady-state for all profiles (right)*

2. Temperature

2.1. Maintaining temperature

When preparing the water baths used in chapter 2, they were first washed and scrubbed with 2 M HCl, then with 70 % ethanol and finally twice with demineralized water. The baths were filled with *Q-POD® Ultrapure Water* and had a cold-finger placed into it. Several rubber tubes of different sizes were used to connect the cold-finger with the cooling tank. Plastic mouthpieces with different size outlets were used to connect the tubes and the openings around these were sealed using plastic strips. Thermometers were placed in the water baths to see if cooling/heating from the cold-finger was being maintained. This was necessary, since the supply of cooling fluid to the cold-finger would periodically be cut off – either from squeezing of the tubes against an edge from the bath or the table or because of a build-up of air bubbles blocking the flow in one of the tubes. The tubes had to be supported by the horizontal microscopes to avoid squeezing. To release any build-up of air bubbles in the tubes, the cold-finger had to be removed from the water bath and tubes manipulated such that gravity would guide the air bubbles through the system. Pictures of the set-up and filling of the water bath can be seen on figure 35.

Figure 95: *Both set-ups with water baths, thermometers, calibration liquids, aquariums, chambers, cold-fingers, rubber tubes, platforms, clamps, sensors, lamps, horizontal microscopes, amperemeters, A/D-converters, motor-controllers, computers and the cooling system below the table (Left). One of the water baths being filled with Ultrapure MiliQ water (Right).*

When working with low temperatures, it is important to avoid freezing of the cooling fluid, as this will ruin the machinery. The cooling fluid was closely observed after lowering of the temperature, but no freezing occurred. Since the set-up would be used for a long period of time, a lid was placed over the cooling fluid to avoid evaporation. To keep the calibration liquids the same temperature as the water bath and avoid exchange of contents, twine was wrapped around the flasks and knotted to keep them suspended in the surface of the bath. The flask containing MiliQ water had to be removed, opened to take in oxygen,

then closed and shaken 2 – 3 times to ensure oxygen saturation before calibration. However, the time spent out of the water bath before calibration was kept to a minimum to avoid the flask adjusting to room temperature, thus affecting the temperature in the water bath when placed back into the bath during calibration. After calibration, the flasks were removed, and the thermometer inspected to confirm that the temperature of the water bath had not been affected. One aquarium was placed permanently in each of the two water baths and only the modelling-wax and capillary chambers were exchanged, using a pair of tweezers, when preparing for measurements of a new tardigrade. Initially, the water baths were placed directly on the magnetic plate used for stirring, but heat from the plate made temperature control more difficult. This effect was eliminated by placing a piece of styrofoam between the water bath and the magnetic plate.

2.2. Low signal at low temperatures

At low temperatures, the signal in millivolt from the sensor is lower – despite oxygen concentrations actually being higher due to the increase in solubility. This is because the diffusion speed and thus the partial pressure of oxygen through the sensors increases with temperature. Therefore, the signal-to-noise ratio is also lower. This only became an issue at 2 °C. Figure 36 shows pictures of profiles measured at 2 °C before and after the modifications that were done to solve this problem.

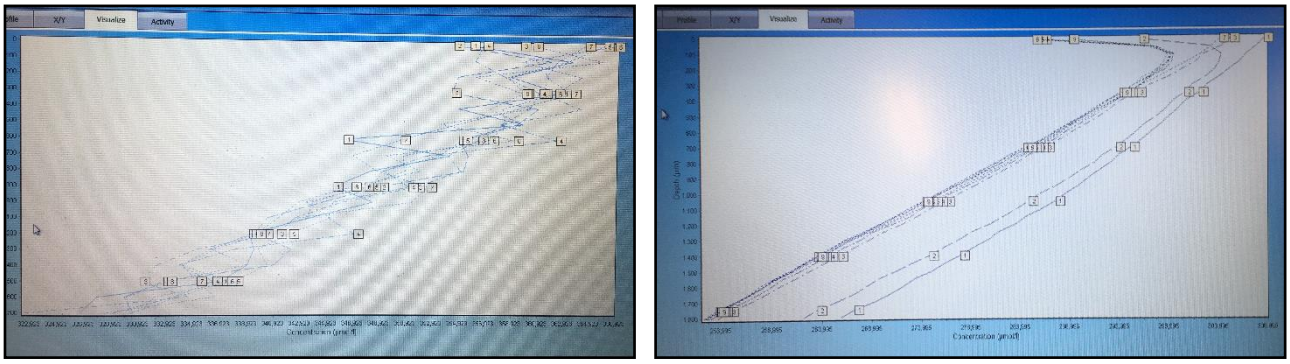

Figure 36: *Profiles measured at 2 °C in chambers containing tardigrades before (left) and after (right) the sensor was replaced, and a grounding cable was added to the set-up.*

The first modification was to replace the sensor with another that had a higher voltage range. Most sensors in the study had ranges from ~ 0 mV in ascorbate to 30 – 130 mV in atmosphere, whereas the range of the sensor used for all measurements at 2 °C in Chapter 2 spanned from ~ 30 mV in ascorbate to ~ 660 mV in atmosphere. This should compensate for the low diffusion speed and increase the signal-to-noise ratio. The second modification was to insert a grounding cable in the multimeter and leave the other end in the

water bath to protect the system against local electrical fluctuations. The grounding cable was used in all following experiments to keep the set-up as consistent as possible.

2.3. Solubility gradient

The first attempt at investigating the effects of temperature on the metabolic rate only included the temperatures 2, 11 & 16 °C and gave some very strange results. Not only did the metabolic rate seem to be higher at 2 °C than at 11 °C, but the way it would change over time also appeared to be highly temperature dependent. At 16 °C, respiration would increase for the first ~ 35 minutes before reaching steady-state – exactly like tardigrades measured at 22 °C. This was also the case for 3 of 6 tardigrades measured at 11 °C – whereas respiration for the other 3 would decrease slightly over time and only one of them reached steady-state. At 2 °C, the respiration for 5 of 6 tardigrades decreased significantly over time with no sign of nearing steady-state. One tardigrade showed increasing respiration, but also no sign of nearing steady-state. These trends can be seen on figure 37. The results were assumed to be indicative of the physiological response to such temperatures by the tardigrades and an acclimatization experiment was designed – where 85 tardigrades were transferred to small petri dishes with MiliQ water that were then sealed with parafilm and incubated in the 2 °C water bath *ON* with the intention of measuring tardigrades that had fully acclimated to the new temperature. However, this experiment was never carried out, since another explanation for the strange results was identified.

Because of the small size of chambers, they return to room temperature almost instantaneously after being removed from the water bath to transfer a tardigrade. This meant the solubility of oxygen in the water would also decrease. When placed back into the water bath, a solubility gradient would therefore be created – causing an oxygen flux from the water bath down through the chamber. The temperature of the chamber and its contents would return to that of the water bath almost instantaneously, but because diffusion is slower at low temperatures, it takes longer for this solubility gradient to be eliminated by oxygen exchange from passive diffusion. The inflation of respiration rate was higher at low temperatures due to the effect of temperature on solubility and took longer to disappear due to the effect of temperature on diffusion speed. The solubility gradient explains both why respiration appears higher at 2 °C than at 11 °C – contrary to what would be expected and why steady-state is not reached at 2 °C. The effect of the solubility gradient is both reversed and more quickly resolved when transferring chambers from low to high temperatures than the reverse – as would be expected if the explanation is correct.

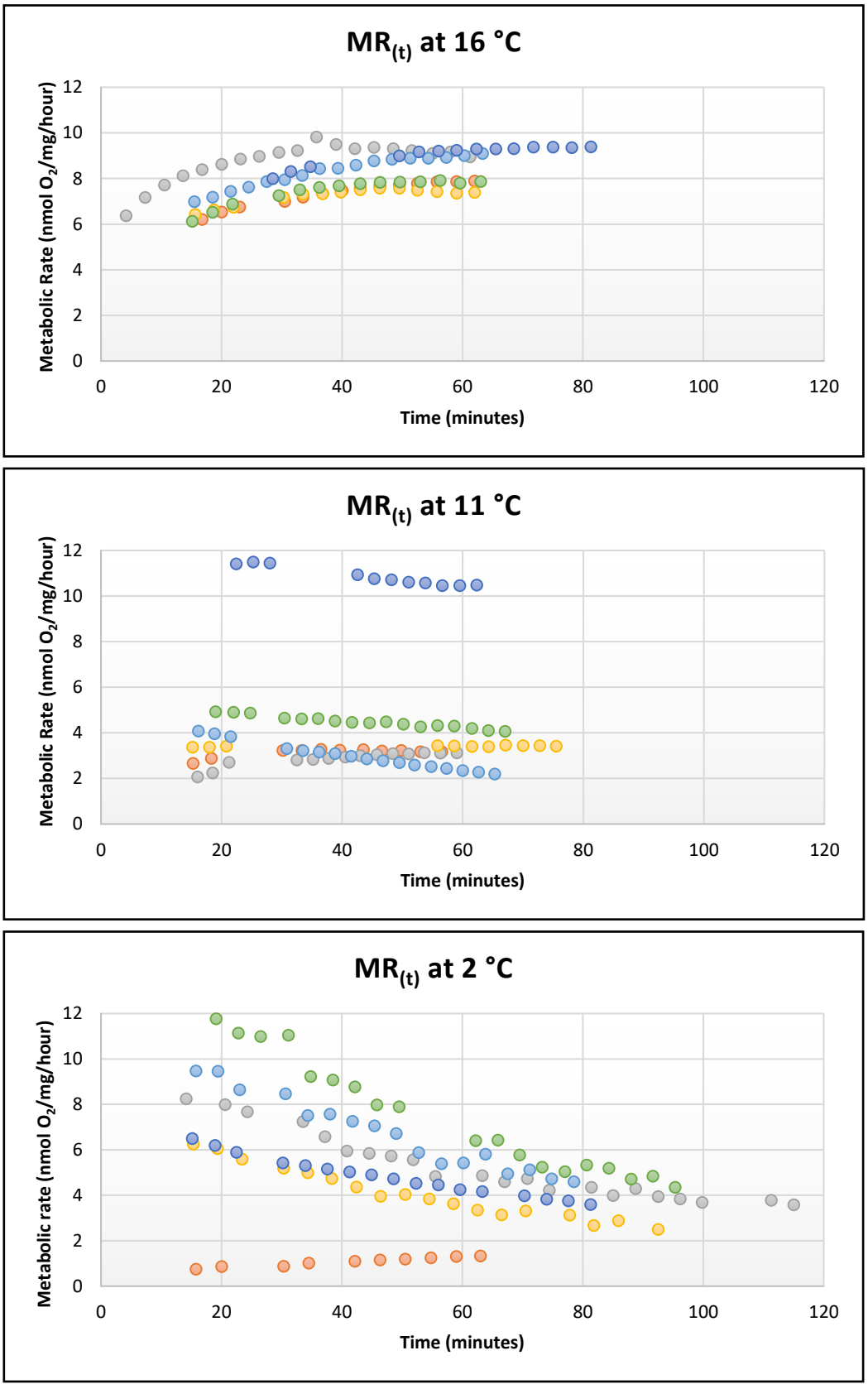

Figure 37: The change in metabolic rate (nmol O2/mg/hour) over time (minutes) for 6 individual tardigrades measured at 16 °C (Top), 11 °C (Middle) and 2 °C (Bottom).

To determine the effects of the solubility gradient at 11 & 16 °C, chambers were incubated *ON* at 24 °C, transferred to the water baths and then profiled until the gradient had completely disappeared. This process can be seen on figure 38 – both from screenshots in *SensorTracePro* and plots of the data in Excel.

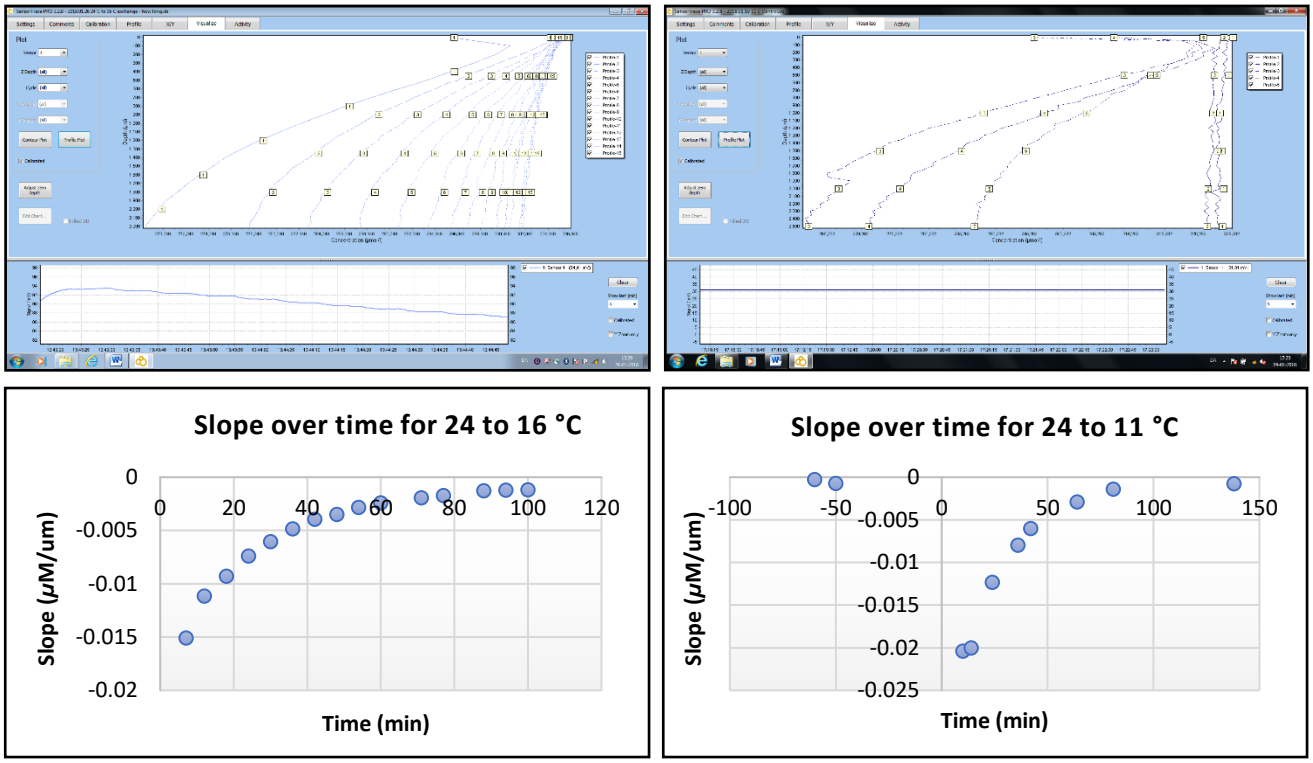

Figure 38: *Screenshots (Top) and Excel plots (Bottom) of the disappearance of the solubility gradient when placing chambers with 24 °C water in a 16 °C (Left) and a 11 °C (Right) water bath. The process takes 100 min. at 16 °C and 150 min. at 11 °C. The first two profiles of the plots on the right are at 24 °C, before the chamber is transferred to 11 °C. The time of transfer is set as t = 0 min.*

The effect is negligent after incubation for 60 minutes at 16 °C and 80 minutes at 11 °C. However, steady-state was reached after 45 minutes and maintained with no significant change in respiration for all 6 tardigrades at 16 °C and 3 of the 6 tardigrades at 11 °C. This strongly suggests that those results represent the actual respiration of the tardigrades – since a remaining solubility gradient would prevent such a steady-state. Those 9 tardigrades were therefore included in the results seen in Chapter 2. The rest of the experiments had to be redone to avoid the effects of a solubility gradient. To accomplish this, a flushing step was added to the procedure. Chambers were flushed with water from the water bath immediately after being placed there, using the customized pipettes. This was done carefully to avoid affecting the tardigrade at the bottom or risk ejecting it from the chamber – as would happen if the flush was too forceful. Immediately after flushing, a profile of the chamber would be measured to ensure that the solubility gradient had been eliminated. After that, the tardigrade was incubated for at least 45 minutes before measuring its respiration.

To test the effectiveness of the flushing step one empty chamber was incubated at 2 °C *ON* and then flushed with deoxygenated water to create a solubility gradient. Another chamber was incubated at 22 °C *ON* then transferred to 2 °C, incubated for 1.5 hours and then flushed with 2 °C water from the water bath. Figure 39 shows screenshots in *SensorTracePro* demonstrating the creation of a solubility gradient when flushing with deoxygenated water and the complete elimination of a solubility gradient that persisted for more than 1.5 hours, when flushing with water from the water bath.

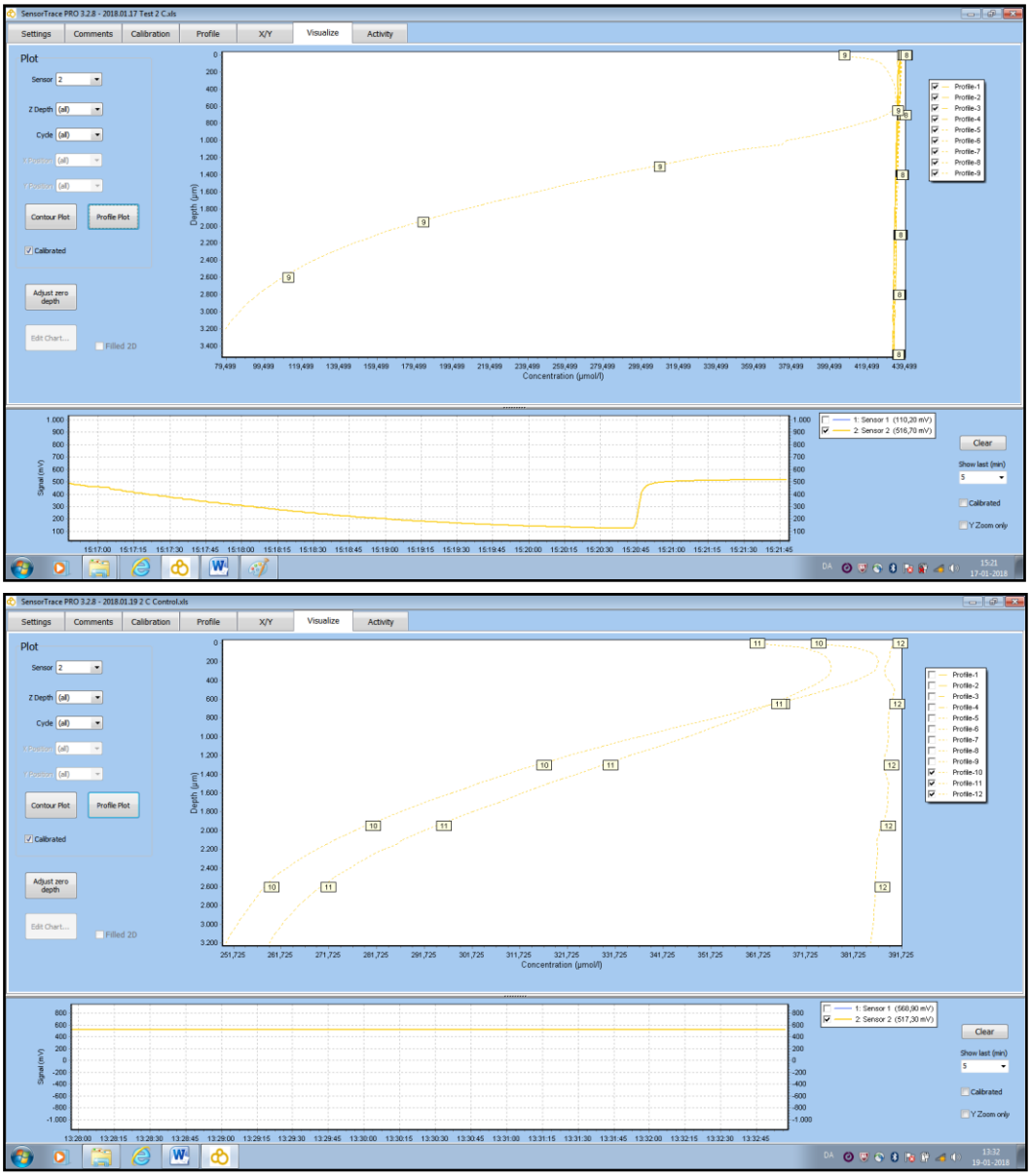

Figure 39: *(Top) Chamber incubated ON at 2 °C and then flushed with deoxygenated water. Profile 1-8 show the oxygen microgradient before flushing and profile 9 shows it after flushing. (Bottom) Chamber incubated at 22 °C ON, then 2 °C for 1.5 hours and then flushed with 2 °C water from the water bath. Profile 10-11 show the remaining solubility gradient after 1.5 hours at 2 °C and profile 12 shows the gradient being eliminated immediately after flushing.*

3. Salinity & Cryptobiosis

3.1. Plotting metabolic rate against time

It takes ~ 30 minutes after transfer of a tardigrade, for the oxygen gradient to establish throughout the chamber. To understand how the metabolic rate of the tardigrade changes in that time, respiration was calculated from the microgradient established near the bottom of the chamber only ~ 3 minutes after transfer. The microgradients were between 400 – 1200 μm long and profiled with a step size of either 50 or 100 μm. The depth of a microgradient was determined from how much data could be included and still have $R^2 > 0.99$ from the second profile on. The second profile was used to ensure $R^2 > 0.99$ across a minimum of 400 μm. The values for metabolic rate determined this way are not as accurate as those determined from whole chambers, due to the lower quantity of data. However, the main interest in $MR_{(t)}$ plots are the trends. To keep those valid, the same depth was used for all calculations of a given tardigrade. Progressively including more data in the calculations of microgradient slopes over time may better approximate the ultimate values, but it distorts the trends. Figure 40 shows the difference in $MR_{(t)}$ plots for one of the tardigrades in 16 ppt NaCl solution described in Chapter 3, depending on whether it was determined from the whole chamber or the bottom 500 μm.

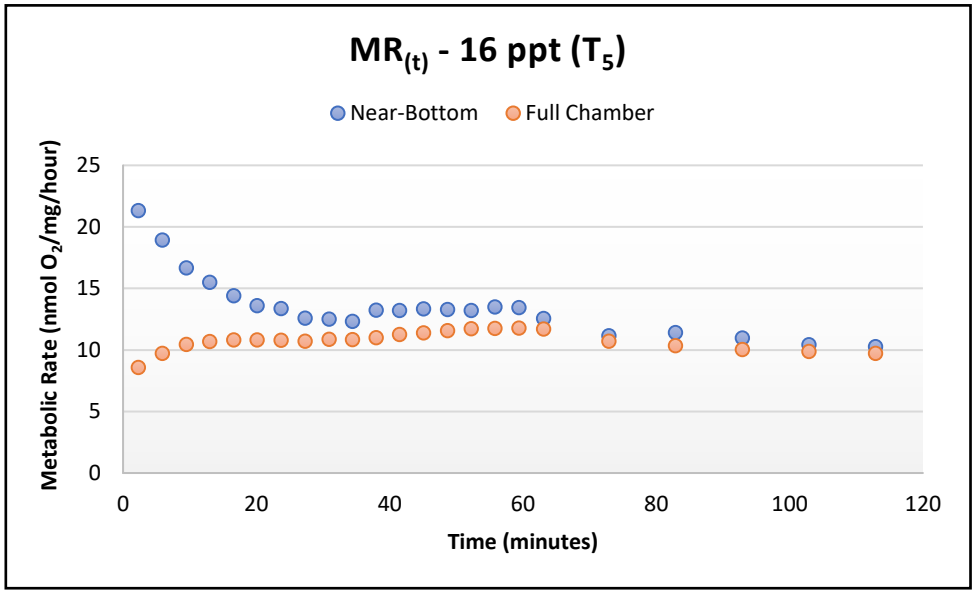

Figure 40: *$MR_{(t)}$ of a tardigrade in 16 ppt NaCl – depending on whether the data used to calculate the metabolic rate was from the whole chamber (orange) or the bottom 500 µm (blue).*

After the first 30 minutes, most of the difference in values has disappeared. However, there is another issue with relying on microgradients near the bottom that is specific to chamber a1 in this study – see appendix I. The radius of a1 decreases near the bottom of the chamber because of narrowing. This changes

the dynamics of the oxygen flux in ways that cannot be easily calculated. Figure 41 shows how narrowing of chamber a1 affects the microgradient measured for the rotifer described in Chapter 4.

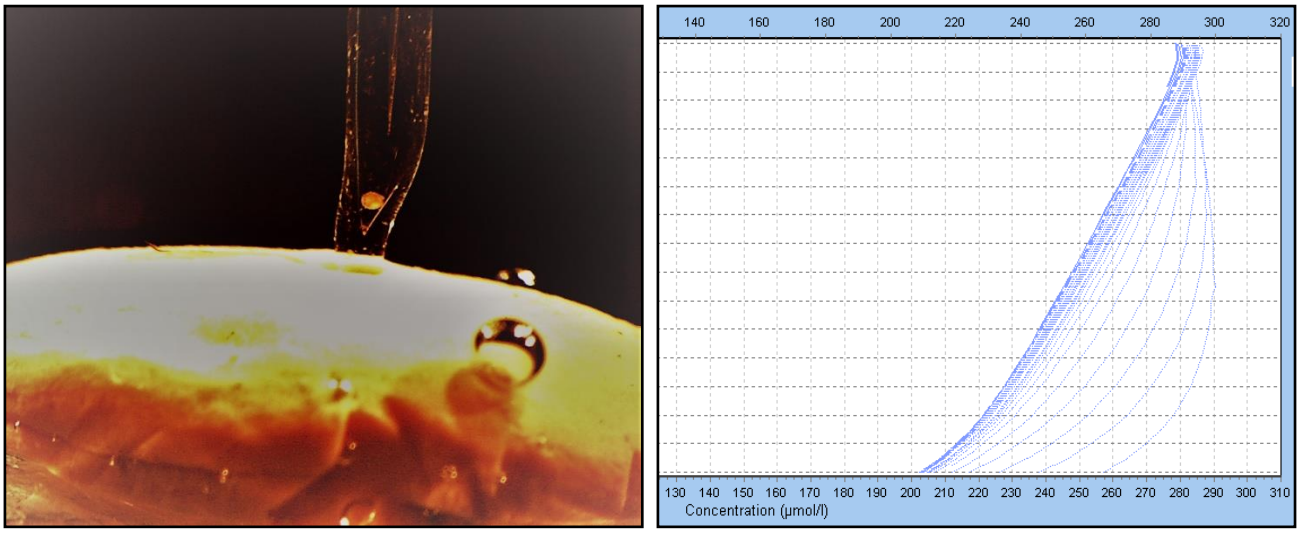

Figure 410: *A picture of the chamber during profiling (Left) and oxygen profiles 1 – 28 in SensorTrace Pro (Right) of the rotifer in chamber a1 across 3000 µm. The picture was taken through the ocular of a horizontal microscope using an iPhone SE camera.*

The narrowing of the chamber matches the change in slope seen for oxygen profiles around 2600 µm. This narrowing effect means that the values seen on the $R_{(t)}$ and $MR_{(t)}$ plots where chamber a1 was used are consistently overestimated. However, since the overestimation is consistent, the trends seen on those plots are still valid – which is what matters most. Insofar as ultimate values are interpreted in Chapters 1 – 3, they are the mean values of steady-state results. Those results were always calculated from microgradients across the parallel area of a chamber – including chamber a1.

3.2. Viability after desiccation

In order to have fully desiccated tuns ready for measurements the day after transfer, the desiccation tubes were moved from wet to dry sand immediately after tardigrades had been transferred and tin-foil placed. This was done due to time-constraints but may have resulted in too rapid desiccation of the tardigrades that contributed to the low viability of tuns from desiccation tubes. It is also possible that the *R. coronifers* were near their limit after ~ 2 years in cryptobiosis and had sustained too much damage for a second desiccation cycle – although the ones that were transferred to desiccation tubes had regained full activity and *ON* viability after the first rehydration. Generally, the viability during this hydration step seemed lower than usual with a survival rate of ~ 50 %. Because of the unsuccessful revival of tuns 1 – 6 during oxygen profiling, the viability of tuns in desiccation tubes was tested with a larger sample size.

Tardigrades were transferred from desiccation tubes to glass bowls and assessed under a stereo-loop. 5 tuns were transferred to MiliQ water and 7 to tap water from Net 4. They were observed 1.5 hours after transfer and again the next day. None of the 5 in MiliQ water regained activity. 1 of the 7 in tap water showed weak movements the next day. 19 tuns from Net 5 were transferred to 2 different glass bowls with tap water. For 10 tuns in one bowl, a lot of bubbles formed on the surface of those tuns and had to be removed with the Irwin loop. One of the tuns regained full activity after 2 hours, but it was of the *M. tardigradum* species and it did not survive *ON*. None of the *R. coronifers* regained activity after 2 hours or *ON*. Net 6 was placed in a petri-dish with oxygen saturated and filtered tap water. 4 tuns were transferred from the net to 4 capillary chambers to see if the chambers affected viability and the remaining 8 were left in the petri dish. After 1.5 hours, 1 of the 4 in chambers was hydrated and dead, while the other 3 were still semi-tuns. After 8 hours, 3 were hydrated and dead, while one was still in semi-tun. Of the 8 in the petri-dish, 2 were dead; 2 were fully active; 3 showed weak activity and 1 was still a semi-tun after 1.5 hours. After 8 hours, 4 were fully active; 1 showed weak activity; 2 were dead and 1 still in semi-tun. Net 7 was placed in a petri-dish filled with tap water with the desiccation tube still attached. It was kept submerged using the lid. After 5 hours, 5 of 16 tardigrades had regained activity. The next day only 3 remained active. Those 3 tardigrades were transferred to the *Whatman 3* paper and two of them were used in Chapter 4 as tuns 9 & 10 where they successfully regained activity.

In total, the survival rate across these viability studies was 19 % (11 out of 58) – not counting the *M. tardigradum* that regained full activity. These observations led to the switch from desiccation tubes to *Whatman 3* filter paper, oxygen saturated tap water instead of MiliQ and broader chambers. This concludes the modifications that were done to the experimental set-ups to obtain the results that will be summarized in the conclusion.

Conclusion

In conclusion, oxygen microgradients provide a simple, flexible and precise method for determining the metabolic rate of tardigrades during many of the physiological adaptations that make them an interesting topic of research. These advantages also make it preferable to the Cartesian diver method which has previously been used for similar studies – although those results have been partially validated here. The method allowed for the determination of metabolic rate in $nmol\ O_2 \cdot mg^{-1} \cdot hour^{-1}$ with regards to both temperature and salinity. The finding that tardigrades that are adapted to colder environments have faster metabolisms is consistent with the results in this study. Novel insights were also gained on how the metabolism of the tardigrades function and how it changes in response to stress. The metabolic rate of *R. coronifer* does not appear to be affected by size. Since size is tightly correlated with age and thus sexual maturity, those do not appear to be factors affecting the metabolic rate either. Furthermore, the cuticle does not appear to actively regulate oxygen uptake. The lack of effect from scaling also means that the bias of the selection step in this study toward larger tardigrades is not a significant issue. The metabolism does not appear to be significantly affected by the movement of tardigrades – since its cessation at 2 °C does not involve more of a decrease in metabolic rate than at other temperature ranges and cessation at 3 – 4 ppt salt solutions coincides with a significant increase in the metabolic rate. The higher metabolic rate of *M. macrocalix* compared to *R. coronifer* can therefore not be explained by its smaller size and more rapid movements – nor by any difference in the environment.

The Q_{10} values for *R. coronifer* suggest a very stable and tightly regulated metabolism with respect to temperature – except for the specific range of 11 – 16 °C which is within the climate of its natural habitat. Not only can there be no *RRTI* as described in the Diver studies since metabolic rate changes significantly between all temperatures, but there can be no *RRTS* range either, since the unstable range is within the Öland climate and the metabolic rate remains stable at 22 – 33 °C which is warmer than it typically gets on Öland. This range of relative temperature dependence (*RRTD*) may be due to hormonal regulation signalling that conditions are optimal for reproduction or due to a temperature-controlled molecular switch between two different metabolic modes. Temperature studies also revealed that the activation energy of the rate-limiting step in *R. coronifer* metabolism is 50.8 kJ/mole O_2. This could be useful for

determining the chemical nature of the *R. coronifer* metabolic pathway. It was measured indirectly since the rate-limiting step itself might not involve oxygen consumption.

The metabolic rate also increases with salinity – most likely due to an osmoregulatory response since no osmoconforming was seen from 0 – 16 ppt. The increase of the tardigrades metabolic rate due to this osmoregulatory response was higher immediately after exposure to the lethal limit than at 3 – 4 ppt and seems to occur faster. It also occurs faster at 0.3 ppt than 3 ppt, although this might simply be because the increase in metabolic rate is smaller. Measuring the metabolic range during the first 5 minutes of exposure at higher resolution would be important to validate this, but it appears to be limited to a 3-fold increase in metabolic rate compared to steady-state in MiliQ water. Mars-analogue levels of perchlorates posed no problem for survival or activity – although it appears to increase metabolic rate more than the same salinity without the perchlorates would. This could be because a lack of transport mechanisms led to a higher osmotic stress from salinity compared to the smaller and physiologically utilized ions of NaCl. The 100x concentration of Mars-analogue perchlorates may simulate desiccation in water due to dehydration – since the metabolic rate of at least one tardigrade seemed uniquely regulated and may have been attempting to enter osmobiosis. This regulation can be described in 5 phases, with phase 3 being especially interesting due to the metabolic rate increasing 286 % over 18 minutes and consistently occurring 60 minutes after the initial exposure to stress. With some adjustments, this could present an opportunity to measure the metabolic rate during successful entry into osmobiosis.

Finally, the change in metabolic rate during termination of anhydrobiosis was found to go through three distinct zones – a high metabolic rate with local peaks, an exponential decrease and a long recuperation period where energy is conserved. The high metabolic rate may be required for the resynthesis and repair of labile structures such as DNA and membranes after e.g. oxidative damage, as well as other modifications such as transcriptional regulation, trehalose degradation and unpacking of organs. The high metabolic rate seen shortly after exposure to water may require organizational structures of the metabolic pathway to be maintained during anhydrobiosis. Barriers for metabolic activity such as inhibitors or a lack of intermediaries, if present, must have been removed within the first 5 minutes of rehydration. The exponential decreases in metabolic rate seem to be correlated with hydration, which might support a recursive-hierarchical description where smaller systems are responsible for the primary modification processes. This observed negative correlation does not seem to fit with the description for termination of anhydrobiosis with regards to artemia cysts – where hydration is thought to facilitate respiration and be

correlated to metabolic rate. The peaks in zone 1 may be to regulate the order and limit overlap of different modification processes and could be caused by the resynthesis of labile structures or metabolic intermediates, removal of inhibitors, or the formation of cellular water channels. Availability of food may play a role in the duration of this recuperation period. In this study, it lasted for more than 24 hours after exposure to water.

To summarize, the project has determined the metabolic rate of tardigrades and how it depends on temperature, salinity and the termination of anhydrobiosis – leading to novel insights into how the tardigrade metabolism functions under those conditions. This answers the problem formulation of the project and provides a method for further inquiry into the energetics of tardigrades.

Perspectives

1. Relevance

This project has elucidated the metabolic rate of the *R. coronifer* species of tardigrades with respect to both normal functions and some of the extraordinary capabilities that make them an interesting research topic. The method can also be used during exposure to a wide array of other conditions such as radiation, toxins and oxidative stress and as an evaluation tool after exposure to any condition such as extreme pressure or empty space. A detailed understanding of tardigrade energetics will allow for the identification of the specific energy requirements for any process of interest. This may prove a valuable tool for chemists and biochemists when describing the molecular mechanisms underlying such processes, which is essential for the potential medical and industrial applications. Furthermore, understanding the metabolism of tardigrades is a key factor for understanding the fundamental question of whether cryptobiosis is truly an ametabolic state and if you can have life without metabolism. In addition to its scientific relevance, this also has implications for our philosophical understanding of life and death.

Finally, metabolism – and specifically metabolic rate is important for the field of ecology and for predicting how ecosystems may be expected to change. Tardigrades are thought to act as pioneer organisms in hazardous environments, facilitating its colonization by other less extremophilic organisms. If humankind decides to terraform Mars, tardigrades may play an important role in that process – given their ecological niche and extremophilic capacities. Understanding the dynamics of their metabolic rate will then be important for predicting the ecological effects. The astrobiological applications of tardigrades also include bioengineering of other organisms to better tolerate space conditions and understanding what mechanisms may be effective for relatively complex multicellular life to survive those conditions. This could provide indications of what to look for when searching for such life elsewhere in the universe – since the same mechanisms may have evolved independently.

2. What is next?

Conditions that would be interesting to investigate further include temperatures between 11 – 16 °C to narrow down the *RRTD* and 2 – 11 °C where movement is suspended; salinities between 4 – 14 ppt to see how the osmoregulatory response changes with salinity in more detail; and replacing small ions with osmolytes such as PEG to study the relationship between cuticle permeability, osmotic stress and entry into osmobiosis. A more thorough chemical analysis of the metabolic rates and activation energy determined in this study would also be valuable. The production of metabolic waste could be determined from pH or CO_2 microgradients – allowing for calculation of the respiratory coefficient and evaluating if auto-toxicity is likely to affect viability during termination of anhydrobiosis. $MR_{(t)}$ plots should give a more detailed description of the first 5 minutes, which might be achieved by optimizing chambers and data collection. Time-frames should be extended to include the entire process of entry into osmobiosis or recuperation after anhydrobiosis. $MR_{(t)}$ plots could also be done for temperature studies like those in Chapter 2. Ideally, salinity or temperature would be changed during measurements on a single tardigrade but unfortunately this would affect the diffusion coefficient of oxygen and thus distort the signal from the sensors – unless somehow accounted for by modelling the changes in diffusion rate. The results of Chapter 4 require validation with higher sample size and more reliable survival rates, as well as a systematic investigation of the effects of time spent in anhydrobiosis and repeated cycles of rehydration.

However, the most interesting experiment would be to measure the oxygen consumption of anhydrobiotic tardigrades in dry state. Unfortunately, the sensors cannot measure accurate microgradients through air due to the much higher overall signal, but figure 42 shows one potential set-up to circumvent this issue.

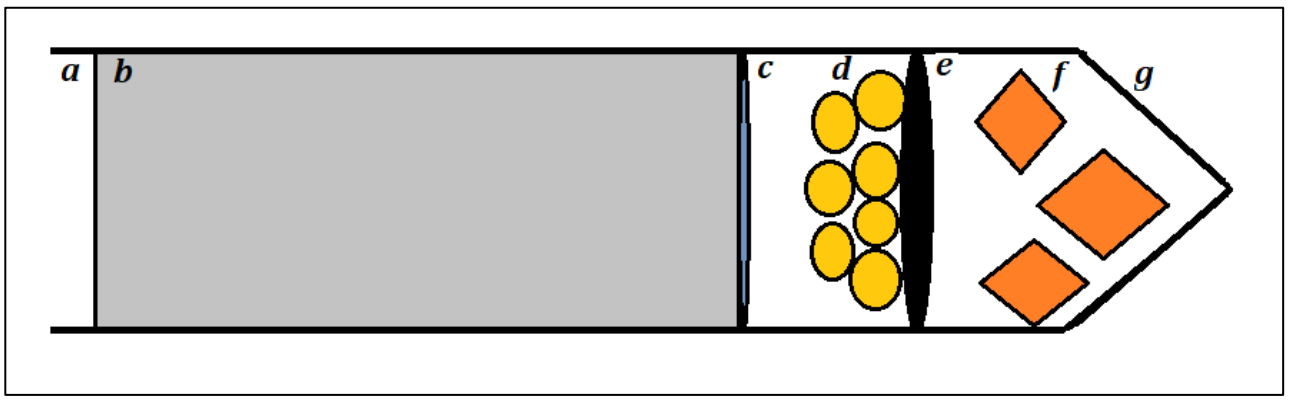

Figure 42: *A schematic drawing of one potential set-up for measuring the oxygen consumption of dry tuns. The figure shows (a) the open end of the chamber, (b) a 1 % agarose phase, (c & e) oxygen-permeable membranes e.g. micropore net, (d) anhydrobiotic R. coronifer tuns, (f) desiccation stones and (g) the collapsed end of chamber.*

The idea is to add a water phase with e.g. 1 % Agarose in one end of the chamber to make it gel-like enough to keep it fixated but liquid enough to let the sensor penetrate and measure oxygen concentration. Before collapsing the chamber, an oxygen permeable membrane is placed underneath the Agarose phase to separate it from the rest of the contents. This could for example be a small piece of micro-pore net. Then, any number of anhydrobiotic tuns can be added to increase the strength of the signal followed by another membrane to keep them isolated. To ensure that the tuns remain completely dry, one or more desiccation stones could be placed below the membrane before collapsing that end of the chamber. By measuring the oxygen microgradient through the Agarose phase, the oxygen consumption of anhydrobiotic tuns could be determined. Controls could be measured of chambers with all the components except any tuns, as well as chambers with tuns that had been inactivated e.g. by heat-treatment. After measurements, both viable and inactivated tuns could be extracted from chambers and rehydrated to see how many of the viable tuns regain activity and ensure that the inactivated tuns do not. It may be necessary to keep all components sterile to eliminate the effect of bacterial respiration – although the controls should account for this. This set-up may provide the most precise quantitative answer available to the question of whether anhydrobiosis is truly ametabolic or not – given the ability to detect oxygen consumption rates as low as 0.7 fmol O_2 per second (Unisense, 2018) and to compile hundreds of tuns in one chamber. The set-up could also be used to measure the metabolic range of single tardigrades during entry into anhydrobiosis – if transferred with water and desiccated in chamber during measurements.

References

Altiero, T. *et al.* (2011) 'Ultraviolet radiation tolerance in hydrated and desiccated eutardigrades', *Journal of Zoological Systematics and Evolutionary Research*, 49(SUPPL.1), pp. 104–110. doi: 10.1111/j.1439-0469.2010.00607.x.

Arakawa, K. (2016) 'No evidence for extensive horizontal gene transfer from the draft genome of a tardigrade', *Proceedings of the National Academy of Sciences*, 113(22), pp. E3057–E3057. doi: 10.1073/pnas.1602711113.

Barnes, R. D. (1982) *Invertebrate Zoology*. Philadelphia: Holt-Saunders International.

Bemm, F. *et al.* (2016) 'Genome of a tardigrade: Horizontal gene transfer or bacterial contamination?', *Proceedings of the National Academy of Sciences*, 113(22), pp. E3054–E3056. doi: 10.1073/pnas.1525116113.

Boothby, T. C. *et al.* (2015) 'Evidence for extensive horizontal gene transfer from the draft genome of a tardigrade', *Proceedings of the National Academy of Sciences*, 112(52), pp. 15976–15981. doi: 10.1073/pnas.1510461112.

Boothby, T. C. *et al.* (2017) 'Tardigrades Use Intrinsically Disordered Proteins to Survive Desiccation', *Molecular Cell*. Elsevier Inc., (65), pp. 975–984. doi: 10.1016/j.molcel.2017.02.018.

Brack, A. (1998) 'The Molecular Origins of Life', *Cambridge University Press*.

Brown, J. H. *et al.* (2004) 'Toward a Metabolic Theory of Ecology', *Ecology*, 85(7), pp. 1771–1789.

Budd, G. E. (2001) 'Tardigrades as "stem-group arthropods": the evidence from the Cambrian fauna', *Zoologischer Anzeiger - A Journal of Comparative Zoology*, 240, pp. 265–279. doi: 10.1078/0044-5231-00034.

Caesar, K., Offenhauser, N. and Lauritzen, M. (2008) 'Gamma-Aminobutyric Acid Modulates Local Brain Oxygen Consumption and Blood Flow in Rat Cerebellar Cortex', *Journal of Cerebral Blood Flow & Metabolism*, 28(5), pp. 906–915. doi: 10.1038/sj.jcbfm.9600581.

Clark, L. C. J. *et al.* (1953) 'Continuous Recording of Blood Oxygen Tensions by Polarography', *Journal of Applied Physiology*, 6, pp. 189–193. doi: 10.1680/udap.2010.163.

Clegg, J. S. (1964) 'the Control of Emergence and Metabolism By External Osmotic Pressure and the Role of Free Glycerol in Developing Cysts of Artemia Salina.', *The Journal of experimental biology*, 41, pp. 879–892.

Clegg, J. S. (1976) 'Interrelationships between Water and Cellular Metabolism in Artemia - V. $^{14}CO_2$ Incorporation', *Journal of Cellular Physiology*, 89(3), pp. 369–380. doi: 10.1002/jcp.1040890303.

Clegg, J. S. (1977) 'Interrelationships between Water and Cellular Metabolism in Artemia - VI. RNA and Protein-synthesis', *Journal of Cellular Physiology*, 91(1), pp. 143–154. doi: 10.1002/jcp.1040910114.

Clegg, J. S. (2001) 'Cryptobiosis - a peculiar state of biological organization', *Comparative Biochemistry and Physiology Part B*, 128, pp. 613–624.

Clegg, J. S. and Cavagnaro, J. (1976) 'Interrelationships between Water and Cellular Metabolism in Artemia - IV. Adeonsine 5'-Triphosphate and cyst hydration', *Journal of Cellular Physiology*, 88(2), pp. 159–166.

Clegg, J. S. and Lovallo, J. (1977) 'Interrelationships between Water and Cellular Metabolism in Artemia - VII. Free Amino Acids', *Journal of Cellular Physiology*, 93(1), pp. 161–168.

Connors, K. A. (1990) *Chemical Kinetics: The Study of Reaction Rates in Solution*. Wiley-VCH; 1st edition.

Cooper, K. W. (1964) 'The first fossil tardigrade: Beorn Leggi Cooper, from cretaceous amber', *Psyche*, 71(2), pp. 41–48.

Crowe, J. H. (1971) 'Anhydrobiosis: An unsolved problem', *American Naturalist*, (105), pp. 563–574. doi: 10.1111/pce.12304.

Crowe, J. H. (1975) 'The physiology of cryptobiosis in Tardigrades', *Mem. Ist. Ital. Idrobiol.*, pp. 37–59.

Crowe, J. H., Carpenter, J. F. and Crowe, L. M. (1998) 'The Role of Vitrification in Anhydrobiosis', *Annual Review of Physiology*, 60(1), pp. 73–103. doi: 10.1146/annurev.physiol.60.1.73.

Crowe, J. H. and Clegg, J. S. (1973) *Anhydrobiosis - Benchmark Papers*. Edited by P. Gray. Stroudsberg, Pennsylvania: Dowden, Hutchinson & Ross, Inc.

Czernekova, M. and Jönsson, K. I. (2016) 'Experimentally induced repeated anhydrobiosis in the eutardigrade Richtersius coronifer', *PLoS ONE*, 11(11), pp. 1–13. doi: 10.1371/journal.pone.0164062.

Dewel, R. and Nelson, D. (1993) *Microscopic Anatomy of Invertebrates, Volume 12: Onychophora, Chilopoda, and Lesser Protostomata*. 12th edn. Edited by W. Harrison. New York.

Edgecombe, G. D. *et al.* (2011) 'Higher-level metazoan relationships: Recent progress and remaining questions', *Organisms Diversity and Evolution*, 11(2), pp. 151–172. doi: 10.1007/s13127-011-0044-4.

Epping, E. H. G., Khalili, A. and Thar, R. (1999) 'Photosynthesis and the dynamics of oxygen consumption in a microbial mat as calculated from transient oxygen microprofiles', *Limnology and Oceanography*, 44(8), pp. 1936–1948. doi: 10.4319/lo.1999.44.8.1936.

Gilmore, C. (2012) *The Oxford Handbook of Philosophy of Death*. Chapter 1: Edited by B. Bradley, F. Feldman, and J. Johansson. New York: Oxford University Press. doi: 10.1093/oxfordhb/9780195388923.001.0001.

Guidetti, R. *et al.* (2012) 'What can we learn from the toughest animals of the Earth? Water bears (tardigrades) as multicellular model organisms in order to perform scientific preparations for lunar exploration', *Planetary and Space Science*. Elsevier, 74(1), pp. 97–102. doi: 10.1016/j.pss.2012.05.021.

Guidetti, R., Altiero, T. and Rebecchi, L. (2011) 'On dormancy strategies in tardigrades', *Journal of Insect Physiology*. Elsevier Ltd, 57(5), pp. 567–576. doi: 10.1016/j.jinsphys.2011.03.003.

Gundersen, J. K. and Jørgensen, B. B. (2012) 'Microstructure of diffusive boundary layers and the oxygen uptake of the sea floor', *Nature*, 1(7), pp. 15796–15799. doi: 10.1017/CBO9781107415324.004.

Gundersen, J. K., Ramsing, N. B. and Glud, R. N. (1998) 'Predicting the signal of O_2 microsensors from physical dimensions, temperature, salinity, and O2 concentration', *Limnol. Oceanogr.*, 43(8), pp. 1932–

1937.

Guppy, M. (2004) 'The biochemistry of metabolic depression: A history of perceptions', *Comparative Biochemistry and Physiology - B Biochemistry and Molecular Biology*, 139(3 SPEC.ISS.), pp. 435–442. doi: 10.1016/j.cbpc.2004.02.019.

Halberg, K. A. *et al.* (2009) 'Cyclomorphosis in Tardigrada: adaptation to environmental constraints.', *The Journal of Experimental Biology*, (212), pp. 2803–2811. doi: 10.1242/jeb.029413.

Halberg, K. A. *et al.* (2013) 'Inorganic ion composition in Tardigrada: cryptobionts contain a large fraction of unidentified organic solutes', *The Journal of Experimental Biology*, (216), pp. 1235–1243. doi: 10.1242/jeb.075531.

Halberg, K. A. and Møbjerg, N. (2012) 'First evidence of epithelial transport in tardigrades : a comparative investigation of organic anion transport', *The Journal of Experimental Biology*, (215), pp. 497–507. doi: 10.1242/jeb.065987.

Hallas, T. E. and W, Y. G. (1972) 'Tardigrada of the soil and litter of a Danish beech forest', *Pedobiologia*, (12), pp. 287–304.

Hashimoto, T. *et al.* (2016) 'Extremotolerant tardigrade genome and improved radiotolerance of human cultured cells by tardigrade-unique protein', *Nature Communications*, 7(12808), pp. 1–14. doi: 10.1038/ncomms12808.

Hecht, M. H. *et al.* (2009) 'Detection of Perchlorate and the Soluble Chemistry of Martian Soil at the Phoenix Lander Site', *Science*, 325(5936), pp. 64–67. doi: 10.1126/science.1172466 Phoenix.

Hengherr, S. *et al.* (2009) 'High-Temperature Tolerance in Anhydrobiotic Tardigrades Is Limited by Glass Transition', *Physiological and Biochemical Zoology*, 82(6), pp. 749–755. doi: 10.1086/605954.

Hickman, C. P. *et al.* (2008) *Integrated Principles of Zoology*. 15th edn, *McGraw-Hill Higher Education*. 15th edn. Edited by D. A. Henricks. New York: Roerig-Blong, J.

Hinton, H. E. and Needham, A. E. (1968) 'Reversible suspension of metabolism and the origin of life', *Proceedings of the Royal Society of London. Series B, Biological Sciences*, 171(1022), pp. 43–57. doi: 10.1098/rspb.1968.0055.

Horikawa, D. D. *et al.* (2006) 'Radiation tolerance in the tardigrade Milnesium tardigradum', *International Journal of Radiation Biology*, 82(12), pp. 843–848. doi: 10.1080/09553000600972956.

Horikawa, D. D. *et al.* (2008) 'Establishment of a Rearing System of the Extremotolerant Tardigrade Ramazzottius varieornatus : A New Model Animal for Astrobiology', *Astrobiology*, 8(3), pp. 549–556. doi: 10.1089/ast.2007.0139.

Hyvönen, R. and Persson, T. (1996) 'Effects of fungivorous and predatory arthropods on nematodes and tardigrades in microcosms with coniferous forest soil', *Biology and Fertility of Soils*, 21, pp. 121–127. doi: 10.1007/BF00336003.

Jennings, P. G. (1975) 'The Signy Island Terrestrial Reference Sites: V. Uptake of Macrobiotus furciger J. Murray (Tardigrada)', *British Antarctic Survey Bulletin*, pp. 161–168.

Jönsson, K. I. (2007) 'Tardigrades as a Potential Model Organism in Space Research', *Astrobiology*, 7(5), pp. 757–766. doi: 10.1089/ast.2006.0088.

Jönsson, K. I. *et al.* (2008) 'Tardigrades survive exposure to space in low Earth orbit', *Current Biology*, 18(17), pp. 729–731. doi: 10.1016/j.cub.2008.06.048.

Jönsson, K. I. *et al.* (2016) 'The fate of the TARDIS offspring: no intergenerational effects of space exposure', *Zoological Journal of the Linnean Society*, 178(4), pp. 924–930. doi: 10.1111/zoj.12499.

Jönsson, K. I. and Bertolani, R. (2001) 'Facts and fiction about long-term survival in tardigrades', *J. Zool., Lond.*, (255), pp. 121–123. doi: 10.1017/S0952836901001169.

Jönsson, K. I., Harms-Ringdahl, M. and Torudd, J. (2005) 'Radiation tolerance in the eutardigrade Richtersius coronifer', *International Journal of Radiation Biology*, 81(9), pp. 649–656. doi: 10.1080/09553000500368453.

Jönsson, K. I. and Schill, R. O. (2007) 'Induction of Hsp70 by desiccation, ionising radiation and heat-shock in the eutardigrade Richtersius coronifer', *Comparative Biochemistry and Physiology - B Biochemistry and Molecular Biology*, 146(4), pp. 456–460. doi: 10.1016/j.cbpb.2006.10.111.

Jönsson, K. I. and Wojcik, A. (2017) 'Tolerance to X-rays and Heavy Ions (Fe, He) in the Tardigrade *Richtersius coronifer* and the Bdelloid Rotifer *Mniobia russeola*', *Astrobiology*, 17(2), pp. 163–167. doi: 10.1089/ast.2015.1462.

Keilin, D. (1959) 'The problem of anabiosis or latent life: history and current concept', *Proceedings of the Royal Society B: Biological Sciences*, 17(150), pp. 149–191.

Kinchin, I. M. (1994) *The Biology of Tardigrades*. 1st edn. London: Portland.

Klekowski, R. Z. and Opalinski, W. (1989) 'Oxygen Consumption in Tardigrada from Spitsbergen', *Polar Biology*, (9), pp. 299–303.

Koutsovoulos, G. *et al.* (2016) 'No evidence for extensive horizontal gene transfer in the genome of the tardigrade *Hypsibius dujardini*', *Proceedings of the National Academy of Sciences*, 113(18), pp. 5053–5058. doi: 10.1073/pnas.1600338113.

Lecoq, J. *et al.* (2009) 'Odor-Evoked Oxygen Consumption by Action Potential and Synaptic Transmission in the Olfactory Bulb.', *The Journal of neuroscience : the official journal of the Society for Neuroscience*, 29(5), pp. 1424–1433. doi: 10.1523/JNEUROSCI.4817-08.2009.

Lenntech (2018) *Osmotic pressure calculator*. Available at: https://www.lenntech.com/calculators/osmotic/osmotic-pressure.htm.

Maas, A. and Waloszek, D. (2001) 'Cambrian derivatives of the early Arthropod stem lineage, Pentastomids, tardigrades and Lobopodians - An "Orsten" perspective', *Zoologischer Anzeiger*, 240, pp. 451–459. doi: 10.1078/0044-5231-00053.

Marchioro, T. *et al.* (2013) 'Somatic musculature of Tardigrada: phylogenetic signal and metameric patterns', *Zoological Journal of the Linnean Society*, (169), pp. 580–603. doi: 10.1111/zoj.12079.

May, R. M., Maria, M. and Guimard, J. (1964) 'Action différentielles des rayons x et ultraviolets sur le tardigrade Macrobiotus areolatus, à l'état actif et desséché.', *Bullentin Biologique de la France et de la Belgique*, (98), pp. 349–367.

Mayhew, J. E. W. (2003) 'A Measured Look at Neuronal Oxygen Consumption', *Neuroscience Perspectives*, 299(February), pp. 1023–1025. doi: 10.1126/science.1082403.

Meteoblue (2018) *Climate Oland*. Available at: https://www.meteoblue.com/en/weather/forecast/modelclimate/oland_norway_3143677 (Accessed: 8 July 2018).

Miller, W. R. (1997) 'Tardigrades: Bears of the Moss', *The Kansas School Naturalist*, 45(3), pp. 1–16.

Møbjerg, N. *et al.* (2011) 'Survival in extreme environments – on the current knowledge of adaptations in tardigrades', *Acta Physiologica*, (202), pp. 409–420. doi: 10.1111/j.1748-1716.2011.02252.x.

Natural History Museum of Copenhagen (2018) *Tardigrada_ZM_2018*, *Zoological Museum*. Available at: https://docs.google.com/spreadsheets/d/1IEj_9O1U41z2cqWFmImVOtuSbokYAHK2Kq_G8rFjuG0/edit#gid=0 (Accessed: 7 June 2018).

Nelson, D. L. and Cox, M. M. (2013) *Lehninger Principles of Biochemistry*. Sixth Edit. Edited by L. Schultz et al. 41 Madison Avenue, New York, NY 10010: Susan Winslow.

Nelson, D. R. (2002) 'Current status of the tardigrada: evolution and ecology.', *Integrative and comparative biology*, 42(3), pp. 652–659. doi: 10.1093/icb/42.3.652.

Neuman, Y. (2006) 'Cryptobiosis: A new theoretical perspective', *Progress in Biophysics and Molecular Biology*, 92(2), pp. 258–267. doi: 10.1016/j.pbiomolbio.2005.11.001.

Neumann, S. *et al.* (2009) 'DNA damage in storage cells of anhydrobiotic tardigrades', *Comparative Biochemistry and Physiology - A Molecular and Integrative Physiology*. Elsevier Inc., 153(4), pp. 425–429. doi: 10.1016/j.cbpa.2009.04.611.

Nichols, P. B. (2005) *Tardigrade evolution and ecology*, *Graduate Theses and Dissertations*. University of South Florida.

Nielsen, P. *et al.* (2007) 'Respiration rates of subitaneous eggs from a marine calanoid copepod: Monitored by nanorespirometry', *Journal of Comparative Physiology B: Biochemical, Systemic, and Environmental Physiology*, 177(3), pp. 287–296. doi: 10.1007/s00360-006-0128-1.

Nøhr Glud, R. *et al.* (1995) 'Calibration and performance of the stirred flux chamber from the benthic lander Elinor', *Deep-Sea Research Part I*, 42(6), pp. 1029–1042. doi: 10.1016/0967-0637(95)00023-Y.

Offenhauser, N. *et al.* (2005) 'Activity-induced tissue oxygenation changes in rat cerebellar cortex: interplay of postsynaptic activation and blood flow', *The Journal of Physiology*, 565(1), pp. 279–294. doi: 10.1113/jphysiol.2005.082776.

Oldham, C. (1994) 'A fast-response oxygen sensor for use on fine-scale and microstructure CTD profilers', *Limnol. Oceanogr.*, 39(8), pp. 1959–1966.

Ono, F. *et al.* (2016) 'Effect of ultra-high pressure on small animals, tardigrades and Artemia', *Cogent Physics*. Cogent, 3(1), pp. 1–8. doi: 10.1080/23311940.2016.1167575.

Osunsanmi, O. (2017) 'The Butcher's Knife Cares Not for the Lamb's Cry - Star Trek: Discovery'. United States of America: CBS Television Distribution.

Persson, D. *et al.* (2011) 'Extreme stress tolerance in tardigrades: surviving space conditions in low earth orbit', *Journal of Zoological Systematics and Evolutionary Research*, 49(Suppl. 1), pp. 90–97. doi: 10.1111/j.1439-0469.2010.00605.x.

Persson, D. *et al.* (2011) 'Extreme stress tolerance in tardigrades: Surviving space conditions in low earth orbit', *Journal of Zoological Systematics and Evolutionary Research*, 49(SUPPL.1), pp. 90–97. doi: 10.1111/j.1439-0469.2010.00605.x.

Pigon, A. and Weglarska, B. (1953) 'The Respiration of Tardigrada: A Study in Animal Anabiosis', *Bull. Acad. Polon. Sci.*, 2(1), pp. 69–72.

Pope, B. (2014) 'Deeper, Deeper, Deeper Still - Cosmos: A Spacetime Odyssey'. United States of America: Fox & National Geographic Channel.

Pouchet, F. A. (1869) *Naturens Vidundere.* PÅ dansk. Edited by P. Mariager. København: Philipsens Forlag.

Ramløv, H. (1989) *Fænomenet Cryptobiose - specielt med henblik på tardigraden Adorybiotus coronifer*. Københavns Universitet.

Ramløv, H. and Westh, P. (1992) 'Survival of the cryptobiotic eutardigrade Adorybiotus coronifer during cooling to -196 °C: Effect of cooling rate, trehalose level, and short-term acclimation', *Cryobiology*, 29(1), pp. 125–130. doi: 10.1016/0011-2240(92)90012-Q.

Ramløv, H. and Westh, P. (2001) 'Cryptobiosis in the Eutardigrade Adorybiotus (Richtersius) coronifer: Tolerance to Alcohols, Temperature and de novo Protein Synthesis', *Zoologischer Anzeiger - A Journal of Comparative Zoology*, 240, pp. 517–523. doi: 10.1078/0044-5231-00062.

Randy, W. R. and Miller, W. R. (2011) 'Tardigrades: These ambling, eight-legged microscopic "bears of the moss" are cute, ubiquitous, all but indestructible and a model organism for education', *American Scientist*, 99(5), pp. 384–391.

Rebecchi, L. *et al.* (2009) 'Survival and DNA degradation in anhydrobiotic tardigrades', *Journal of Experimental Biology*, 212(24), pp. 4033–4039. doi: 10.1242/jeb.033266.

Rebecchi, L. *et al.* (2011) 'Resistance of the anhydrobiotic eutardigrade Paramacrobiotus richtersi to space flight (LIFE – TARSE mission on FOTON-M3)', *Journal of Zoological Systematics and Evolutionary Research*, 49(Suppl. 1), pp. 98–103. doi: 10.1111/j.1439-0469.2010.00606.x.

Rebecchi, L., Altiero, T. and Guidetti, R. (2007) 'Anhydrobiosis: the extreme limit of desiccation tolerance', *Isj*, 4, pp. 65–81. doi: 10.1242/jeb.02179.

Revsbech, N. P. (1989) 'An oxygen microelectrode with a guard cathode.', *Limnology and Oceanography.*, 34(2), pp. 472–476.

Revsbech, N. P. (1989) 'Diffusion characteristics of microbial communities determined by use of oxygen microsensors', *Journal of Microbiological Methods*, 9(2), pp. 111–122. doi: 10.1016/0167-7012(89)90061-4.

Reyes, B. A., Pendergast, J. S. and Yamazaki, S. (2008) 'Mammalian Peripheral Circadian Oscillators Are Temperature Compensated', *J Biol Rhythms*, 23(1), pp. 95–98. doi: 10.1111/j.1468-1331.2010.03161.x.Clinical.

Riedel, T. E. *et al.* (2013) 'Oxygen consumption rates of bacteria under nutrient-limited conditions', *Applied and Environmental Microbiology*, 79(16), pp. 4921–4931. doi: 10.1128/AEM.00756-13.

Rizzo, A. M. *et al.* (2015) 'Space Flight Effects on Antioxidant Molecules in Dry Tardigrades : The

TARDIKISS Experiment', *BioMed Research International*, 2015(i), pp. 1–7. doi: http://dx.doi.org/10.1155/2015/167642.

Romano, F. A. (2003) 'On water bears', *Florida Entomologist*, 86(2), pp. 134–137. doi: 10.1653/0015-4040(2003)086[0134:OWB]2.0.CO;2.

Sands, C. J. *et al.* (2008) 'Phylum Tardigrada: An "individual" approach', *Cladistics*, 24(6), pp. 861–871. doi: 10.1111/j.1096-0031.2008.00219.x.

Schill, R. O., Steinbrück, G. H. B. and Köhler, H. (2004) 'Stress gene (hsp70) sequences and quantitative expression in Milnesium tardigradum (Tardigrada) during active and cryptobiotic stages', *The Journal of Experimental Biology*, 207, pp. 1607–1613. doi: 10.1242/jeb.00935.

Seki, K. and Toyoshima, M. (1998) 'Preserving tardigrades under pressure', *Nature*, 395(6705), pp. 853–854. doi: 10.1038/27576.

Severinghaus, J. W. (2002) 'The Invention and Development of Blood Gas Analysis', *Anesthesiology*, 97(1), pp. 253–256.

Stec, D. *et al.* (2016) 'Estimating optimal sample size for tardigrade morphometry', *Zoological Journal of the Linnean Society*, 178(4), pp. 776–784. doi: 10.1111/zoj.12404.

Tanaka, S. *et al.* (2015) 'Novel mitochondria-targeted heat-soluble proteins identified in the anhydrobiotic tardigrade improve osmotic tolerance of human cells', *PLoS ONE*, 10(2), pp. 1–15. doi: 10.1371/journal.pone.0118272.

Tenlen, J. R. *et al.* (2016) 'Correction for Boothby et al., Evidence for extensive horizontal gene transfer from the draft genome of a tardigrade', *Proceedings of the National Academy of Sciences*, 113(36), pp. E5364–E5364. doi: 10.1073/pnas.1613046113.

The Planetary Society (2011) *Phobos Life Project*. Available at: http://www.planetary.org/explore/projects/life/ (Accessed: 24 May 2017).

Thompson, J. K., Peterson, M. R. and Freeman, R. D. (2003) 'Single-Neuro Activity and Tissue Oxygenation in the Cerebral Cortex', *Science*, 299(February), pp. 1070–1072. doi: 10.1126/science.1079220.

Thompson, J. K., Peterson, M. R. and Freeman, R. D. (2005) 'Separate Spatial Scales Determine Neural Activity-Dependent Changes in Tissue Oxygen within Central Visual Pathways', *Journal of Neuroscience*, 25(39), pp. 9046–9058. doi: 10.1523/JNEUROSCI.2127-05.2005.

Unisense (2016) *MicroRespiration System User Manual*. Aarhus N 8200, Denmark.

Unisense (2018) *Nano Respiration System*. Available at: http://www.unisense.com/NanoRespiration_System (Accessed: 8 July 2018).

Vasanthan, T. *et al.* (2017) 'G-Equivalent Acceleration Tolerance in the Eutardigrade Species *Hypsibius dujardini*', *Astrobiology*, 17(1), pp. 55–60. doi: 10.1089/ast.2015.1439.

Wadsworth, J. and Cockell, C. S. (2017) 'Perchlorates on Mars enhance the bacteriocidal effects of UV light', *Scientific Reports*. Springer US, 7(1), pp. 1–8. doi: 10.1038/s41598-017-04910-3.

Watanabe, M. *et al.* (2002) 'Mechanism allowing an insect to survive complete dehydration and extreme

temperatures', *Journal of Experimental Biology*, 205(18), pp. 2799–2802.

Wełnicz, W. *et al.* (2011) 'Anhydrobiosis in tardigrades — The last decade', *Journal of Insect Physiology*, 57, pp. 577–583. doi: 10.1016/j.jinsphys.2011.03.019.

Weronika, E. and Kaczmarek, Ł. (2016) 'Tardigrades in Space Research - Past and Future', *Orig Life Evol Biosph*. doi: 10.1007/s11084-016-9522-1.

Westh, P. (1990) *Biokemiske aspekter af cryptobiose - Eksperimentelt belyst med tardigrader*. Københavns Universitet.

Wright, J. C. W. (2001) 'Cryptobiosis 300 Years on from van Leuwenhoek: What Have We Learned about Tardigrades ?', *Zoologischer Anzeiger*, 240(August 2000), pp. 563–582.

Wright, J. C., Westh, P. and Ramløv, H. (1992) 'Cryptobiosis in Tardigrada', *Biological Reviews*, 67(1), pp. 1–29. doi: 10.1111/j.1469-185X.1992.tb01657.x.

Yoshida, Y. *et al.* (2017) *Comparative genomics of the tardigrades Hypsibius dujardini and Ramazzottius varieornatus*, *PLoS Biology*. doi: 10.1371/journal.pbio.2002266.

Appendix I – Capillary chambers

Chamber A1: Length = 2.841 mm; Radius = $\frac{(690\ \mu m + 725.7\ \mu m)}{4}$ = 353.925 μm. A = 3.93525024079 · 10^{-3} cm^2.

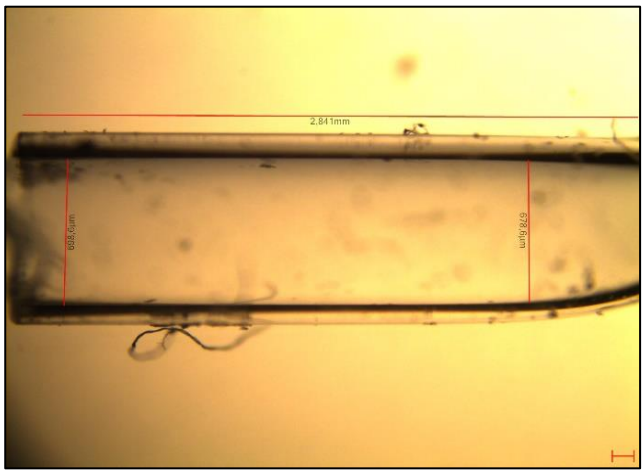

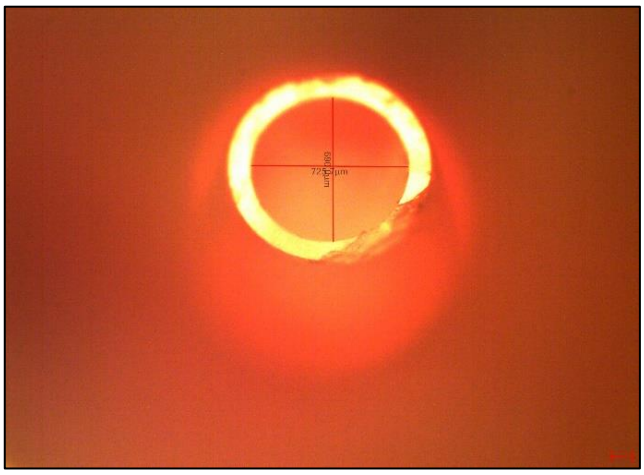

Chamber A2: Length = 2.501 mm; Radius = $\frac{(720\ \mu m + 697.1\ \mu m)}{4}$ = 354.275 μm. A = 3.9430373065 · 10^{-3} cm^2.

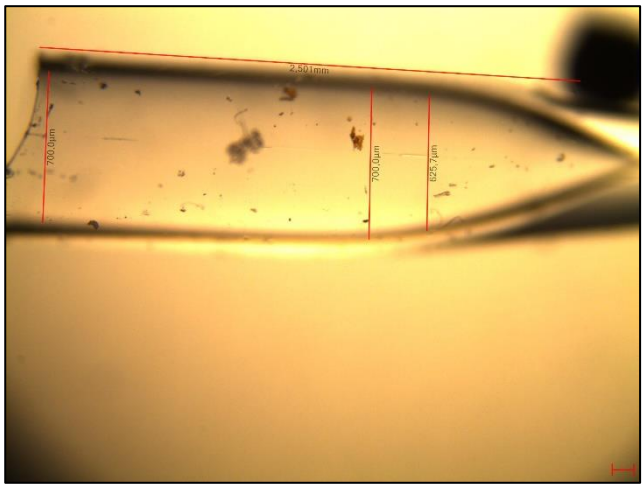

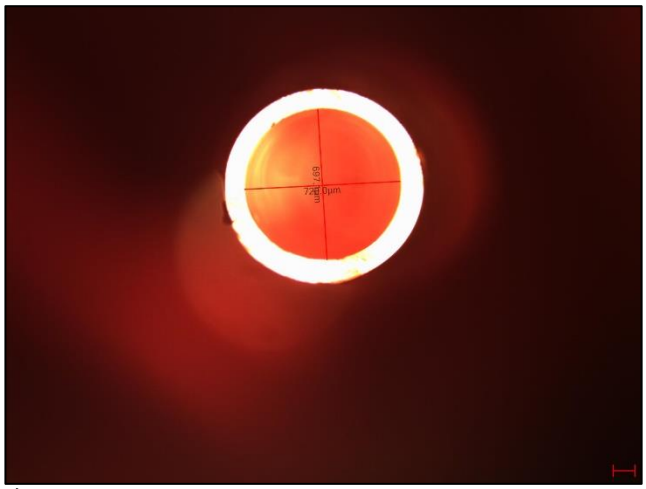

Chamber A3: Length = 2.620 mm; Radius = $\frac{(660\ \mu m + 655.7\ \mu m)}{4}$ = 328.925 μm. A = 3.39894110491 · 10^{-3} cm^2.

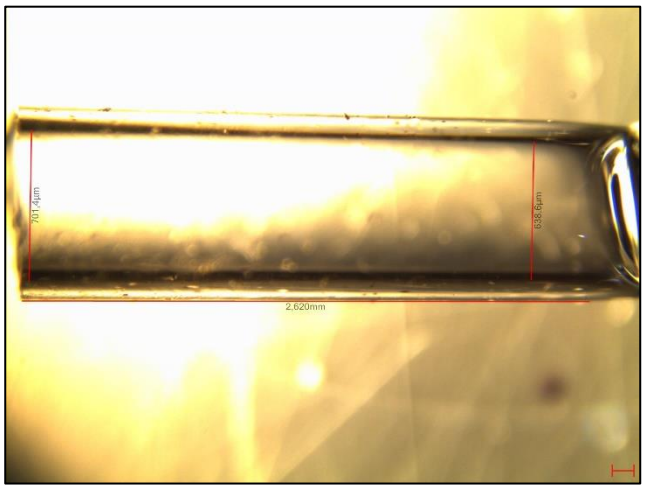

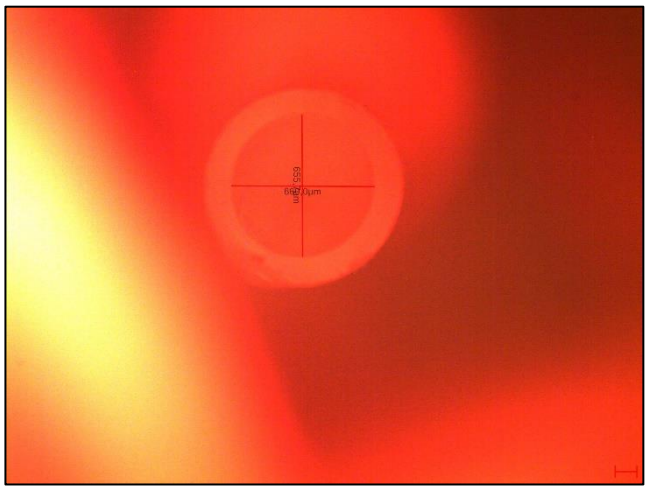

Chamber A4: Length = 2.806 mm; Radius = $\frac{(717.9\ \mu m + 722{,}9\ \mu m)}{4}$ = 360.2 μm. A = 407602922911 · 10^{-3} cm^2.

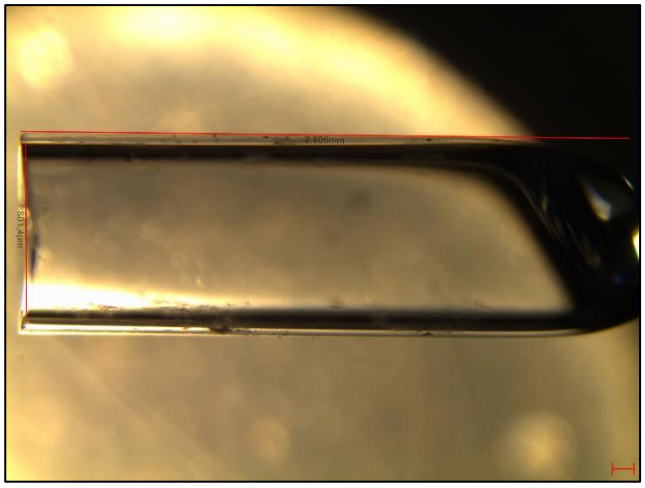


Chamber B1: Length = 2.709 mm; Radius = $\frac{(660\ \mu m + 660\ \mu m)}{4}$ = 330.0 μm. A = 3.42119439976 · 10^{-3} cm^2.

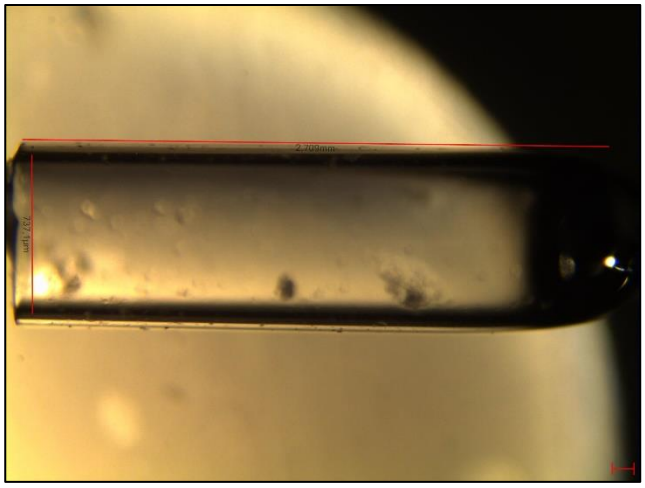
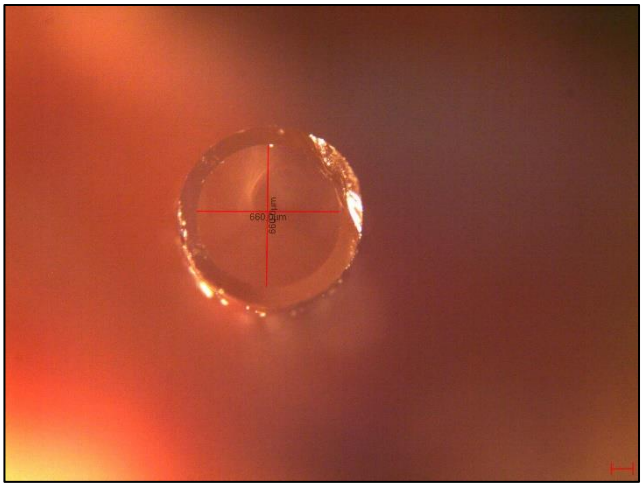

Chamber B2: Length = 2.034 mm; Radius = $\frac{(640\ \mu m + 640\ \mu m)}{4}$ = 320.0 μm. A = 3.21699087728 · 10^{-3} cm^2.

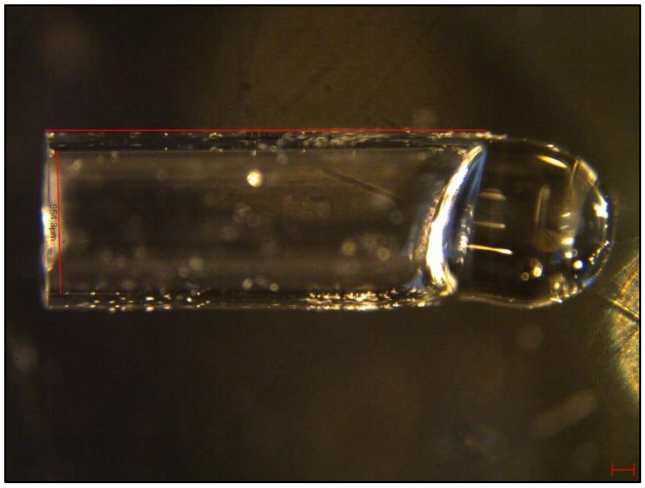
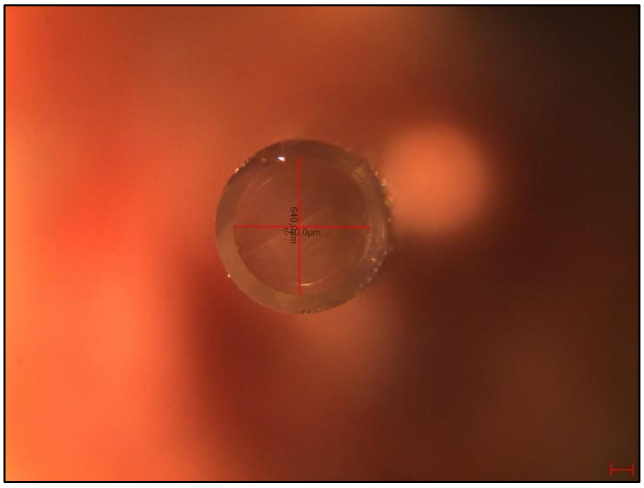

Chamber B3: Length = 2.764 mm; Radius = $\frac{(591.4\ \mu m + 591.4\ \mu m)}{4}$ = 295.7 μm. A = 2.74696117825 · 10^{-3} cm^2.

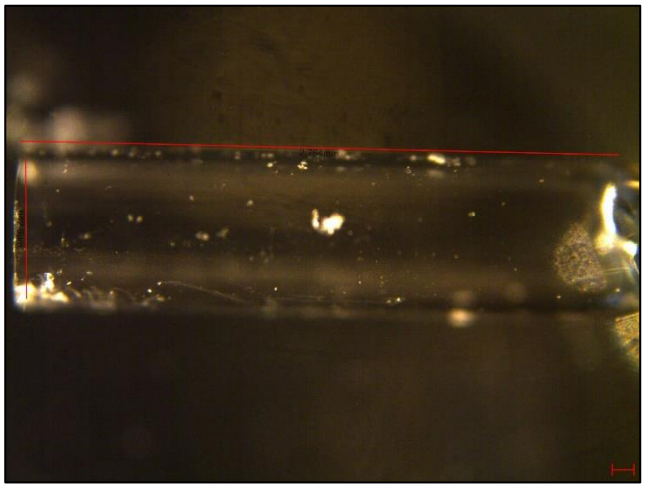
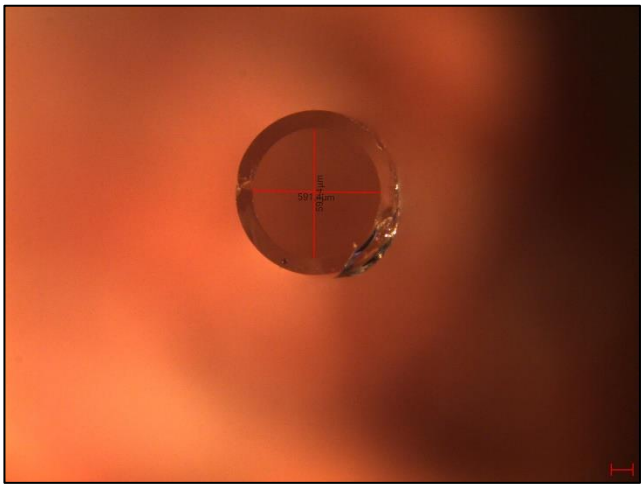

Chamber B4: Length = 2.200 mm; Radius = $\frac{(594.3\ \mu m + 594.3\ \mu m)}{4}$ = 297.15 μm. A = 2.77396732972 · 10^{-3} cm^2.

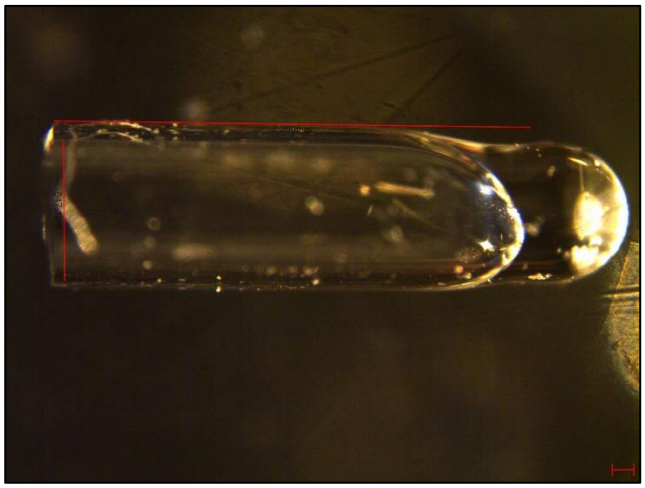
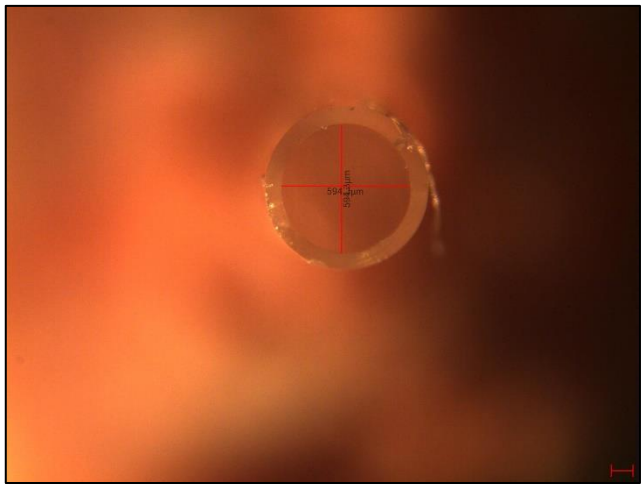

Chamber C1: Length = 2.000 mm; Radius = $\frac{(630\ \mu m + 630\ \mu m)}{4}$ = 315.0 μm. A = 3.11724531052 · 10^{-3} cm^2.

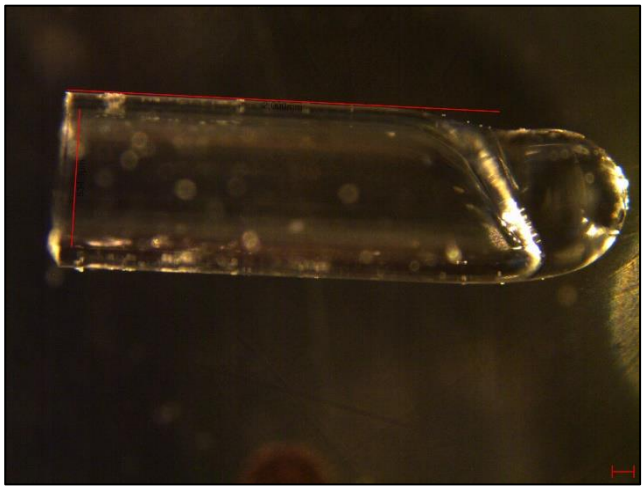
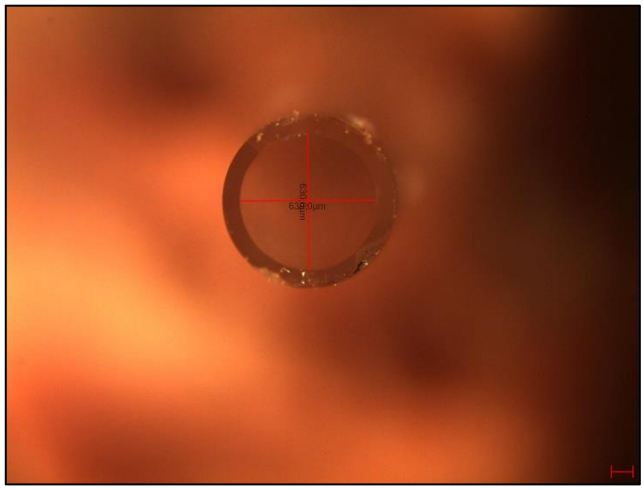

Average length ≈ 2.5 mm. Average radius ≈ 330 μm. Average diameter ≈ 660 μm.

Appendix II – Seawater and Gases Table

Conditions used in this study have been highlighted.

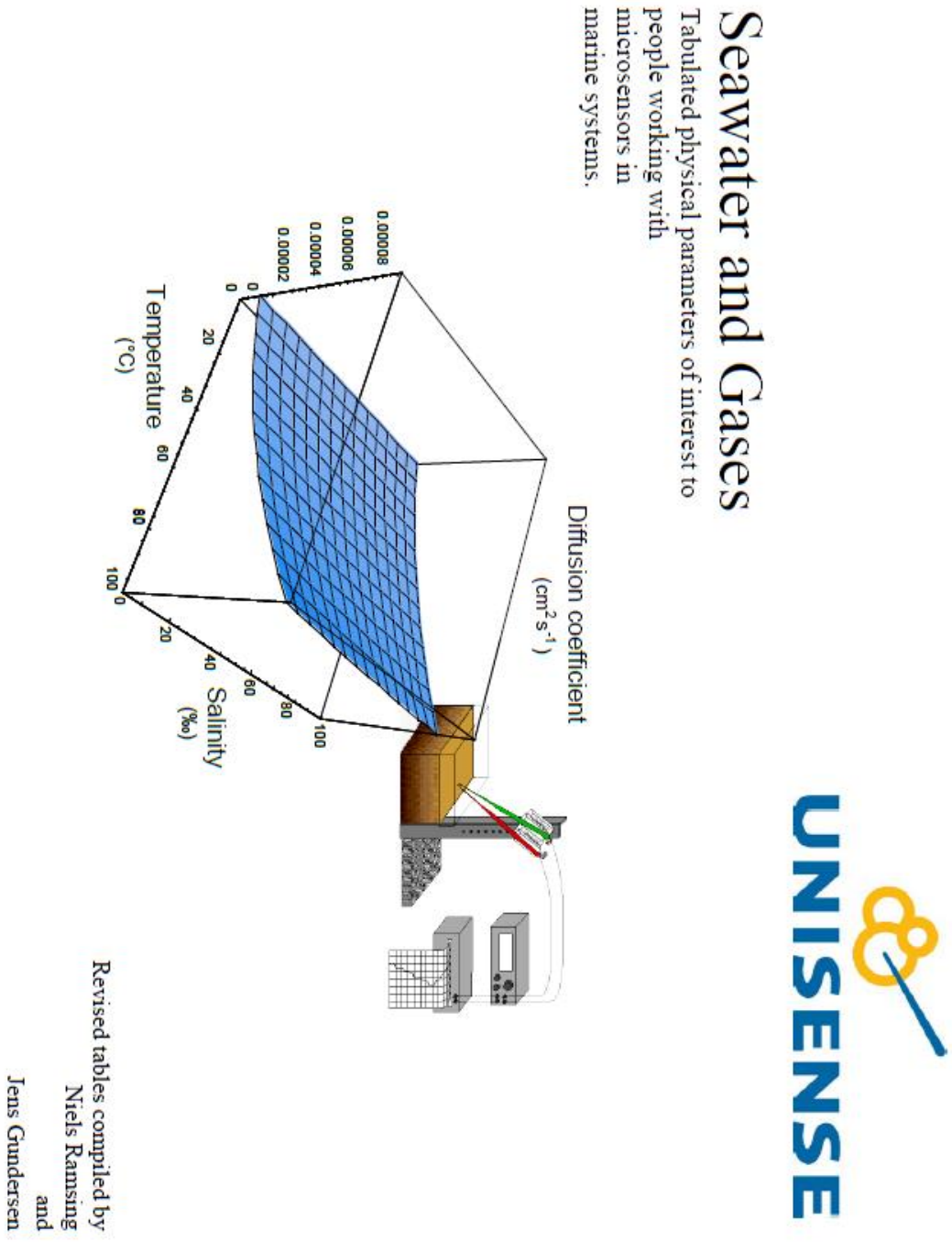

Content

Cover page: Diffusion coefficient for oxygen at various temperatures & salinities

diffO2 = Diffusivity of oxygen in distilled water at 10°C
= 1.57*10^-5 cm2 s-1
Table from Broeker & Peng, 1974,
estimated from Himmelblau, 1964
The value at 10 °C is used to scale the calculated Di[T,S,P]

To calculate diffusion coefficient for other gasses

To get diffusivity of	*multiply table values by*
H2	1.9470
N2	0.8301
He	2.6602
Ar	0.7573
Rn	0.5825
CO	0.8495
CO2	0.7961
CH4	0.8495
N2O	1.0049
H2S	0.7573
SO2	0.7476

Di[T,S,P] = the diffusion constant of oxygen at Temperature T (0≤T≤40 °C)
and salinity S, (0<S<40‰) at pressure P, (0<P<1000bar) => cm2 s-1
Calculated from formula:
Di[T2,S2,P2]=Di[T1,S1,P1]*(dynvisc[T1,S1,P1]/dynvisc[T2,S2,P2])*(T2/T1)
Equation from: Li & Gregory, 1974, Geochim. Cosmochim, 38:703-714
using Di[T1,S1,P1]=difO2 with T1=10°C, S1=0‰ and P1=1bar (see above)

solO2[T,S] = solubility of oxygen at temperature T (0≤T≤40 °C)
and salinity S, (0<S<40‰) at pressure P = 1 bar => µmol kg-1
formula found in Garcia and Gordon. 1992,
Oxygen solubility in seawater: Better fitting equations,
(calulated for any salinity)
Limnol. Oceanogr. 37:1307-1312

Oxygen conversion factors
0.032 mg/µmol
0.02241 ml/µmol
1.428 mg/ml

dens[T,S] = density of seawater at temperature T (0≤T≤40)
and salinity S, (0<S<40‰) at pressure P = 1 bar => g cm-3
Equation from:Standard Methods for examination of water and
wastewater 1992, 18 th ed. Edited by A Greenberg et al. p 2-48
"2520 C. Density method"
reprinted from: Millero & Poisson, 1981.
International one-atmosphere equation of state of seawater,
Deep Sea Res. 28:625

dynvisc[T,S,P] = dynamic viscosity of seawater at temperature T (0≤T≤40)
and salinity S, (0<S<40‰) at pressure P, (0<P<1000bar)
=> cp = centi poise = 10*^3 Pa s = 10*^-2 g cm-1 s-1
Formula from: Chemical Oceanography vol. 4, 1975, 2'ed. Edited by
Riley, Table 25, p 338, developed by Millero, 1974
with pressure corrections by Matthäus,1972

kinvisc[T,S] = kinematic viscosity of water at temperature T (0≤T≤40)
and salinity S, (0<S<40‰) at pressure P = 1 bar
=> cp g-1 cm3 = 10*^-2 cm2 s-1
Calculated from dynamic viscosity:
kinvisc[T,S] = dynvisc[T,S]/dens[T,S]

Schmidt number [T,S] = (kinematic viscosity / diffusion coefficient) at Temperature
T, (0≤T≤40°C) and salinity S, (0<S<40‰) at pressure P = 1 bar
=> Dimensionless

DATA-TABLE 1 *by Niels Ramsing & Jens Gundersen*

Diffusion coefficient for oxygen at different temperatures and salinities of seawater

Units: 10^-5 cm2 s-1

Salinity	Temperature (°C)																				
(‰)	0.0	1.0	2.0	3.0	4.0	5.0	6.0	7.0	8.0	9.0	10.0	11.0	12.0	13.0	14.0	15.0	16.0	17.0	18.0	19.0	20.0
0.0	1.1041	1.1465	1.1899	1.2344	1.2798	1.3261	1.3734	1.4214	1.4702	1.5198	1.5700	1.6209	1.6723	1.7243	1.7769	1.8300	1.8836	1.9377	1.9924	2.0478	2.1039
1.0	1.1026	1.1448	1.1881	1.2324	1.2777	1.3239	1.3709	1.4188	1.4675	1.5169	1.5669	1.6176	1.6689	1.7208	1.7732	1.8261	1.8796	1.9336	1.9882	2.0434	2.0993
2.0	1.1011	1.1432	1.1863	1.2305	1.2756	1.3216	1.3685	1.4162	1.4647	1.5140	1.5639	1.6144	1.6656	1.7173	1.7695	1.8223	1.8756	1.9295	1.9839	2.0390	2.0949
3.0	1.0996	1.1415	1.1845	1.2285	1.2735	1.3193	1.3661	1.4137	1.4620	1.5111	1.5608	1.6112	1.6622	1.7137	1.7658	1.8185	1.8717	1.9254	1.9797	2.0347	2.0904
4.0	1.0981	1.1399	1.1827	1.2266	1.2714	1.3171	1.3637	1.4111	1.4593	1.5082	1.5578	1.6080	1.6588	1.7102	1.7622	1.8147	1.8677	1.9213	1.9755	2.0304	2.0860
5.0	1.0966	1.1382	1.1809	1.2246	1.2693	1.3148	1.3613	1.4085	1.4566	1.5053	1.5547	1.6048	1.6555	1.7068	1.7586	1.8109	1.8638	1.9173	1.9714	2.0261	2.0815
6.0	1.0950	1.1366	1.1792	1.2227	1.2672	1.3126	1.3589	1.4060	1.4539	1.5024	1.5517	1.6017	1.6522	1.7033	1.7550	1.8072	1.8599	1.9133	1.9672	2.0218	2.0771
7.0	1.0935	1.1350	1.1774	1.2208	1.2651	1.3104	1.3565	1.4034	1.4512	1.4996	1.5487	1.5985	1.6489	1.6998	1.7514	1.8034	1.8560	1.9092	1.9631	2.0175	2.0727
8.0	1.0921	1.1333	1.1756	1.2189	1.2631	1.3082	1.3541	1.4009	1.4485	1.4968	1.5457	1.5953	1.6456	1.6964	1.7478	1.7997	1.8522	1.9053	1.9589	2.0133	2.0684
9.0	1.0906	1.1317	1.1738	1.2169	1.2610	1.3060	1.3518	1.3984	1.4458	1.4939	1.5427	1.5922	1.6423	1.6930	1.7442	1.7960	1.8483	1.9013	1.9548	2.0090	2.0640
10.0	1.0891	1.1301	1.1721	1.2150	1.2589	1.3037	1.3494	1.3959	1.4431	1.4911	1.5398	1.5891	1.6390	1.6895	1.7406	1.7923	1.8445	1.8973	1.9507	2.0048	2.0597
11.0	1.0876	1.1285	1.1703	1.2131	1.2569	1.3015	1.3471	1.3934	1.4405	1.4883	1.5368	1.5860	1.6358	1.6861	1.7371	1.7886	1.8407	1.8934	1.9467	2.0006	2.0554
12.0	1.0861	1.1268	1.1686	1.2112	1.2549	1.2994	1.3447	1.3909	1.4378	1.4855	1.5339	1.5829	1.6325	1.6828	1.7336	1.7849	1.8369	1.8894	1.9426	1.9965	2.0511
13.0	1.0846	1.1252	1.1668	1.2093	1.2528	1.2972	1.3424	1.3884	1.4352	1.4827	1.5309	1.5798	1.6293	1.6794	1.7300	1.7813	1.8331	1.8855	1.9386	1.9923	2.0468
14.0	1.0832	1.1236	1.1651	1.2075	1.2508	1.2950	1.3401	1.3859	1.4326	1.4799	1.5280	1.5767	1.6261	1.6760	1.7265	1.7776	1.8293	1.8816	1.9345	1.9881	2.0425
15.0	1.0817	1.1220	1.1633	1.2056	1.2488	1.2928	1.3377	1.3835	1.4300	1.4772	1.5251	1.5737	1.6229	1.6727	1.7231	1.7740	1.8256	1.8777	1.9305	1.9840	2.0383
16.0	1.0802	1.1204	1.1616	1.2037	1.2467	1.2907	1.3354	1.3810	1.4274	1.4744	1.5222	1.5706	1.6197	1.6693	1.7196	1.7704	1.8218	1.8739	1.9265	1.9799	2.0340
17.0	1.0788	1.1188	1.1599	1.2018	1.2447	1.2885	1.3331	1.3786	1.4248	1.4717	1.5193	1.5676	1.6165	1.6660	1.7161	1.7668	1.8181	1.8700	1.9226	1.9758	2.0298
18.0	1.0773	1.1173	1.1581	1.2000	1.2427	1.2864	1.3308	1.3761	1.4222	1.4690	1.5164	1.5646	1.6133	1.6627	1.7127	1.7633	1.8144	1.8662	1.9186	1.9717	2.0256
19.0	1.0759	1.1157	1.1564	1.1981	1.2407	1.2842	1.3286	1.3737	1.4196	1.4662	1.5136	1.5615	1.6102	1.6594	1.7093	1.7597	1.8107	1.8624	1.9147	1.9677	2.0215
20.0	1.0744	1.1141	1.1547	1.1963	1.2388	1.2821	1.3263	1.3713	1.4170	1.4635	1.5107	1.5585	1.6070	1.6561	1.7058	1.7561	1.8070	1.8586	1.9108	1.9636	2.0173
21.0	1.0730	1.1125	1.1530	1.1944	1.2368	1.2800	1.3240	1.3689	1.4145	1.4608	1.5078	1.5556	1.6039	1.6529	1.7024	1.7526	1.8034	1.8548	1.9068	1.9596	2.0132
22.0	1.0716	1.1110	1.1513	1.1926	1.2348	1.2779	1.3218	1.3665	1.4119	1.4581	1.5050	1.5526	1.6008	1.6496	1.6990	1.7491	1.7997	1.8510	1.9030	1.9556	2.0090
23.0	1.0701	1.1094	1.1496	1.1908	1.2328	1.2757	1.3195	1.3641	1.4094	1.4554	1.5022	1.5496	1.5977	1.6464	1.6957	1.7456	1.7961	1.8473	1.8991	1.9516	2.0049
24.0	1.0687	1.1078	1.1479	1.1889	1.2309	1.2736	1.3173	1.3617	1.4068	1.4528	1.4994	1.5467	1.5946	1.6431	1.6923	1.7421	1.7925	1.8435	1.8952	1.9476	2.0008
25.0	1.0673	1.1063	1.1462	1.1871	1.2289	1.2715	1.3150	1.3593	1.4043	1.4501	1.4966	1.5437	1.5915	1.6399	1.6890	1.7386	1.7889	1.8398	1.8914	1.9437	1.9968
26.0	1.0658	1.1047	1.1446	1.1853	1.2269	1.2694	1.3128	1.3569	1.4018	1.4474	1.4938	1.5408	1.5884	1.6367	1.6856	1.7351	1.7853	1.8361	1.8875	1.9397	1.9927
27.0	1.0644	1.1032	1.1429	1.1835	1.2250	1.2674	1.3106	1.3545	1.3993	1.4448	1.4910	1.5378	1.5854	1.6335	1.6823	1.7317	1.7817	1.8324	1.8837	1.9358	1.9887
28.0	1.0630	1.1016	1.1412	1.1817	1.2231	1.2653	1.3083	1.3522	1.3968	1.4422	1.4882	1.5349	1.5823	1.6303	1.6790	1.7283	1.7782	1.8287	1.8799	1.9319	1.9847
29.0	1.0616	1.1001	1.1395	1.1799	1.2211	1.2632	1.3061	1.3498	1.3943	1.4395	1.4854	1.5320	1.5793	1.6272	1.6757	1.7248	1.7746	1.8250	1.8761	1.9280	1.9806
30.0	1.0602	1.0986	1.1379	1.1781	1.2192	1.2612	1.3039	1.3475	1.3918	1.4369	1.4827	1.5291	1.5763	1.6240	1.6724	1.7214	1.7711	1.8214	1.8724	1.9241	1.9767
31.0	1.0588	1.0970	1.1362	1.1763	1.2173	1.2591	1.3017	1.3452	1.3894	1.4343	1.4799	1.5263	1.5732	1.6209	1.6691	1.7180	1.7676	1.8177	1.8686	1.9203	1.9727
32.0	1.0574	1.0955	1.1346	1.1745	1.2154	1.2570	1.2996	1.3429	1.3869	1.4317	1.4772	1.5234	1.5702	1.6177	1.6659	1.7146	1.7640	1.8141	1.8649	1.9164	1.9687
33.0	1.0560	1.0940	1.1329	1.1728	1.2135	1.2550	1.2974	1.3405	1.3845	1.4291	1.4745	1.5205	1.5673	1.6146	1.6626	1.7113	1.7606	1.8105	1.8612	1.9126	1.9648
34.0	1.0546	1.0925	1.1313	1.1710	1.2116	1.2530	1.2952	1.3382	1.3820	1.4265	1.4718	1.5177	1.5643	1.6115	1.6594	1.7079	1.7571	1.8069	1.8575	1.9087	1.9608
35.0	1.0532	1.0910	1.1296	1.1692	1.2097	1.2509	1.2930	1.3359	1.3796	1.4240	1.4691	1.5149	1.5613	1.6084	1.6562	1.7046	1.7536	1.8033	1.8538	1.9049	1.9569
36.0	1.0518	1.0895	1.1280	1.1675	1.2078	1.2489	1.2909	1.3336	1.3772	1.4214	1.4664	1.5120	1.5584	1.6053	1.6530	1.7012	1.7502	1.7998	1.8501	1.9012	1.9530
37.0	1.0504	1.0880	1.1264	1.1657	1.2059	1.2469	1.2887	1.3314	1.3747	1.4189	1.4637	1.5092	1.5554	1.6023	1.6498	1.6979	1.7467	1.7962	1.8464	1.8974	1.9492
38.0	1.0491	1.0865	1.1248	1.1639	1.2040	1.2449	1.2866	1.3291	1.3723	1.4163	1.4610	1.5064	1.5525	1.5992	1.6466	1.6946	1.7433	1.7927	1.8428	1.8936	1.9453
39.0	1.0477	1.0850	1.1231	1.1622	1.2021	1.2429	1.2845	1.3268	1.3699	1.4138	1.4584	1.5036	1.5496	1.5962	1.6434	1.6913	1.7399	1.7892	1.8391	1.8899	1.9414
40.0	1.0463	1.0835	1.1215	1.1605	1.2003	1.2409	1.2823	1.3246	1.3675	1.4113	1.4557	1.5008	1.5466	1.5931	1.6403	1.6880	1.7365	1.7857	1.8355	1.8862	1.9376

DATA-TABLE 2 *by Niels Ramsing & Jens Gundersen*

Diffusion coefficient for oxygen at different temperatures and salinities of seawater

Units: 10^-5 cm2 s-1

Salinity	Temperature (°C)																				
(‰)	20.0	21.0	22.0	23.0	24.0	25.0	26.0	27.0	28.0	29.0	30.0	31.0	32.0	33.0	34.0	35.0	36.0	37.0	38.0	39.0	40.0
0.0	2.1039	2.1608	2.2186	2.2776	2.3379	2.3999	2.4637	2.5297	2.5984	2.6703	2.7458	2.8256	2.9106	3.0016	3.0997	3.2063	3.3228	3.4512	3.5939	3.7536	3.9342
1.0	2.0993	2.1561	2.2139	2.2727	2.3330	2.3948	2.4584	2.5243	2.5929	2.6645	2.7398	2.8194	2.9042	2.9949	3.0926	3.1987	3.3147	3.4425	3.5843	3.7431	3.9225
2.0	2.0949	2.1515	2.2091	2.2679	2.3280	2.3897	2.4532	2.5190	2.5873	2.6588	2.7339	2.8133	2.8977	2.9881	3.0855	3.1912	3.3066	3.4337	3.5748	3.7326	3.9108
3.0	2.0904	2.1469	2.2044	2.2631	2.3230	2.3846	2.4480	2.5136	2.5818	2.6531	2.7280	2.8072	2.8914	2.9814	3.0784	3.1837	3.2986	3.4251	3.5653	3.7222	3.8992
4.0	2.0860	2.1424	2.1997	2.2583	2.3181	2.3795	2.4428	2.5083	2.5763	2.6474	2.7222	2.8011	2.8850	2.9748	3.0714	3.1762	3.2906	3.4164	3.5559	3.7118	3.8877
5.0	2.0815	2.1378	2.1951	2.2535	2.3132	2.3745	2.4376	2.5030	2.5709	2.6418	2.7163	2.7950	2.8787	2.9681	3.0644	3.1688	3.2826	3.4078	3.5466	3.7015	3.8762
6.0	2.0771	2.1333	2.1904	2.2487	2.3083	2.3695	2.4325	2.4977	2.5654	2.6362	2.7105	2.7890	2.8724	2.9615	3.0574	3.1614	3.2747	3.3993	3.5373	3.6913	3.8648
7.0	2.0727	2.1288	2.1858	2.2440	2.3034	2.3645	2.4274	2.4924	2.5600	2.6306	2.7047	2.7830	2.8661	2.9549	3.0505	3.1540	3.2668	3.3908	3.5280	3.6811	3.8534
8.0	2.0684	2.1243	2.1812	2.2392	2.2986	2.3595	2.4222	2.4872	2.5546	2.6250	2.6990	2.7770	2.8599	2.9484	3.0436	3.1467	3.2590	3.3823	3.5188	3.6710	3.8421
9.0	2.0640	2.1198	2.1766	2.2345	2.2938	2.3545	2.4172	2.4819	2.5492	2.6195	2.6932	2.7710	2.8536	2.9419	3.0367	3.1394	3.2512	3.3739	3.5096	3.6609	3.8309
10.0	2.0597	2.1154	2.1720	2.2298	2.2890	2.3496	2.4121	2.4767	2.5439	2.6140	2.6875	2.7651	2.8475	2.9354	3.0299	3.1321	3.2434	3.3655	3.5005	3.6508	3.8198
11.0	2.0554	2.1109	2.1675	2.2252	2.2842	2.3447	2.4071	2.4716	2.5385	2.6085	2.6818	2.7592	2.8413	2.9289	3.0231	3.1249	3.2357	3.3572	3.4914	3.6409	3.8087
12.0	2.0511	2.1065	2.1630	2.2205	2.2794	2.3398	2.4020	2.4664	2.5332	2.6030	2.6761	2.7533	2.8352	2.9225	3.0163	3.1177	3.2280	3.3489	3.4824	3.6310	3.7977
13.0	2.0468	2.1021	2.1584	2.2159	2.2746	2.3350	2.3971	2.4613	2.5279	2.5975	2.6705	2.7474	2.8290	2.9161	3.0095	3.1105	3.2203	3.3406	3.4734	3.6211	3.7867
14.0	2.0425	2.0977	2.1539	2.2113	2.2699	2.3301	2.3921	2.4561	2.5227	2.5921	2.6649	2.7416	2.8230	2.9097	3.0028	3.1034	3.2127	3.3324	3.4645	3.6113	3.7759
15.0	2.0383	2.0934	2.1495	2.2067	2.2652	2.3253	2.3871	2.4511	2.5174	2.5867	2.6593	2.7358	2.8169	2.9034	2.9961	3.0963	3.2051	3.3242	3.4556	3.6015	3.7650
16.0	2.0340	2.0890	2.1450	2.2021	2.2605	2.3205	2.3822	2.4460	2.5122	2.5813	2.6537	2.7300	2.8109	2.8970	2.9895	3.0892	3.1976	3.3161	3.4468	3.5918	3.7543
17.0	2.0298	2.0847	2.1406	2.1976	2.2559	2.3157	2.3773	2.4409	2.5070	2.5759	2.6482	2.7243	2.8049	2.8908	2.9828	3.0822	3.1901	3.3080	3.4380	3.5822	3.7436
18.0	2.0256	2.0804	2.1362	2.1930	2.2512	2.3109	2.3724	2.4359	2.5018	2.5706	2.6426	2.7185	2.7989	2.8845	2.9762	3.0752	3.1826	3.3000	3.4292	3.5726	3.7329
19.0	2.0215	2.0761	2.1318	2.1885	2.2466	2.3062	2.3675	2.4309	2.4967	2.5653	2.6371	2.7128	2.7929	2.8782	2.9697	3.0682	3.1751	3.2920	3.4205	3.5630	3.7223
20.0	2.0173	2.0718	2.1274	2.1840	2.2420	2.3014	2.3626	2.4259	2.4915	2.5600	2.6317	2.7071	2.7870	2.8720	2.9631	3.0613	3.1677	3.2840	3.4118	3.5535	3.7118
21.0	2.0132	2.0676	2.1230	2.1795	2.2374	2.2967	2.3578	2.4209	2.4864	2.5547	2.6262	2.7014	2.7811	2.8658	2.9566	3.0543	3.1603	3.2760	3.4032	3.5441	3.7013
22.0	2.0090	2.0634	2.1187	2.1751	2.2328	2.2920	2.3530	2.4160	2.4813	2.5494	2.6208	2.6958	2.7752	2.8597	2.9501	3.0475	3.1530	3.2681	3.3946	3.5347	3.6909
23.0	2.0049	2.0591	2.1143	2.1706	2.2282	2.2873	2.3482	2.4111	2.4763	2.5442	2.6153	2.6902	2.7694	2.8536	2.9436	3.0406	3.1457	3.2603	3.3861	3.5253	3.6806
24.0	2.0008	2.0549	2.1100	2.1662	2.2237	2.2827	2.3434	2.4061	2.4712	2.5390	2.6100	2.6846	2.7635	2.8474	2.9372	3.0338	3.1384	3.2524	3.3776	3.5160	3.6703
25.0	1.9968	2.0508	2.1057	2.1618	2.2192	2.2781	2.3387	2.4013	2.4662	2.5338	2.6046	2.6790	2.7577	2.8414	2.9308	3.0270	3.1312	3.2447	3.3692	3.5068	3.6601
26.0	1.9927	2.0466	2.1014	2.1574	2.2147	2.2734	2.3339	2.3964	2.4612	2.5286	2.5992	2.6735	2.7519	2.8353	2.9244	3.0203	3.1240	3.2369	3.3608	3.4976	3.6499
27.0	1.9887	2.0424	2.0972	2.1530	2.2102	2.2688	2.3292	2.3915	2.4562	2.5235	2.5939	2.6680	2.7462	2.8293	2.9181	3.0135	3.1168	3.2292	3.3524	3.4884	3.6398
28.0	1.9847	2.0383	2.0929	2.1487	2.2057	2.2643	2.3245	2.3867	2.4512	2.5184	2.5886	2.6624	2.7404	2.8233	2.9118	3.0069	3.1097	3.2215	3.3441	3.4793	3.6297
29.0	1.9806	2.0342	2.0887	2.1444	2.2013	2.2597	2.3198	2.3819	2.4463	2.5133	2.5833	2.6570	2.7347	2.8173	2.9055	3.0002	3.1025	3.2139	3.3358	3.4703	3.6197
30.0	1.9767	2.0301	2.0845	2.1400	2.1969	2.2552	2.3152	2.3771	2.4413	2.5082	2.5781	2.6515	2.7290	2.8114	2.8992	2.9936	3.0955	3.2063	3.3276	3.4613	3.6098
31.0	1.9727	2.0260	2.0803	2.1357	2.1925	2.2506	2.3105	2.3723	2.4364	2.5031	2.5728	2.6461	2.7234	2.8054	2.8930	2.9869	3.0884	3.1987	3.3194	3.4523	3.5999
32.0	1.9687	2.0219	2.0761	2.1315	2.1881	2.2461	2.3059	2.3676	2.4315	2.4981	2.5676	2.6407	2.7177	2.7995	2.8868	2.9804	3.0814	3.1912	3.3112	3.4434	3.5900
33.0	1.9648	2.0179	2.0720	2.1272	2.1837	2.2417	2.3013	2.3629	2.4267	2.4931	2.5624	2.6353	2.7121	2.7936	2.8806	2.9738	3.0744	3.1837	3.3031	3.4345	3.5802
34.0	1.9608	2.0138	2.0678	2.1229	2.1793	2.2372	2.2967	2.3581	2.4218	2.4881	2.5573	2.6299	2.7065	2.7878	2.8744	2.9673	3.0675	3.1762	3.2950	3.4257	3.5705
35.0	1.9569	2.0098	2.0637	2.1187	2.1750	2.2327	2.2921	2.3535	2.4170	2.4831	2.5521	2.6246	2.7010	2.7820	2.8683	2.9608	3.0606	3.1688	3.2870	3.4169	3.5608
36.0	1.9530	2.0058	2.0596	2.1145	2.1707	2.2283	2.2876	2.3488	2.4122	2.4781	2.5470	2.6192	2.6954	2.7762	2.8622	2.9543	3.0537	3.1614	3.2790	3.4082	3.5512
37.0	1.9492	2.0018	2.0555	2.1103	2.1664	2.2239	2.2830	2.3441	2.4074	2.4732	2.5419	2.6139	2.6899	2.7704	2.8561	2.9479	3.0468	3.1540	3.2710	3.3995	3.5416
38.0	1.9453	1.9979	2.0514	2.1061	2.1621	2.2195	2.2785	2.3395	2.4026	2.4682	2.5368	2.6086	2.6844	2.7646	2.8500	2.9415	3.0400	3.1467	3.2631	3.3908	3.5321
39.0	1.9414	1.9939	2.0474	2.1020	2.1578	2.2151	2.2740	2.3349	2.3978	2.4633	2.5317	2.6034	2.6789	2.7589	2.8440	2.9351	3.0332	3.1394	3.2552	3.3822	3.5226
40.0	1.9376	1.9900	2.0433	2.0978	2.1536	2.2107	2.2696	2.3303	2.3931	2.4584	2.5266	2.5981	2.6735	2.7532	2.8380	2.9288	3.0264	3.1322	3.2474	3.3737	3.5132

DATA-TABLE 6 *by Niels Ramsing & Jens Gundersen*

Oxygen solubility at different temperatures and salinities of seawater

Units: µmol/l

Salinity	Temperature (°C)																				
(‰)	0.0	1.0	2.0	3.0	4.0	5.0	6.0	7.0	8.0	9.0	10.0	11.0	12.0	13.0	14.0	15.0	16.0	17.0	18.0	19.0	20.0
0.0	456.6	444.0	431.9	420.4	409.4	398.9	388.8	379.2	369.9	361.1	352.6	344.4	336.6	329.1	321.9	314.9	308.3	301.8	295.6	289.7	283.9
1.0	453.5	441.0	429.0	417.6	406.7	396.3	386.3	376.7	367.6	358.8	350.4	342.3	334.5	327.1	319.9	313.0	306.4	300.0	293.9	287.9	282.2
2.0	450.4	438.0	426.1	414.8	404.0	393.6	383.7	374.3	365.2	356.5	348.1	340.1	332.4	325.0	317.9	311.1	304.5	298.2	292.1	286.2	280.6
3.0	447.3	435.0	423.2	412.0	401.3	391.0	381.2	371.8	362.8	354.2	345.9	338.0	330.4	323.0	316.0	309.2	302.7	296.4	290.4	284.5	278.9
4.0	444.2	432.0	420.4	409.2	398.6	388.5	378.7	369.4	360.5	351.9	343.7	335.9	328.3	321.0	314.0	307.3	300.9	294.6	288.6	282.9	277.3
5.0	441.1	429.1	417.5	406.5	396.0	385.9	376.3	367.0	358.2	349.7	341.6	333.7	326.2	319.0	312.1	305.5	299.0	292.9	286.9	281.2	275.7
6.0	438.1	426.1	414.7	403.8	393.3	383.3	373.8	364.6	355.9	347.5	339.4	331.6	324.2	317.1	310.2	303.6	297.2	291.1	285.2	279.5	274.0
7.0	435.1	423.2	411.9	401.1	390.7	380.8	371.3	362.3	353.6	345.2	337.2	329.6	322.2	315.1	308.3	301.7	295.4	289.4	283.5	277.9	272.4
8.0	432.1	420.3	409.1	398.4	388.1	378.3	368.9	359.9	351.3	343.0	335.1	327.5	320.2	313.1	306.4	299.9	293.6	287.6	281.8	276.2	270.8
9.0	429.1	417.5	406.3	395.7	385.5	375.8	366.5	357.6	349.0	340.8	333.0	325.4	318.2	311.2	304.5	298.1	291.9	285.9	280.1	274.6	269.2
10.0	426.1	414.6	403.6	393.0	383.0	373.3	364.1	355.2	346.8	338.6	330.8	323.4	316.2	309.3	302.6	296.2	290.1	284.2	278.5	273.0	267.6
11.0	423.2	411.8	400.8	390.4	380.4	370.8	361.7	352.9	344.5	336.5	328.7	321.3	314.2	307.3	300.8	294.4	288.3	282.5	276.8	271.3	266.1
12.0	420.3	409.0	398.1	387.8	377.9	368.4	359.3	350.6	342.3	334.3	326.7	319.3	312.2	305.4	298.9	292.6	286.6	280.8	275.1	269.7	264.5
13.0	417.4	406.2	395.4	385.2	375.3	366.0	357.0	348.3	340.1	332.2	324.6	317.3	310.3	303.5	297.1	290.8	284.8	279.1	273.5	268.1	262.9
14.0	414.5	403.4	392.7	382.6	372.8	363.5	354.6	346.1	337.9	330.0	322.5	315.3	308.3	301.7	295.2	289.1	283.1	277.4	271.9	266.5	261.4
15.0	411.7	400.6	390.1	380.0	370.4	361.1	352.3	343.8	335.7	327.9	320.5	313.3	306.4	299.8	293.4	287.3	281.4	275.7	270.2	265.0	259.9
16.0	408.8	397.9	387.4	377.4	367.9	358.7	350.0	341.6	333.5	325.8	318.4	311.3	304.5	297.9	291.6	285.5	279.7	274.0	268.6	263.4	258.3
17.0	406.0	395.2	384.8	374.9	365.4	356.4	347.7	339.4	331.4	323.7	316.4	309.4	302.6	296.1	289.8	283.8	278.0	272.4	267.0	261.8	256.8
18.0	403.2	392.5	382.2	372.4	363.0	354.0	345.4	337.2	329.2	321.7	314.4	307.4	300.7	294.2	288.0	282.1	276.3	270.8	265.4	260.3	255.3
19.0	400.4	389.8	379.6	369.9	360.6	351.7	343.1	335.0	327.1	319.6	312.4	305.5	298.8	292.4	286.3	280.3	274.6	269.1	263.8	258.7	253.8
20.0	397.7	387.1	377.0	367.4	358.2	349.3	340.9	332.8	325.0	317.6	310.4	303.5	296.9	290.6	284.5	278.6	273.0	267.5	262.3	257.2	252.3
21.0	394.9	384.5	374.5	364.9	355.8	347.0	338.6	330.6	322.9	315.5	308.4	301.6	295.1	288.8	282.7	276.9	271.3	265.9	260.7	255.7	250.8
22.0	392.2	381.8	371.9	362.4	353.4	344.7	336.4	328.5	320.8	313.5	306.5	299.7	293.2	287.0	281.0	275.2	269.7	264.3	259.1	254.1	249.3
23.0	389.5	379.2	369.4	360.0	351.0	342.4	334.2	326.3	318.7	311.5	304.5	297.8	291.4	285.2	279.3	273.5	268.0	262.7	257.6	252.6	247.9
24.0	386.8	376.6	366.9	357.6	348.7	340.2	332.0	324.2	316.7	309.5	302.6	295.9	289.6	283.4	277.5	271.9	266.4	261.1	256.0	251.1	246.4
25.0	384.1	374.0	364.4	355.2	346.4	337.9	329.8	322.1	314.6	307.5	300.7	294.1	287.8	281.7	275.8	270.2	264.8	259.5	254.5	249.6	244.9
26.0	381.5	371.5	361.9	352.8	344.0	335.7	327.7	320.0	312.6	305.5	298.7	292.2	285.9	279.9	274.1	268.5	263.2	258.0	253.0	248.2	243.5
27.0	378.8	368.9	359.5	350.4	341.7	333.4	325.5	317.9	310.6	303.6	296.8	290.4	284.2	278.2	272.4	266.9	261.6	256.4	251.5	246.7	242.1
28.0	376.2	366.4	357.0	348.0	339.5	331.2	323.4	315.8	308.6	301.6	294.9	288.5	282.4	276.5	270.7	265.3	260.0	254.9	250.0	245.2	240.6
29.0	373.6	363.9	354.6	345.7	337.2	329.0	321.2	313.8	306.6	299.7	293.1	286.7	280.6	274.7	269.1	263.6	258.4	253.3	248.5	243.8	239.2
30.0	371.0	361.4	352.2	343.4	334.9	326.9	319.1	311.7	304.6	297.8	291.2	284.9	278.8	273.0	267.4	262.0	256.8	251.8	247.0	242.3	237.8
31.0	368.5	358.9	349.8	341.1	332.7	324.7	317.0	309.7	302.6	295.9	289.3	283.1	277.1	271.3	265.8	260.4	255.3	250.3	245.5	240.9	236.4
32.0	365.9	356.5	347.4	338.8	330.5	322.5	314.9	307.7	300.7	294.0	287.5	281.3	275.4	269.6	264.1	258.8	253.7	248.8	244.0	239.4	235.0
33.0	363.4	354.0	345.1	336.5	328.3	320.4	312.9	305.6	298.7	292.1	285.7	279.5	273.6	268.0	262.5	257.2	252.2	247.3	242.6	238.0	233.6
34.0	360.9	351.6	342.7	334.2	326.1	318.3	310.8	303.7	296.8	290.2	283.9	277.8	271.9	266.3	260.9	255.7	250.6	245.8	241.1	236.6	232.2
35.0	358.4	349.2	340.4	332.0	323.9	316.2	308.8	301.7	294.9	288.3	282.0	276.0	270.2	264.6	259.3	254.1	249.1	244.3	239.7	235.2	230.9
36.0	355.9	346.8	338.1	329.7	321.7	314.1	306.7	299.7	293.0	286.5	280.3	274.3	268.5	263.0	257.7	252.5	247.6	242.8	238.2	233.8	229.5
37.0	353.5	344.4	335.8	327.5	319.6	312.0	304.7	297.7	291.1	284.6	278.5	272.5	266.8	261.4	256.1	251.0	246.1	241.4	236.8	232.4	228.2
38.0	351.0	342.0	333.5	325.3	317.4	309.9	302.7	295.8	289.2	282.8	276.7	270.8	265.2	259.7	254.5	249.5	244.6	239.9	235.4	231.0	226.8
39.0	348.6	339.7	331.2	323.1	315.3	307.9	300.7	293.9	287.3	281.0	274.9	269.1	263.5	258.1	252.9	247.9	243.1	238.5	234.0	229.7	225.5
40.0	346.2	337.4	329.0	320.9	313.2	305.8	298.7	292.0	285.4	279.2	273.2	267.4	261.8	256.5	251.4	246.4	241.6	237.0	232.6	228.3	224.1

DATA-TABLE 7 *by Niels Ramsing & Jens Gundersen*

Oxygen solubility at different temperatures and salinities of seawater

Units: µmol/l

Salinity	Temperature (°C)																				
(‰)	20.0	21.0	22.0	23.0	24.0	25.0	26.0	27.0	28.0	29.0	30.0	31.0	32.0	33.0	34.0	35.0	36.0	37.0	38.0	39.0	40.0
0.0	283.9	278.3	273.0	267.8	262.8	257.9	253.2	248.7	244.3	240.0	235.9	231.9	228.0	224.2	220.5	217.0	213.5	210.1	206.7	203.5	200.4
1.0	282.2	276.7	271.4	266.3	261.3	256.5	251.8	247.3	243.0	238.7	234.6	230.6	226.8	223.0	219.4	215.8	212.3	209.0	205.7	202.5	199.3
2.0	280.6	275.1	269.8	264.7	259.8	255.0	250.4	245.9	241.6	237.4	233.3	229.4	225.6	221.8	218.2	214.7	211.2	207.9	204.6	201.4	198.3
3.0	278.9	273.5	268.3	263.2	258.3	253.6	249.0	244.6	240.3	236.1	232.1	228.1	224.3	220.6	217.0	213.5	210.1	206.8	203.6	200.4	197.3
4.0	277.3	271.9	266.7	261.7	256.8	252.1	247.6	243.2	238.9	234.8	230.8	226.9	223.1	219.5	215.9	212.4	209.0	205.7	202.5	199.4	196.3
5.0	275.7	270.3	265.2	260.2	255.4	250.7	246.2	241.8	237.6	233.5	229.5	225.7	221.9	218.3	214.7	211.3	207.9	204.6	201.4	198.3	195.3
6.0	274.0	268.7	263.6	258.7	253.9	249.3	244.8	240.5	236.3	232.2	228.3	224.4	220.7	217.1	213.6	210.2	206.8	203.6	200.4	197.3	194.3
7.0	272.4	267.2	262.1	257.2	252.5	247.9	243.4	239.1	235.0	230.9	227.0	223.2	219.5	215.9	212.4	209.0	205.7	202.5	199.4	196.3	193.3
8.0	270.8	265.6	260.6	255.7	251.0	246.5	242.1	237.8	233.7	229.7	225.8	222.0	218.3	214.8	211.3	207.9	204.7	201.5	198.3	195.3	192.3
9.0	269.2	264.1	259.1	254.2	249.6	245.1	240.7	236.5	232.4	228.4	224.5	220.8	217.2	213.6	210.2	206.8	203.6	200.4	197.3	194.3	191.3
10.0	267.6	262.5	257.6	252.8	248.2	243.7	239.4	235.2	231.1	227.1	223.3	219.6	216.0	212.5	209.1	205.7	202.5	199.4	196.3	193.3	190.3
11.0	266.1	261.0	256.1	251.3	246.7	242.3	238.0	233.8	229.8	225.9	222.1	218.4	214.8	211.3	208.0	204.7	201.4	198.3	195.3	192.3	189.4
12.0	264.5	259.5	254.6	249.9	245.3	240.9	236.7	232.5	228.5	224.6	220.9	217.2	213.7	210.2	206.8	203.6	200.4	197.3	194.2	191.3	188.4
13.0	262.9	257.9	253.1	248.4	243.9	239.6	235.3	231.2	227.3	223.4	219.7	216.0	212.5	209.1	205.7	202.5	199.3	196.2	193.2	190.3	187.4
14.0	261.4	256.4	251.6	247.0	242.5	238.2	234.0	229.9	226.0	222.2	218.5	214.9	211.4	208.0	204.6	201.4	198.3	195.2	192.2	189.3	186.5
15.0	259.9	254.9	250.2	245.6	241.1	236.8	232.7	228.6	224.7	220.9	217.3	213.7	210.2	206.8	203.6	200.4	197.2	194.2	191.2	188.3	185.5
16.0	258.3	253.4	248.7	244.2	239.8	235.5	231.4	227.4	223.5	219.7	216.1	212.5	209.1	205.7	202.5	199.3	196.2	193.2	190.2	187.4	184.6
17.0	256.8	252.0	247.3	242.8	238.4	234.2	230.1	226.1	222.2	218.5	214.9	211.4	208.0	204.6	201.4	198.2	195.2	192.2	189.3	186.4	183.6
18.0	255.3	250.5	245.9	241.4	237.0	232.8	228.8	224.8	221.0	217.3	213.7	210.2	206.8	203.5	200.3	197.2	194.1	191.2	188.3	185.4	182.7
19.0	253.8	249.0	244.4	240.0	235.7	231.5	227.5	223.6	219.8	216.1	212.5	209.1	205.7	202.4	199.2	196.1	193.1	190.2	187.3	184.5	181.7
20.0	252.3	247.6	243.0	238.6	234.3	230.2	226.2	222.3	218.6	214.9	211.4	207.9	204.6	201.3	198.2	195.1	192.1	189.2	186.3	183.5	180.8
21.0	250.8	246.1	241.6	237.2	233.0	228.9	224.9	221.1	217.3	213.7	210.2	206.8	203.5	200.3	197.1	194.1	191.1	188.2	185.4	182.6	179.9
22.0	249.3	244.7	240.2	235.8	231.7	227.6	223.6	219.8	216.1	212.5	209.1	205.7	202.4	199.2	196.1	193.0	190.1	187.2	184.4	181.6	179.0
23.0	247.9	243.2	238.8	234.5	230.3	226.3	222.4	218.6	214.9	211.4	207.9	204.6	201.3	198.1	195.0	192.0	189.1	186.2	183.4	180.7	178.0
24.0	246.4	241.8	237.4	233.1	229.0	225.0	221.1	217.4	213.7	210.2	206.8	203.4	200.2	197.1	194.0	191.0	188.1	185.2	182.5	179.8	177.1
25.0	244.9	240.4	236.0	231.8	227.7	223.7	219.9	216.2	212.5	209.0	205.6	202.3	199.1	196.0	193.0	190.0	187.1	184.3	181.5	178.8	176.2
26.0	243.5	239.0	234.7	230.5	226.4	222.5	218.6	214.9	211.4	207.9	204.5	201.2	198.0	194.9	191.9	189.0	186.1	183.3	180.6	177.9	175.3
27.0	242.1	237.6	233.3	229.1	225.1	221.2	217.4	213.7	210.2	206.7	203.4	200.1	197.0	193.9	190.9	188.0	185.1	182.4	179.6	177.0	174.4
28.0	240.6	236.2	231.9	227.8	223.8	219.9	216.2	212.5	209.0	205.6	202.3	199.0	195.9	192.9	189.9	187.0	184.2	181.4	178.7	176.1	173.5
29.0	239.2	234.8	230.6	226.5	222.5	218.7	215.0	211.4	207.9	204.5	201.2	198.0	194.8	191.8	188.9	186.0	183.2	180.5	177.8	175.2	172.6
30.0	237.8	233.5	229.3	225.2	221.3	217.4	213.7	210.2	206.7	203.3	200.1	196.9	193.8	190.8	187.9	185.0	182.2	179.5	176.9	174.3	171.7
31.0	236.4	232.1	227.9	223.9	220.0	216.2	212.5	209.0	205.5	202.2	199.0	195.8	192.7	189.8	186.9	184.0	181.3	178.6	175.9	173.4	170.9
32.0	235.0	230.7	226.6	222.6	218.7	215.0	211.3	207.8	204.4	201.1	197.9	194.7	191.7	188.7	185.9	183.0	180.3	177.6	175.0	172.5	170.0
33.0	233.6	229.4	225.3	221.3	217.5	213.8	210.1	206.7	203.3	200.0	196.8	193.7	190.7	187.7	184.9	182.1	179.4	176.7	174.1	171.6	169.1
34.0	232.2	228.0	224.0	220.0	216.2	212.5	209.0	205.5	202.1	198.9	195.7	192.6	189.6	186.7	183.9	181.1	178.4	175.8	173.2	170.7	168.2
35.0	230.9	226.7	222.7	218.8	215.0	211.3	207.8	204.3	201.0	197.8	194.6	191.6	188.6	185.7	182.9	180.1	177.5	174.9	172.3	169.8	167.4
36.0	229.5	225.4	221.4	217.5	213.8	210.1	206.6	203.2	199.9	196.7	193.6	190.5	187.6	184.7	181.9	179.2	176.5	173.9	171.4	168.9	166.5
37.0	228.2	224.1	220.1	216.2	212.5	208.9	205.4	202.1	198.8	195.6	192.5	189.5	186.6	183.7	180.9	178.2	175.6	173.0	170.5	168.1	165.7
38.0	226.8	222.7	218.8	215.0	211.3	207.7	204.3	200.9	197.7	194.5	191.4	188.5	185.6	182.7	180.0	177.3	174.7	172.1	169.6	167.2	164.8
39.0	225.5	221.4	217.5	213.8	210.1	206.6	203.1	199.8	196.6	193.4	190.4	187.4	184.5	181.7	179.0	176.3	173.8	171.2	168.7	166.3	164.0
40.0	224.1	220.1	216.3	212.5	208.9	205.4	202.0	198.7	195.5	192.4	189.3	186.4	183.5	180.8	178.1	175.4	172.8	170.3	167.9	165.5	163.1

Appendix III – Envco Conductivity to Salinity Table

Conversion Table for Changing Conductivity into Salinity

Conductivity*							Salinity
0°C	5°C	10°C	15°C	20°C	25°C	30°C	ppt
1.200	1.400	1.500	1.700	2.000	2.200	2.400	1
2.220	2.500	2.900	3.300	3.700	4.100	4.500	2
3.200	3.700	4.200	4.700	5.300	5.900	6.500	3
4.100	4.700	5.400	6.100	6.900	7.600	8.400	4
5.000	5.800	6.600	7.500	8.400	9.300	10.300	5
5.900	6.800	7.900	8.800	9.900	11.000	12.100	6
6.700	7.800	8.900	10.100	11.300	12.600	13.900	7
7.600	8.800	10.100	11.400	12.800	14.200	15.700	8
8.500	9.800	11.200	12.700	14.200	15.800	17.400	9
9.300	10.800	12.300	13.900	15.600	17.300	19.100	10
10.200	11.800	13.400	15.200	17.000	18.900	20.800	11
11.000	12.800	14.500	16.500	18.900	20.400	22.500	12
11.900	13.700	15.600	17.600	19.700	21.900	24.100	13
12.600	14.600	16.700	18.700	21.100	23.400	25.800	14
13.400	15.600	17.800	20.100	22.400	24.900	27.400	15
14.200	16.400	18.800	21.200	23.800	26.400	29.100	16
15.000	17.400	19.800	22.400	25.100	27.800	30.700	17
15.800	18.300	20.900	23.600	26.400	29.300	32.300	18
16.600	14.200	21.900	24.800	27.700	30.700	33.900	19
17.400	20.100	23.000	25.900	29.000	32.200	35.500	20
18.200	21.100	24.000	27.100	30.300	33.600	37.000	21
19.000	22.000	25.100	28.300	31.600	35.000	38.600	22
19.800	22.900	26.100	29.400	32.900	36.500	40.100	23
20.600	23.800	27.100	30.600	34.200	37.900	41.700	24
21.400	24.700	28.100	31.700	35.400	39.300	43.200	25
22.100	25.500	29.100	32.800	36.700	40.700	44.800	26
22.800	26.400	30.100	33.900	37.900	42.100	46.300	27
23.600	27.300	31.100	35.100	39.200	43.500	47.800	28
24.400	28.100	32.100	36.200	40.400	44.800	49.400	29
25.200	29.000	33.100	37.300	41.700	46.200	50.900	30
26.000	30.000	34.100	38.500	43.000	47.600	52.400	31
26.800	30.900	35.100	39.600	44.200	49.000	53.900	32
27.500	31.700	36.100	40.700	45.400	50.300	55.400	33
28.300	32.600	37.100	41.800	46.700	51.700	56.800	34
29.100	33.500	38.100	42.900	47.900	53.000	58.300	35
29.700	34.200	39.000	44.000	49.100	54.400	59.800	36
30.500	35.100	40.000	45.100	50.300	55.700	61.300	37
31.200	36.000	41.000	46.200	51.500	57.100	62.800	38
32.000	36.800	41.900	47.200	52.700	58.400	64.200	39
32.700	37.700	42.900	48.300	53.900	59.700	65.700	40

* Conductivity values are given in millisiemens/cm
Data derived from the equation of P.K. Weyl, Limnology and Oceanography; 9,75 (1964).